THE FEASIBILITY STUDY FOR ELECTRONIC IMAGING SYSTEM WITH THE PHOTOHELIOGRAPH

E.L. Svensson and F.L. Schaff

WESTINGHOUSE DEFENSE AND ELECTRONIC SYSTEMS CENTER
Systems Development Division
Baltimore, Maryland

Contract No. NASW-2184

February 1972

Final Report for Period February 1971 to January 1972

Prepared for

NATIONAL AERONAUTICS AND SPACE ADMINISTRATION
Headquarters
Washington, D.C.

THE FEASIBILITY STUDY FOR ELECTRONIC IMAGING SYSTEM WITH THE PHOTOHELIOGRAPH

E.L. Svensson and F.L. Schaff

WESTINGHOUSE DEFENSE AND ELECTRONIC SYSTEMS CENTER
Systems Development Division
Baltimore, Maryland

Contract No. NASW-2184

February 1972

Final Report for Period February 1971 to January 1972

Prepared for

NATIONAL AERONAUTICS AND SPACE ADMINISTRATION
Headquarters
Washington, D.C.

1. Report No.	2. Government Accession No.	3. Recipient's Catalog No.

4. Title and Subtitle	5. Report Date
THE FEASIBILITY STUDY FOR ELECTRONIC IMAGING SYSTEM WITH THE PHOTOHELIOGRAPH	7 Feb 1972
	6. Performing Organization Code 72-0089
7. Author(s) E.L. Svensson and F.L. Schaff	8. Performing Organization Report No.
9. Performing Organization Name and Address Westinghouse Defense and Electronic Systems Center Systems Development Division Baltimore, Maryland 21203	10. Work Unit No.
	11. Contract or Grant No. Contract No. NASW-2184
12. Sponsoring Agency Name and Address National Aeronautics and Space Administration Headquarters Washington, D.C.	13. Type of Report and Period Covered Final Feb 71 to Jan 72
	14. Sponsoring Agency Code

15. Supplementary Notes

16. Abstract

17. Key Words	18. Distribution Statement
Photoheliograph High-Resolution, Slow-Scan TV	

19. Security Classif. (of this report)	20. Security Classif. (of this page)	21. No. of Pages	22. Price
Unclassified	Unclassified		

TP-147

TABLE OF CONTENTS

LIST OF ILLUSTRATIONS

LIST OF TABLES

FOREWORD

This final report represents the results of a 9-month study to determine the feasibility of using an Electronic Image System (EIS) as a scientific data gathering device for the NASA/California Institute of Technology Photoheliograph program.

Acknowledgement is given to NASA-Headquarters, NASA Marshall Space Flight Center, the California Institute of Technology, and Ball Brothers Research Corporation for their aid in providing the system characteristics and information needed to perform the EIS study.

Westinghouse personnel contributing to the study program were:

Emil L. Svensson	Principal Investigator
Fred L. Schaff	Associate Principal Investigator
Dr. A.S. Jensen	Consultant on Sensor Technology
C. Sturtevant	Telemetry Capabilities
D.T. Provine	Data Handling and Film Techniques
K. Badertscher	Computer Programming
F.J. Kaisler	Optics
W. Hayden	Project Administration

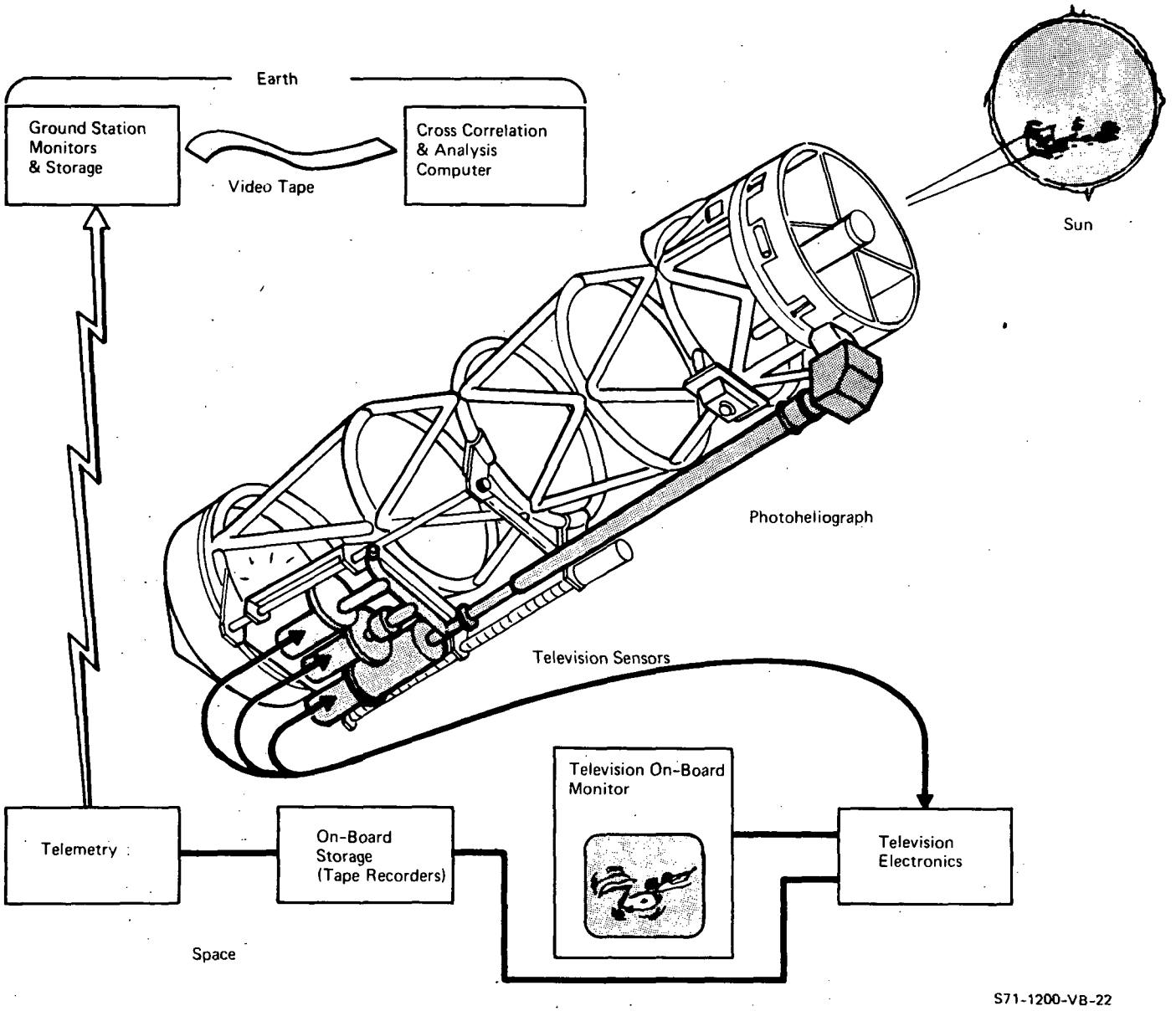

Photoheliograph with Electronic Imaging System

1. INTRODUCTION

The Photoheliograph program will be the highest resolution investigation of the sun presently planned. It is a multistage program starting with the present 65-centimeter aperture, then the 1.5-meter aperture, and finally culminating in the 3.0-meter aperture (Large Space Telescope). However, each instrument will be no better than the instrumentation between the telescope and final hard copy used for scientific analysis. Image detection is of major importance since information lost cannot be recovered. With this in mind, early versions of the photoheliograph have been designed with film as the sensor because of its undisputably high resolution capability and historical experience. However, film also incurs the disadvantages of large bulk, radiation damage susceptability, low sensitivity, difficulty in data reduction, variations in density from frame to frame, and most importantly, the lack of real-time information plus the requirement of physical recovery of exposed film. Westinghouse Electric Corporation was selected to review the state of the art of electronic imaging systems to determine the possibility of deriving approaches capable of achieving the requirements of the Photoheliograph program.

The initial study approach was directed in the following six areas.

- Determination of characteristics of the solar activity within the spectral response of the photoheliograph.
- Determination of characteristics of the space vehicles which could carry the photoheliograph, specifically the stability and data handling capabilities.
- Analysis of the capability of the ground based data gathering network to assimilate the generated information.
- The characteristics of the photoheliograph and the associated spectral filters.
- The results anticipated by the Principal Investigator.
- The state of the art of electronic imaging sensors.

The result of this effort could then be used to define the optimum sensor and the television/telemetry system which would best meet the overall requirements. In addition, brief supporting studies were made to compare the results with film and also to determine if any changes external to the electronic imaging system could be made to improve overall system capability when used with an electronic imaging system (EIS).

Early in the study, it was determined that two major tradeoff areas existed which impacted on the overall program regardless of whether film or electronic imagery was used. The first was that the state of the art in spacecraft stabilization was inadequate for the spacial resolution of the photoheliograph. This resulted in the need for high-sensitivity sensors used with short exposure times which, typically, cause a reduction in resolution. The possibilities of additional image motion compensation within the photoheliograph were considered and television systems optimized for IMC or non-IMC are discussed. The second problem area is in the total data handling capability of the typical vehicle. With film, the problem is total bulk and transfer capability. With the EIS, the problem must consider the vehicle data storage capability, the telemetry bandwidth, the downlink signal-to-noise ratio, and the total time over ground tracking stations. This problem is discussed based on present and predicted mission capabilities.

All available sensors were studied within the constraints of the experiment to determine if there was a single outstanding candidate which could be used with any variation of the present or future Photoheliograph program. Lacking this perfect candidate, all sensors were characterized so that an optimum match could be obtained. The tradeoffs are between sensitivity, resolution, overall system complexity, and sensor growth capability. The first three items were compared to the requirements of the 65-centimeter photoheliograph mounted on the ATM-B. The growth factor is then considered for the larger aperture Photoheliographs along with the growth required in spacecraft stability and data handling capability before an overall improvement is obtained.

The final section is devoted to specifying a system or systems which would contain the television subsystem, the data storage devices, the telemetry interface circuitry, a display subsystem for the astronauts, and the

controls required for overall operation. The system is patterned around the 65-centimeter photoheliograph but would have growth potential for future missions.

Appendix A considers a possible change to the photoheliograph which would provide an improved EIS by increasing the format size. Appendix B makes comparisons between film and EIS on overall performance. Appendix C describes a computer program designed to compute EIS signal current and signal-to-noise ratios for spectral characteristics, optics, filter characteristics, and the sensor.

2. SCIENTIFIC REQUIREMENTS

This section describes the characteristics of the sun, the photoheliograph, and the scientific objectives of the program and their impact on the EIS. These characteristics define the limits of sensitivity, resolution, frame time, and total frames of information required from the EIS.

2.1 SOLAR CHARACTERISTICS

The sun can roughly be described as a disc, subtending approximately a 32-minute field of view when viewed from earth and radiating energy at a black body temperature of 5,900°K. Figure 2-1 (reference 1) illustrates the black body continuum curve and the energy received at the surface through the atmosphere. The spectral intensity variations, as a function of weather conditions and scattering in the atmosphere, limit the spacial resolution to about 0.5 arc-sec on rare occasions and more than 1.0 arc-sec typically even in clear weather. Thus, it is obvious that accurate and repeatable measurements of the solar energy, and thereby a broader

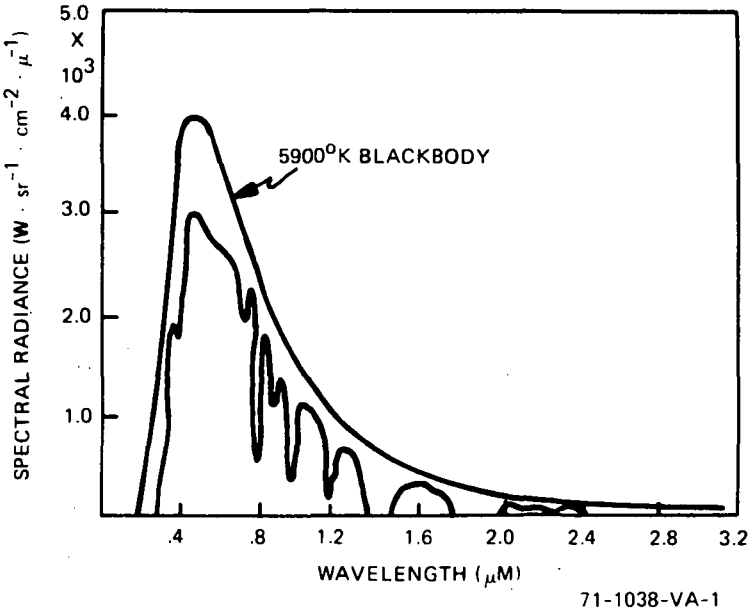

Figure 2-1. Approximate Solar Spectrum

understanding of plasma physics, can be obtained only from sensors located outside the earth's atmosphere. The photoheliograph is designed to have greater spacial and spectral resolution capabilities than would be usable in an earthbound device.

The absolute value of solar radiance has been well defined from earlier missions and could serve as a calibration for this mission. The important requirement is that the EIS sensitivity with wavelength be accurately defined and remain constant throughout the mission so that TV frames taken during the mission can be compared. Spectral resolution is completely defined by the filters on the photoheliograph and requires only that the EIS have sufficient sensitivity at all wavelengths of interest.

Table 2-1 shows a more accurate representation of the solar energy including the Fraunhofer absorption lines, their approximate width, and the energy levels. Each line represents a discrete absorption of energy by a particular ionization. The finite width of the line is an indication of variations in motion or doppler shift of the atoms, and the total energy difference from the solar mean is an indication of the relative quantity of each atom. The photoheliograph, by scanning both its narrow field of view and spectral width, can map these values with reference to particular solar events. The values in the table are averages over the entire solar disc; and, thus, local regions (particularly in sunspots, etc) should deviate significantly from these values.

A third definition of solar characteristics is also required to define the EIS. The rate of change of the detail under observation must be known since it will determine the frame times, the time between frames, total number of frames, and the mix between the three cameras and four spectral filters attached to the Photoheliograph. The solar features are put into two categories: one of short-lived features and one of long-lived features. Actual occurrences will be somewhat unpredictable until launch, but planning based on previous occurrences will be used by the Principal Investigator to cover any likely events.

Short-lived features are those whose occurrence will be less than an orbit including fine structure and motions of photospheric granules, fine structures and motions of chromospheric network features, chromospheric

TABLE 2-1

SOLAR RADIANCE FOR PHOTOHELIOGRAPH

λ (Å)	Fλ *	Spectral Width (Å)	Strong Fraunhofer Lines	λ (Å)	Fλ *	Spectral Width (Å)	Strong Fraunhofer Lines
2000	0.04			5000	3.57		
2200	0.141			5167.3	0.45	0.88	Mg I
2400	0.19			5122.7	0.34	1.27	Mg I
2600	0.39			5183.6	0.31	1.62	Mg I
2795.4	-	22	Mg II	5500	3.25		
2800	0.85			5890	0.12	0.83	Na I
2802.3	-	22	Mg II	5895.9	0.14	0.6	Na I
2851.6	-	9.6	Mg II	6000	2.86		
2881.1	-	2.6	Si I	6500	2.54		
3000	1.65			6562.8	0.390	4.1	HI(Hα)
3200	2.24						
3400	2.68						
3581.2	0.10	2.3	fe I				
3600	3.03						
3700	3.15						
3734.9	0.03	3.1	fe I				
3800	3.35						
3820.5	0.07	1.8	fe I				
3900	3.54						
3933.7	0.21	19.1	Ca II				
3968.5	0.22	14.4	Ca II				
4000	3.71						
4045.8	0.08	1.25	fe I				
4100	3.82						
4101.7	0.82	3.0	HI (H δ)				
4200	3.90						
4226.7	0.08	1.41	Ca I				
4300	3.91						
4340.5	0.63	2.89	HI(Hγ)				
4383.6	0.12	1.05	fe I				
4400	3.90						
4500	3.87						
4600	3.82						
4800	3.71						
4861.3	0.55	3.75	HI (Hβ)				

* Watt·Steradian^{-1} Å^{-1}·cm^{-2} x 10^{-1}

Reference 2: Astrophysical Quantities; Allen, C.W.; Athlone Press; 1963

oscillations, motion in prominences, detailed structure of filaments, etc. An estimate of the maximum rate of change which might occur can be inferred from a solar flare which occurred on 8 August 1968 in an active area where on 7 August a major flare was predicted. The flare expanded from nonexistence to 800 million square miles in 2-1/2 minutes. This corresponds to an average expansion of 0.4 arc-sec/sec or twice the photoheliograph diffraction limit per second. This obviously demonstrates the desirability of repeating a frame per camera every 3 seconds or faster under maximum conditions.

Long-lived features are those which exist with little change from one earth orbit to the next. Typical of this type are growth of active regions, life histories of sunspots, patrol observations to catch flare details, etc. The long-lived features require the same spacial and spectral resolution as the short-lived events but do not impact the frame and recycling times of the EIS. The most difficult problem will be registration of frames from orbit to orbit, both spacially and in relative intensity. Both problems place restraints not only on the EIS but also on the photoheliograph.

2.2 PHOTOHELIOGRAPH CHARACTERISTICS

The photoheliograph is essentially a large reflector telescope designed to observe the solar energy in three bands from the far ultraviolet through the visible to the Hydrogen Alpha line in the visible red. The telescope focuses a 2 arc-min square section of the sun's surface ($\approx 1/200$ of the solar disc) onto a 21- by 21-millimeter format with a diffraction limit of 1,320 TV lines or 33 lp/mm at the EIS input. The major characteristics of the photoheliograph that affect the EIS are detailed in table 2-2. The total mirror losses are (R^4) the reflectivity value of each of 4 mirrors. In addition, the T# shown includes an estimate for the losses in the beam-splitters which divide the incoming energy onto the three scientific cameras plus the standard scan, spotting telescope. The image motion compensation device is not included since its use is not yet established.

Table 2-3 contains pertinent details of the spectral filters used with each of the three EIS's. A series of wideband filters in the visible band are also likely, but these will parallel the tunable birefringent filter and will have neutral density filters to reduce the intensity to the same level as

TABLE 2-2

PHOTOHELIOGRAPH TELESCOPE DETAILS

Aperture	65 cm	1.5 m
Focal Length	3,250 cm	3,250 cm
f/#	50	22
Image Plane	21 x 21 mm	21 x 21 mm
Obscuration	20 percent	20 percent
Mirror Reflectivity (total)	92 to 65 percent	92 to 65 percent
T/#	79 to 111	35 to 49
FOV	2 x 2 min	2 x 2 min
Diffraction Limit	0.2 sec	0.09 sec
Diffraction Limit (@ format)	33 lp/mm	75 lp/mm
Total TV Lines	1,320	3,000

TABLE 2-3

PHOTOHELIOGRAPH FILTER DETAILS

a. Ultraviolet	
Type	Interference
Bandwidth	100 Å
Band Center	2,200 Å
Peak Transmission	15 percent
b. Visible	
Type	Tunable Birefringent
Bandwidth	≈1/4 Å
Band Center	Tunable (4,000 to 6,000 Å)
Peak Transmission	≈5 percent
c. Hydrogen Alpha	
Type	Fabry-Perot Interferometer
Bandwidth	1/2 Å
Band Center	6,563 Å

the tunable birefringent filter. The Hydrogen Alpha and the ultraviolet filters are available, and their parameters are accurately defined. However, the tunable birefringent filter is under development, and both spectral width and peak transmission values may change. Anticipated filter widths of 1/8 Å at 4000 Å and 1/4 Å at 6000 Å are included in the calculations.

The overall optical schematic, shown in figure 2-2, illustrates two possible configurations. One configuration requires one camera to operate with broadband filters in both the ultraviolet and the visible; the other two cameras are used for the Hydrogen Alpha and the birefringent filters alone. This approach allows greater utilization of the birefringent filter but at a cost of energy lost in the broadband beamsplitters and the inability to use a solar blind photocathode in the ultraviolet camera to reduce spectral discrimination required from the ultraviolet filters. A second approach uses dichroic beamsplitters which both reduce unwanted energy relative to desired energy in each direction and increases the relative intensity of the desired energy. Also, one camera is used exclusively for ultraviolet which allows a solar blind photocathode to use the sensor as a visible light filter. Thus, for purposes of EIS evaluation, it has been assumed that the second approach is more likely to be used, and all computations are based on this assumption. The characteristics of the mirrors, beamsplitters, etc are further described in the following item list.

Items 1, 2, 3, 4: All mirrors for the main telescope. Total reflectivity is R^4.

If mirrors are coated with enhanced silver.

$\lambda > 4500$ Å $R \approx 95$ percent

$\lambda < 4500$ Å R degrades to 20 percent at 2000 Å

If mirrors are coated with aluminum

$\lambda > 3500$ Å $R \approx 85$-90 percent

2000 Å $\leq \lambda \leq$ 2500 Å $R \approx 75$ percent

Item 5, 6: Ultraviolet - visible dichroic beamsplitters

$\lambda > 2500$ Å $T \approx 85$ percent

$\lambda < 2500$ Å $R \approx 90$ percent

Item 7: Red - visible dichroic beamsplitter

$\lambda > 6000$ Å $T \approx 90$ percent

$\lambda < 6000$ Å $R \approx 90$ percent

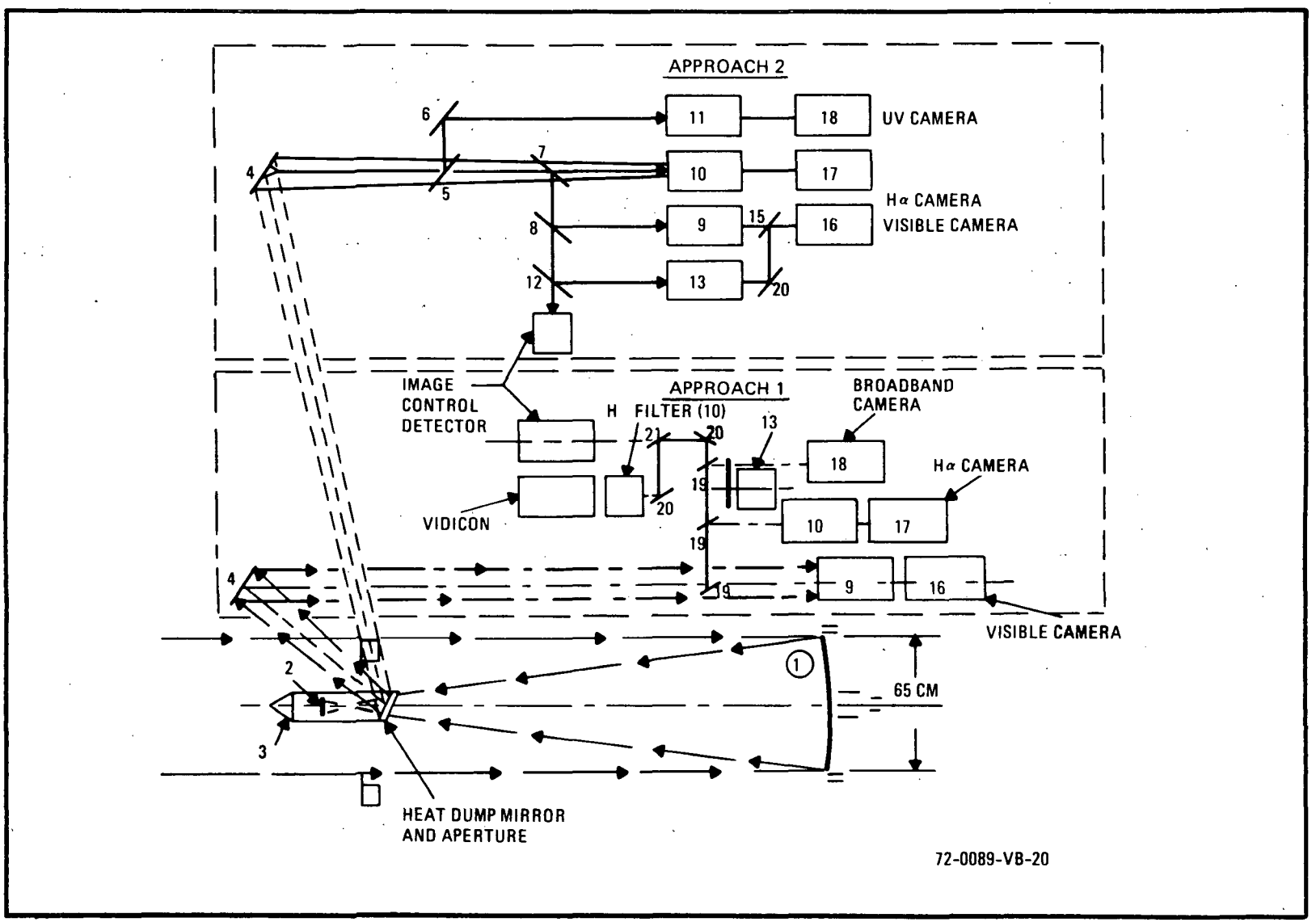

Figure 2-2. Photoheliograph Optical Schematic

Item 8, 12, 15:	Flip-out flats - silvered mirrors. Item 8 and 12 flip-out to give input to image and focus control. Item 15 flip-out to use Zeiss birefringent filter or broadband visible filter wheel.
Item 9:	Zeiss birefringent filter, tunable
Item 10:	Halle Hydrogen Alpha filter
Item 11:	Ultraviolet interference filter
Item 13:	Broad band visible filters on wheel plus neutral density filters to reduce intensity.
Item 16, 17, 18:	Cameras, EIS, or film.
Item 19:	Broadband beamsplitters
	$T \approx 45$ percent
	$R \approx 45$ percent
Item 20:	Broadband silvered mirrors
	$R \approx 95$ percent
Item 21:	Red - visible dichroic beamsplitter
	$\lambda > 6000$ Å $R \approx 90$ percent
	$\lambda > 6000$ Å $T \approx 90$ percent

With these values defined for the photoheliograph and the solar output obtained from table 2-1, the net intensity to the EIS can be obtained. The computer program of Appendix C was designed to do this computation for any desired set of telescope characteristics, filters, photocathodes, sensors, and electronics, but the four basic power levels are determined here for reference. These levels are the two fixed filters, the ultraviolet and the Hydrogen Alpha, and the anticipated minimum and maximum values obtained with the Zeiss birefringent filter. The computation is simply the equation for the irradiance at the large of an extended distant object

$$H = \frac{\pi N}{4(T\#)^2(m+1)^2} \qquad W \cdot M^{-2}$$

Where: N = radiance of source (table 1-1)

m = image size/object size $\rightarrow$ 0 for this case

$T\#$ = telescope $f\#/\sqrt{Tr}$

and where: Tr = multiple of all losses including mirror reflectivities, the beamsplitter losses, and the obscuration loss.

The filter width and filter transmission values must also be factored in to obtain the net power presented to the sensor. Table 2-4 shows the step by step values and the final results. Table 2-5 shows the results for the 65-cm aperture telescope and those anticipated from the future 1.5-meter aperture telescope. These values will then serve as the basis for all power considerations required throughout the document. Although these do not represent final values, they are the latest available estimates and should be accurate enough to make a fair evaluation of the EIS problem.

TABLE 2-4
SELECTED IRRADIANCE COMPUTATIONS

Name	Units	Symbol	Ultraviolet 2200Å	Visible Minimum 4045.8Å	Visible Maximum 5500Å	Hα 6562.8Å
Radiance	$W \cdot Sr^{-1} \cdot \AA^{-1} \cdot m^{-2}$	N	1.41×10^{2}	7.8×10^{1}	3.25×10^{3}	3.9×10^{2}
f#	none		50	50	50	50
(1-Obscuration)	none		0.8	0.8	0.8	0.8
Mirror	none		0.75^{4}	0.85^{4}	0.9^{4}	0.9^{4}
Beamsplitter	none		0.9	0.85x0.90x0.95	0.85x0.90x0.95	0.85x0.90
Net Transmission	none	Tr	0.204	0.302	0.380	0.400
Spectral	none	T#	111	91	81	79
Irradiance	$W \cdot \AA^{-1} \cdot m^{-2}$	H	9.03×10^{-3}	7.4×10^{-3}	3.9×10^{-1}	4.94×10^{-2}
Filter Width	A		100	0.125	0.25	0.50
Filter Transmission	none		0.15	0.05	0.05	0.10
Net Irradiance	$W \cdot M^{-2}$		1.36×10^{-1}	4.62×10^{-5}	4.86×10^{-3}	2.46×10^{-3}

72-0089-T26

TABLE 2-5

NET ENERGY TO PHOTOHELIOGRAPH SENSORS

	65 cm	1.5 Meter
Hydrogen Alpha	2.5×10^{-3} w/m^2	5.6×10^{-3} w/m^2
Ultraviolet	1.4×10^{-1}	3.2×10^{-1}
Visible Continuum	4.9×10^{-3}	1.1×10^{-2}
Visible Minimum	4.6×10^{-5}	1.0×10^{-4}

3. ENVIRONMENT

The photoheliograph and the EIS performance are both dependent on the environment in which they operate. This section describes the more important considerations and the constraints which are placed upon the operating ability of the system.

3.1 VEHICLE CONSIDERATIONS

3.1.1 Types of Vehicles

The photoheliograph is not presently programmed for a specific mission. However, the 65-centimeter version was designed to be contained in the Apollo Telescope Mount (ATM) "B" model. Considerable planning has been done with the ATM attached to a Skylab-B which is not greatly different from the "A" mission. Therefore, a considerable amount of analysis is available to predict how the 65-centimeter photoheliograph would perform on the Skylab/ATM "B". This mission, as defined in reference 9 is used as the baseline for the remainder of this section.

Other projected missions for present and larger photoheliographs are the ATM-B on the Space Shuttle, a sortie vehicle mated with space shuttle, and the Research Applications Module (RAM). For nearer term missions, both an advanced OSO and a stratospheric balloon have been suggested as possible vehicles for the 65-centimeter photoheliograph.

For any vehicle, three characteristics strongly influence the Photoheliograph and the EIS: vehicle stability; onboard data handling capability; and form factor (size, weight, and volume) alloted for the experiment.

The Skylab B/ATM-B mission has been defined sufficiently to estimate these values and will be used as a baseline to establish the constraints placed on the experiment by the spacecraft.

3.1.2 Stability

Initially, the value used in the photoheliograph system definition was the jitter value of $\pm$ 1 arc second/second as defined in references 3 and 4.

This particular requirement has been modified and replaced with the long-term stability requirements of tables 3-1 and 3-2 which are excerpted from reference 10. These latter values only show the extremes and do not consider higher order motions within the extremes. Recent information, reference 15, indicates that no major changes have occurred in the design of the stability system of either the Skylab or the ATM. Furthermore, although the jitter rate is no longer a system requirement, the ± 1 arc-sec/sec value is still obtained from computer simulations.

TABLE 3-1
SKYLAB B CONTROL SYSTEM REQUIREMENTS

System Axis	Command Pointing Uncertainty	Stability for 15 minutes
X (pitch)	± 4 arc-min	± 9 arc-min
Y (yaw)	± 4	± 9
Z (roll)	± 10	± 7.5

TABLE 3-2
ATM-B CONTROL SYSTEM REQUIREMENTS

System Axis	Command Pointing Uncertainty	Stability for 15 minutes
X (pitch)	± 2.5 arc-sec	± 2.5 arc-sec
Y (yaw)	± 2.5 arc-sec	± 2.5 arc-sec
Z (roll)	± 10 arc-min	± 7.5 arc-min

Figure 3-1 shows the effect on the photoheliograph's limiting resolution versus the spacecraft stability. It is obvious that, if the old jitter requirement is real, exposures of tens of milliseconds are required to maintain resolution. On the other hand, if the 15-minute stability value can be scaled linearly, exposures of more than 1 second can be obtained without resolution degradation. However there will be higher frequency and

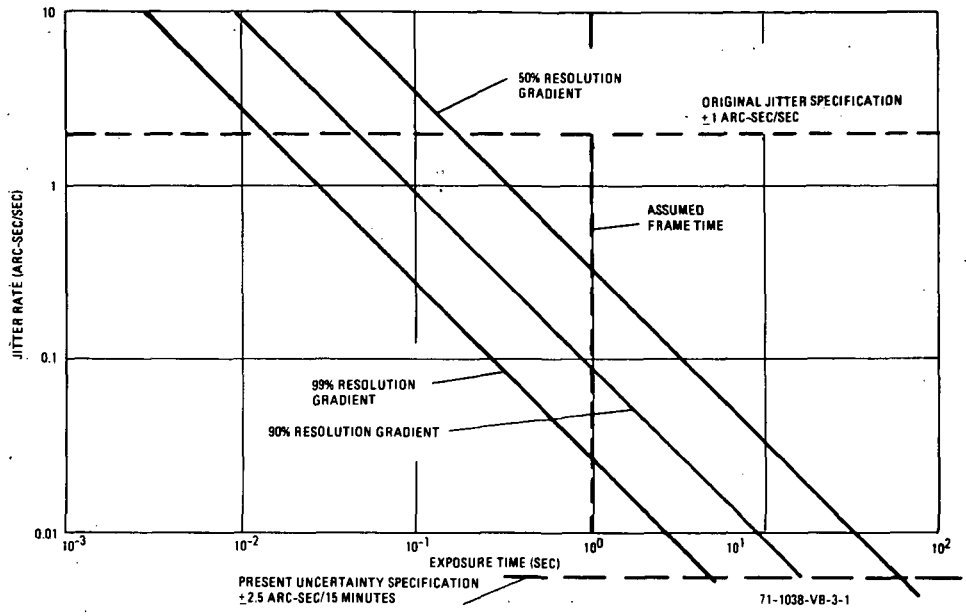

Figure 3-1. Spacecraft Jitter Rate Versus Exposure Time for a Given Resolution Loss

amplitude values of jitter regardless of the ability to predict the value, and true values will not be obtained until the results of ATM-A are analyzed. Therefore, a television system capable of utilizing the spacial resolution capabilities of the photoheliograph must either incorporate a variable exposure time or assume additional image motion compensation (IMC) within the photoheliograph itself.

Schemes to provide IMC within the photoheliograph are under active consideration. These systems would provide sufficient stability to allow exposure times up to the limit set by the frame recycle time required by the solar motion. However, all work is of a conceptual nature, and there is no plan to proceed with a feasibility model to demonstrate characteristics. Therefore, the EIS study must consider the possibility that IMC will not be available (at least for the first launch). In that case, the study must be conducted for both an IMC photoheliograph and a non-IMC photoheliograph.

Figure 3-2 shows the effects of spacecraft stability on both the 65-cm and 1.5-meter photoliographs in a form that can select an exposure time to

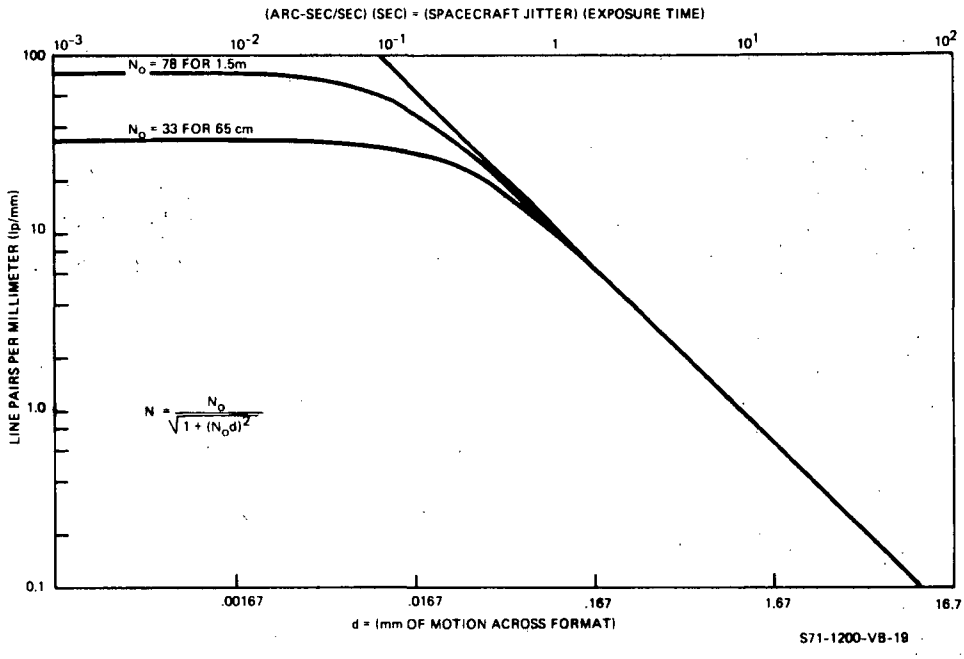

Figure 3-2. Effects of Stability on Limiting Resolution

to provide a particular resolution limit for a given spacecraft jitter rate. Here again, it is obvious that jitter rates of $\pm$ 1 arc-sec/sec must be compensated by exposure times of 10^{-1} or 10^{-2} to prevent serious loss of resolution.

A more important value is the effect of the spacecraft motion on the photoheliograph's modulation transfer function (MTF). Figure 3-3 shows this effect as the motion normal to the photoheliograph pointing axis causes a shift of one line pair at the limiting resolution (see reference 16 for full explanation). The square wave target has a more severe effect than a sine-wave target, but the square wave target will be used to determine figures 3-4 and 3-5 for ease of calculation. Both figures show the loss in MTF for values of the abscissa of figure 3-2. For the 65-cm photoheliograph, a value of X = 0.1 causes a reduction of MTF at every point but still has a finite value at the diffraction limit of the telescope. X = 0.1 for the 1.5-meter telescope seriously reduces the MTF, and X = 1.0 is unacceptable for both.

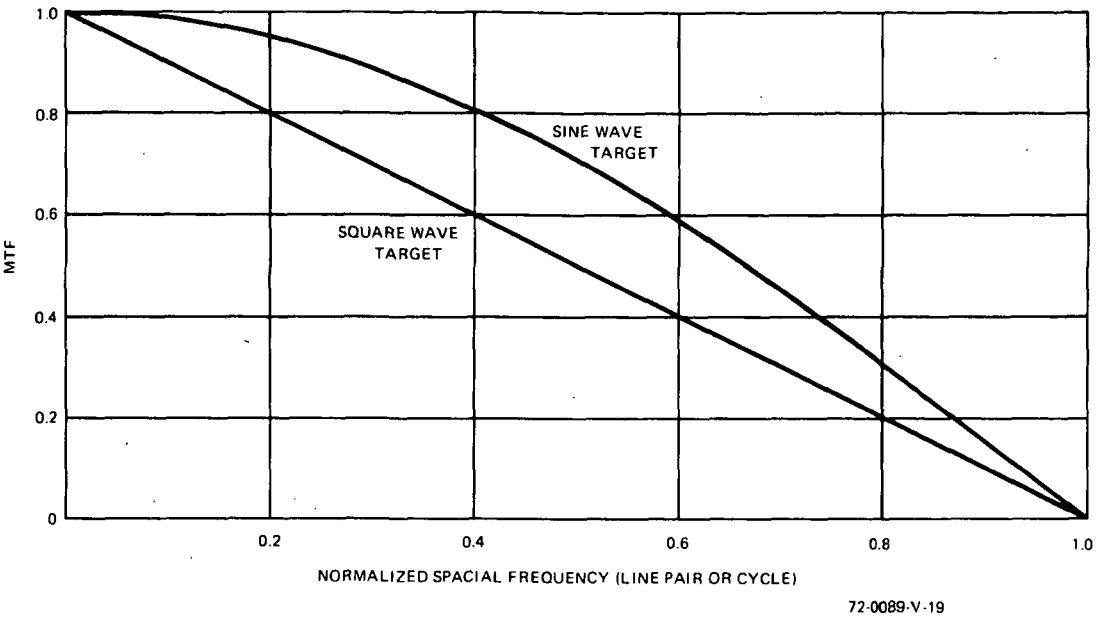

Figure 3-3. Loss in MTF Due to Motion of Target Relative to Sensor

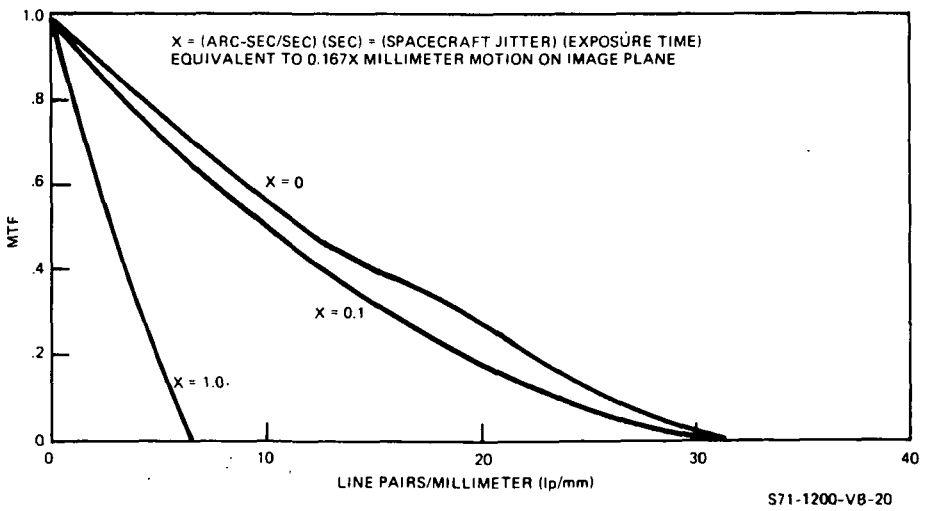

Figure 3-4. Effects of Lateral Motion on MTF of a 65-cm Photoheliograph

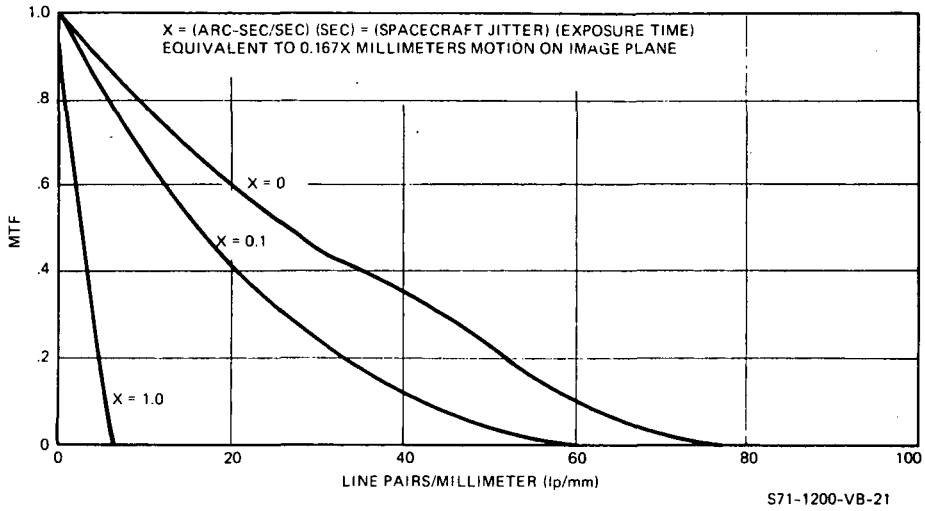

Figure 3-5. Effects of Lateral Motion on MTF of a 1.5-Meter Photoheliograph (f/22, 0.2 Central Obscuration)

The conclusion is that stability is of utmost importance to the successful outcome of the photoheliograph program and that short exposure times by a sensitive EIS offer a necessary and satisfactory solution.

3.1.3 Data Handling

3.1.3.1 Overall Description

A block diagram showing the major parts of the data handling subsystem is presented in figure 3-6. There are three ways of handling the data:

- Convert the sensor video to digital signals, process, store, and transmit digitally.
- Record the sensor video directly as an analog signal then convert to digital on playback for the downlink.
- Record, playback, and transmit analog video signals.

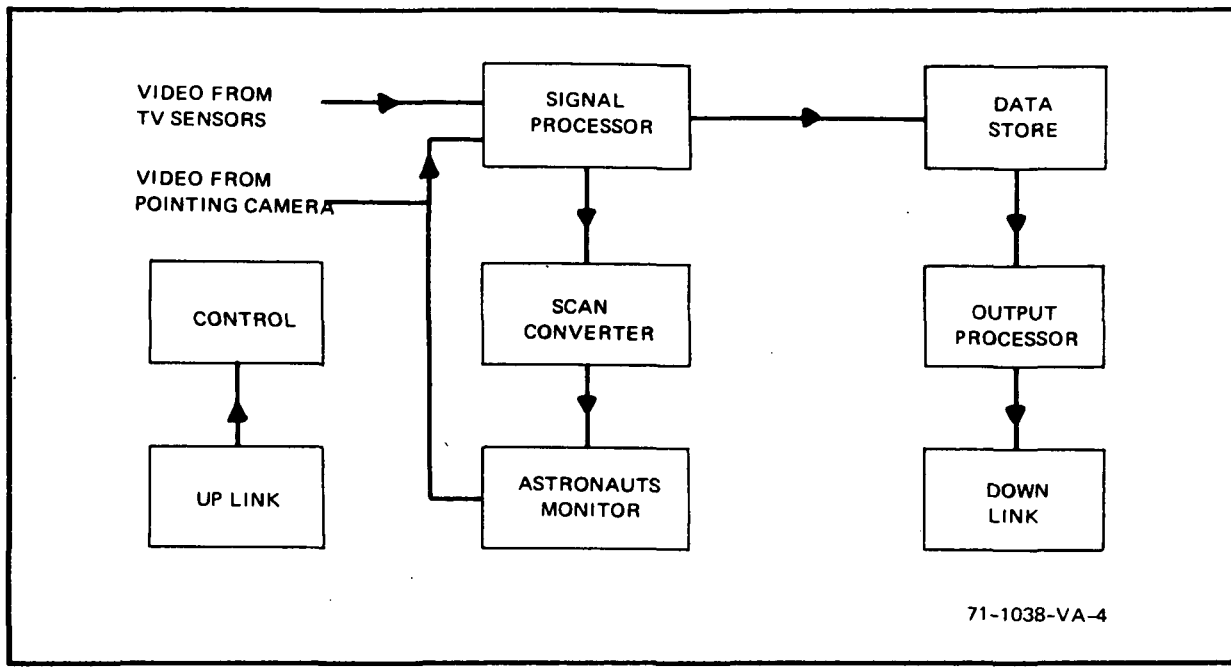

Figure 3-6. Data Handling Subsystem

Although each of the parts of the data handling subsystem may be significantly different in each of the above combinations, a short description of each block in figure 3-6 will be given.

a. Signal Processor

This unit serves as the buffer between the incoming video signals and the video storage unit. In an all analog system, this unit may be a small part of the tape recorder, but in an all-digital approach utilizing bandwidth reduction techniques, this unit would be larger than all the rest of the data handling units.

b. Data Store

The data store will most likely be either an analog or digital tape recorder and will be a critical component of the system. At present, no unit has the capacity to handle the worst-case information output of the TV sensors.

c. Output Processor

This unit is the interface between the data store and the downlink.

d. Downlink

The downlink, a basic unit of the spacecraft, allows transfer of the data from the data handling subsystem to ground stations. Although not a part of the photoheliograph, the downlink parameters represent a set of limits on the data handling subsystem.

e. Scan Converter and Astronaut's Monitor

Besides viewing the output from the pointing camera, the astronauts require some views of the FOV of the photoheliograph's three sensors. Since the onboard monitors and the pointing camera are set to work at the standard 525-line, 2 to 1 interlace, 30-frame-per-second rate, some form of scan converter is necessary. A simple way of accomplishing this task would be to furnish a separate monitor utilizing a direct view storage tube (DVST) with some overscanning capability. This would allow viewing of the slow-scan sensors with little degradation at a fraction of the complexity of any type of scan converter.

3.1.3.2 Spacecraft Data Storage

For a 1-second frame time, 1,500-scan-line-per-frame system with approximately equal horizontal and vertical resolution (1,350 TV lines), the required bandwidth is 1100 kHz. The bandwidth can be sharply limited by an appropriate filter to the required value without losing any information.

If the signal is digitized, the sampling rate is twice the above bandwidth, and the total bit rate depends upon the number of bits used for amplitude information. Including the quantizing noise due to digitizing, the incoming analog sensor signal is equal to one-half the rms random noise level in the incoming signal. Table 3-3 gives the maximum signal-to-noise ratio that can be obtained by the given number of bits.

The number of bits used in table 3-3 does not include any provision for synchronizing signals placed outside the amplitude limits of the video in order to minimize the memory capacity required by the system. For the expected video signals, 5 bits of quantizing are not adequate and 6 bits are

TABLE 3-3
BIT VERSUS S/N RATIO

Number of bits	S/N Ratio	S/N Ratio (dB)
3	14	23
4	28	29
5	56	35
6	110	41
7	220	47
8	440	53

barely adequate. Therefore, 7 bits will be used in all digital considerations. The bit rate, therefore, is 13×10^6 per second.

For the same selection of parameters, an analog recorder or memory would require a 1100 kHz input bandwidth.

Table 3-4 illustrates the best available space-qualified tape recorders. Obviously, digital recorders do not have the available input rates for the baseline system and cannot be used. Analog versions of the digital recorders are uncommon, Odetics has the only active development contract. The unit is an FM system, having a response of dc to 60 kHz and is considered developmental. Analog recorders are limited to the two RCA units and are considerably more complex. Also, they are not standard or off-the-shelf recorders. The SH series are all engineering or developmental models and no production units have been made. The ERTS recorder is presently nearing completion of the development verification phase, and the prototype will be entering qualification shortly.

This recorder, if modified to store 110 minutes of 1100-kHz information and to playback at 4 to 5 MHz, should be compatible with the input rates considered likely from reference 6 and also with the downlink discussed in paragraph 3.1.4.

There are several types of data storage besides tape recorders which are developmental or require excessive power and volume for the 10^{10} to 10^{12} bits storage required. Table 3-5 is a comparison of the costs, power, and volume for various memory devices and conclusively shows the advantage of magnetic tape recorders in the reasonable future for large-capacity storage.

TABLE 3-4

TAPE RECORDERS FOR SPACEBORNE APPLICATIONS

MODEL	SIZE (IN)	WEIGHT (LB)	TAPE SPEED (IN/SEC)	POWER (W)	BIT CAPACITY	RECORDING TIME (MIN)	BANDWIDTH	COST ($)
LEACH SERIES 2000	7.6x7.1x5.3 290 $in.^3$	10 to 15	0.1 to 100	5 to 25	$1.4x10^8$ per track 7 tracks max.	12 at max BW	100KB/sec max record 200KB/sec max reproduce	25-50K
ODETICS SESP-71-2	9x12x5.5 600 $in.^3$	16	1 or 4 record 8 re-produce	20	$2.14x10^8$ per track $1.5x10^9$ total 7 tracks	100 high BW 400 low BW	64KB/sec or 256KB/sec record 512KB/sec reproduce	50K
ECHO SCIENCE LS-2	9x10.5x6 570 $in.^3$	12	3.6 record 19.1 re-produce	22	$1.93x10^8$ total 5 tracks	67, repro-duce time 11.5	48KB/sec record 256KB/sec reproduce	50K
RCA SH-HL-2	11x15x6 1000 $in.^3$	30	2.5 or 10	65	Analog Helical Scan	60 High BW 480 low BW	4MHz or 0.5 MHz	100K
RCA ERTS VTR	Transport 21.5x15x6.5 Electronics 16.8x16x7 3900 $in.^3$ total	74	12	280 Peak 88 Steady	Analog Transverse Scan	30 at 4 MHz or 110 at 1100 kHz	4MHz	250K

71-1038-T-5-1

TABLE 3-5

COMPARISON OF MEMORY DEVICES

	COST PER BIT (CENTS) (MIL VERSIONS)		PRESENT CHARACTERISTICS (PER MEGABIT)	
	CURRENT	1976 PROJECTED	POWER (WATTS)	VOLUME (IN^3)
BIPOLAR RANDOM ACCESS MEMORY (RAM)	10	1.2	2.500	1,000
HYBRID BIPOLAR RAM	5	0.5	350	300
FULLY DECODED MOS RAM	1.8	0.4	50	50
BIPOLAR SHIFT REGISTER (SR)	100	50	1,100	1,000
STATIC MOS SR	2.4	0.6	7	100
DYNAMIC MOS SR	0.8	0.2	3.3	40
MAGNETIC CORE	8	4	750	1,500
MAGNETIC WIRE	14	6	310	1,600
MAGNETIC DRUM	0.9	0.7	--	130
MAGNETIC BUBBLE	--	0.001 (~1980)	--	--
MAGNETO-ACOUSTIC	--	0.2 (~1980)	--	--
CHARGED COUPLED DEVICES	--	0.1 (~1980)	--	--
SPACE TAPE RECORDERS	0.005	0.004	0.025	0.3

72-0089-T-18

3.1.4 Data Link for Solar Astronomy

3.1.4.1 General

In the photoheliograph experiment, video tape recordings will be made of the pictures during the orbit. It is necessary that suitable data link equipment be available to send this information to ground stations for analysis.

The capability of such a data link depends on numerous factors such as the number of resolution elements per picture, the frame rate, recording time per orbit, time sharing of experiments on same data link, percentage of data to be transmitted, number and location of ground stations suitably equipped, and total time in view of the receiving antennas. Some of these are subjected to tradeoff considerations.

Because of the great expenses involved in establishing, equipping, and operating satellite tracking stations, it is unrealistic to consider new sites. Fortunately, an ample variety is available from the Manned Space Flight Network (MSFN) and the Space Tracking and Data Acquisition Network (STADAN). It is appropriate to review the existing capabilities of these facilities for handling relatively wide-band video signals and to ascertain any known plans for future improvements. This information may then be used for guidance in planning.

3.1.4.2 Spacecraft Data Handling

Section 2 defined certain requirements for the photoheliograph as if it were an independent vehicle. However, considerable planning has been done to provide an integrated spacecraft concept mating the photoheliograph with the ATM-B (reference 9). The following information gives a representative set of conditions for overall photoheliograph operation.

The data and communication systems in Skylab B are changed considerably from the Skylab A systems. The two PCM and VHF/UHF transmission systems in the AM and ATM are replaced with one central PCM system and S-band transmitters located in the AM. A Skylab communication terminal is added to the OWS to provide real-time voice, uplink commands, and downlink data monitoring.

The baseline system includes capability for transmission of the solar astronomy video data and a portion of the earth resource data. The main method of data retrieval for earth resources is the return of data tapes in the CSM.

The overall block diagram of figure 3-7 illustrates the anticipated system. The video switch chooses between television from either the OWS or the CSM and the video from solar astronomy. This data can then be stored in the video recorders or sent directly to the pre-mod processor for real-time telemetry.

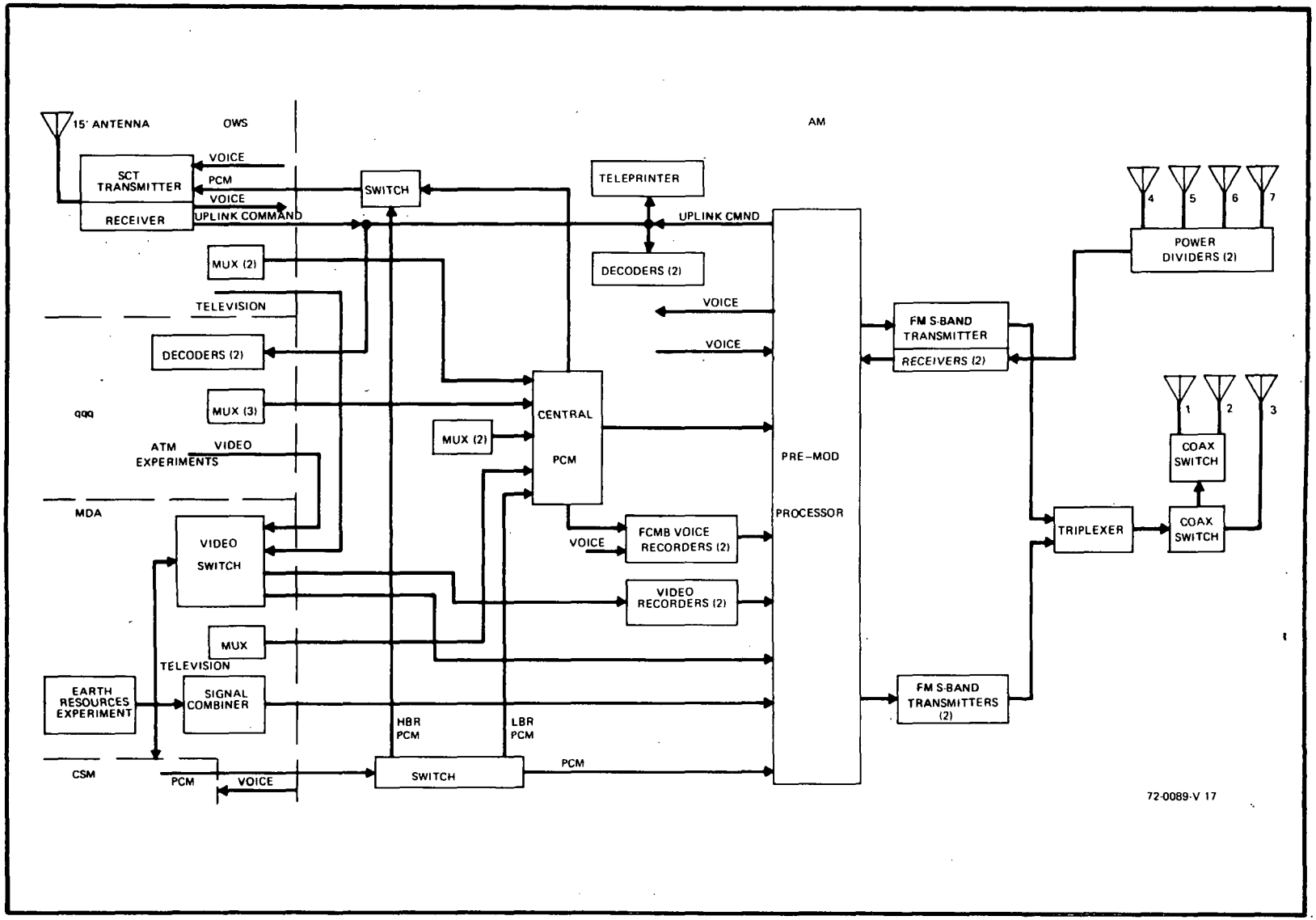

Figure 3-7. Skylab B/ATM B Overall Data Handling Block Diagram

An onboard programmer for the photoheliograph programs the output of the 5 cameras to two channels provided for recording. The two video channels of 1.6 MHz each are recorded on separate channels with a 90-minute record capability and a 30-minute playback at 4.8 MHz. Some of the recorder capacity may be shared with a portable, handheld commercial format imaging system from the OA, but it is likely that most of this video will be transmitted in real-time and at times other than those when the astronauts would be involved in a solar astronomy experiment.

Finally, as a data link, there are two FM S-band transmitters which can provide any two of the following:

- *Video recorder No. 1 up to 5 MHz*
- Video recorder No. 2 up to 5 MHz
- Earth resources data up to 5 MBPS
- TV from OA up to 5 MHz
- Real-time video from solar astronomy up to 5 MHz.

The total transmission time available will depend on the number of tracking sites and the acceptable limits of signal to noise as determined by transmitter power and antenna gain plus receiver antenna gain. The percentage of time within the maximum limit will be determined by NASA mission planning for the particular mission.

3.1.4.3 Capabilities of Existing Ground Stations

3.1.4.3.1 Manned Space Flight Network (MSN). - The Apollo Unified S-band System, used by the Manned Space Flight Network, utilizes two carriers simultaneously. One of these is phase modulated and the other is frequency modulated. The PM carrier, at 2287.5 MHz, is modulated with the range code, telemetry on a 1.024-MHz subcarrier and voice on a 1.25-MHz subcarrier. Alternate provisions are made for emergency voice and key. The FM carrier at 2272.5 MHz is modulated with the TV signal. Alternate arrangements are available for handling voice and telemetry on this carrier.

The original provisions for television were for an analog signal having a basic picture format of 10 frames per second, 320 lines per frame with an aspect ratio of 4:3. The resolution was further limited by 500-kHz base and low-pass filtering.

At the ground receiver, the FM signal from the antenna is amplified by a low-noise preamplifier, the predetection bandwidth is selected from filters with 1- and 4-MHz noise bandwidth, further amplified, limited, and amplified again to give a level of -10 dBm at 50 MHz. An output is available at this point.

Normally, this signal is converted to a 120-MHz IF and is introduced to the carrier frequency demodulator. The television signal is completely demodulated in the first modulation tracking loop. The baseband television signal is routed through a low-pass filter to the video output.

The system was modified to provide a 2-MHz bandwidth instead of the original 500 kHz in order to accommodate color television for Apollo.

Plans for Skylab B called for new carrier demodulators capable of handling either 15-MBPS data or high resolution TV up to 20-MHz RF bandwidth at the Texas/NTTF sites. It is now planned that this will be implemented to handle the need of the Earth Resources Technology Satellite (ERTS). The TV base bandwidth that can be handled depends on the modulation index employed. If, as an estimate, the index were 1 Carson's rule, it would indicate a 5-MHz base bandwidth capability.

The Manned Space Flight Network includes three stations having 85-foot-diameter antennas: Goldstone, Canberra, and Madrid. The other stations have 30-foot-diameter antennas and are located at Carnarvon, Bermuda, Corpus Christi, Cape Kennedy, Guymas, Hawaii, Guam, Ascension, Canary Islands, Grand Bahama, Antigua, and 3 ships.

3.1.4.3.2 Space Tracking and Data Acquisition Network (STADAN). - Several of the ground stations of the STADAN network that are used for the Applications Technology Satellite (ATS) program have capability for receiving relatively wide-band television signals. These stations are at Rosman, North Carolina; Mojave-Barstow, California; and a transportable station intended for Cooby Creek, Australia. There is an 85-foot antenna at Rosman having a gain of 57.5 dB. The others have 40-foot antennas with gains of 50.8 dB.

These stations use a low-noise preamplifier having a 25°K noise temperature, 30-dB gain, and a 200-MHz RF bandwidth (4.0 to 4.2 GHz). The overall system noise temperature of the 4-GHz receiving subsystem, including antenna, ground and galactic noise, is 60°K at zenith.

The frequency down converter accepts a 4-GHz FM or PM RF carrier and converts it to a 70-MHz IF signal. The IF amplifier discriminator unit filters, amplifies, and demodulates the FM and PM signals. First, the unit filters the IF signal with a 30-MHz bandwidth filter. The output goes to a baseband amplifier which has a passband < 10 Hz to > 10 MHz. The signal is then split into two equal parts. One is filtered with a 4-MHz low-pass filter to provide 1.0 Vp-p into 75 ohms for TV. The other is filtered with a 400-Hz bandpass filter for 4.5-, 6.0-, or 7.5-MHz subcarriers.

3.1.4.4 Recommendations for Solar Astronomy Data Link

Existing ground stations have the capability for acquiring and tracking the spacecraft signals. They also have the additional communications facilities for commands, voice, and telemetry links that might be required for either manned or unmanned spacecraft. The stations are spaced around the globe and are tied together by extensive communications networks. Practical and economic considerations strongly dictate that these stations are used for programs such as the one under consideration here.

The existing MSFN communication facilities, as used with Apollo, provide for a 2-MHz television baseband. This is less than desired for the solar astronomy experiments. It is expected that this network will be modified to provide a 5-MHz bandwidth for ERTS and solar astronomy.

The analysis of Skylab B data recovery considers a 4-site network and utilizes 2-degree contact data. A 4-site network is considered for wide-band data and permits minimum modification. Only 15 orbits were analyzed since a closely repetitive pattern is established after 15 orbits and takes approximately 1 day. The MSFN 85-foot antenna sites are included only where a unique advantage is gained by doing so. Data recovery of the Skylab B scientific data is assumed to occur in the following manner: Solar astronomy and earth resources are not performed simultaneously. Capability will be provided for a high data rate for 4 consecutive orbits per day, with a maximum of 45 minutes recorded data per orbit. This requires 15 minutes of dump time. The other orbits during the day provide less capability for data dump time. The repetitive pattern is shown in table 3-6. It is apparent that the TEX/NTTF sites can come close to handling the desired 15 minutes of data readout on orbits 14, 15, 1, 2 (which are consecutive). Additional

TABLE 3-6

SKYLAB TRACKING DATA 4 SITES NETWORK

Orbit	TEX/NTTF	MAD	AGO	Assumed Experiment Telemetry Activity	Total Time Available Per Orbit (Minutes)
1	15.4	9.4	-	SA	24.8
2	12.3	10.2	-	SA	22.5
3	8.9	8.2	-	-	17.1
4	10.2	-	-	ER	10.2
5	10.2	-	-	ER	10.2
6	9.9	-	7.3	ER	17.2
7	-	-	10.1	-	10.1
8	-	-	7.9	-	7.9
9	-	-	4.6	-	4.6
10	-	-	6.6	-	6.6
11	-	-	9.7	-	9.7
12	-	9.2	9.2	-	18.4
13	-	10.1	-	-	10.1
14	13.4	9.1	-	SA	22.5
15	15.5	9.2	-	SA	24.7

SA = Solar Astronomy ER = Earth Resources

S71-1200-VA-8

time could be had by using the other stations and/or additional orbits. The plans assumed that the following MSFN equipment capabilities would be operational.

a. All stations (Unified S-Band System)

(1) Feed System - linear 2200 to 2300 MHz

(2) 4 wide-band receivers, FM or PM

(3) 30-MHz IF bandwidth

b. TEX and NTFF

New carrier demodulators capable of handling either 15-MBPS data or high-resolution TV up to 20-MHz RF bandwidth (5-MHz video). Other sites are limited to 4.5-MHz filtered or 10 MHz-unfiltered RF bandwidths (1.1- or 2.5-MHz video). Alternately, the existing 4-MHz video capability of the three STADAN stations could be considered.

Data received at the ground stations will be stored on magnetic tape for later analysis by the Principal Investigator. Stations should also have

certain real-time data link with a central location. The planned recorder configuration is as follows.

a. All Stations

(1) 1 each VR - 660 (dual recorders at 85-foot sites). Wide-band video tape recorders (30 Hz to 4.2 MHz) - 1 channel.

(2) 1 each Model FR - 1900 14 track data recorders (400 Hz to 2 MHz)

b. TEX and NFTF

1 each ERTS Recorder (0 to 19 MHz)

It seems appropriate to consider the data link capabilities described above as the most likely to be available and, therefore, to use these parameters as constraints in defining the solar astronomy data subsystem.

4. SENSOR EVALUATION

4.1 INTRODUCTION

At the start of the study, most known photosensitive devices were considered. For completeness, these devices and their problems will be mentioned.

The first devices considered and discarded were line arrays and point source detectors. In both cases, the spacecraft stability and the frame rate required would necessitate a mechanical scanner faster than the present state of the art. Furthermore, if an electronic beam scanner would be placed in front of either a line array or point source, it is the equivalent of sensors which are considered. Basically, either are useful only if at least one axis of scan is provided by the vehicle motion.

The solid-state square array eliminates most of the aforementioned problems but is still only as sensitive as a silicon diode vidicon, and development has not achieved the resolution or the uniformity of a silicon diode vidicon.

Thus, the primary candidate sensors for this study fall in the broad category of vacuum tube, deflected electron beam sensors. This is still a broad definition to choose the optimum device for the photoheliograph experiment. The more likely candidates will be discussed individually, and others with marginal applicability will be grouped together. To allow direct comparison between sensors, the following list of constraints and definitions will be used wherever possible. Several changes resulting since the interim report reflect a more detailed picture of the EIS.

a. The 21-by21-millimeter square active format defined for the photoheliograph will be used.

b. All resolution curves will be in 1p/mm at the optimum operating point. If the sensor has multiple imaging elements, a magnification of unity will be used unless another value is theoretically fixed.

c. The input sensitivity of each sensor will be described in terms of $W \cdot m^{-2}$ for monochromatic light at several wavelengths within the range of the photoheliograph.

d. Each sensor's photoresponse will be mA/watt so that the sensitivity in item c can readily be scaled to any other wavelength or filter width.

e. The television characteristics are chosen as ones which can reasonably adhere to the requirements of the photoheliograph mission. If changes do occur they should not be so extensive that results cannot be scaled.

(1) Frame time = 1 second - This is sufficiently fast to allow successive frames within the expected scene movement time while allowing a reasonable exposure time.

(2) Line number = 1,500 TV lines - This represents the 1,300-TV line photoheliograph resolution times the Kell factor.

(3) Video bandwidth = 1100 kHz - This value provides sufficient pixels to utilize the photoheliograph diffraction limit while minimizing recorder storage requirements and maximizing signal to noise.

f. The signal-to-noise ratio described for each sensor is based on optimized sensor operation within the television constraints previously listed. Depending on the sensor, the limiting noise element may be the sensor itself or the video amplifier.

g. Exposure Time - Continuous exposure for the 1-second frame rate is assumed. If the sensor is a charge storage type, the effects of shorter exposure times may be scaled. Nonintegrating sensors such as the image dissector require continuous exposure.

4.2 GENERAL COMPARISON

No single sensor is presently available which can fully meet the present and future photoheliograph requirements. The sensors that are considered in this report can be put into three general classifications.

a. Those sensors which are satisfactory in resolution but are lacking in one or more areas such as sensitivity, signal-to-noise ratio, reliability, electronic complexity, or frame time capability.

b. Those sensors which are satisfactory in sensitivity and most of the others in item a but lacking in resolution.

c. Those sensors which are not optimum in either category a or b but represent a compromise.

Typically, the return beam vidicon (RBV) and the image dissector (ID) fall in category a. The intensified silicon sensor (ISS), the image isocon (II), and the secondary electron conduction (SEC) sensors fall in category b. The standard vidicon (V), silicon vidicon (SV), focus projection and scanning (FPS) vidicon, and intensified vidicon (IV) fall in the third category. Each of the sensors considered are compared in each important parameter in the following paragraphs.

Two other sensors considered but not discussed in this study are the image orthicon and the plumbicon. The first is similar to the image isocon but inferior in sensitivity, resolution, and signal-to-noise ratio. The second is a special form of vidicon optimized for unity gamma and a spectral response near the human eye. One other sensor, the optechon or grating storage tube, potentially has the resolution plus some other characteristics necessary for the photoheliograph program, but it was not included because of its high developmental risk.

Some but not all of the sensors used for evaluation are listed below:

V	Westinghouse WX5160 and GEC 1311-001	Vidicon
SV	Amperex S10XQA and RCA C23136	Silicon Vidicon
II	RCA C21095C	Image Isocon
ID	ITT F4052	Image Dissector
RBV	RCA C23084C	Return Beam Vidicon
FPS	GE Z7940	Focus Projection and Scanning
SEC	Westinghouse WL30654	Secondary Electron Conduction
ISS	Westinghouse WX31841 and RCA C21117C	Intensified Silicon Sensor
I	Westinghouse WX31787 and RCA C33020	Intensifier (only)

4.3 SENSITIVITY

Sensitivity is one figure of merit for an electronic imaging sensor. Typically, this value is described in terms of the sensor's response to a broadband source of light such as a 2,854°K tungsten light. Until recently, photometric units such as footcandles (lumens/foot^2) or footlamberts were commonly used. These units represent a convolution integration between the illumination of a 2,042°K blackbody, the sensor's spectral response, and the eye's spectral response. Thus, if the sensor has sensitivity beyond either the eye's or the illumination's response, it would not be shown in the result. Furthermore, a solar blind ultraviolet photocathode would, by this definition, have zero sensitivity. The radiometric definition removes the eye's response from the integration and is defined by the actual watts per square meter on the sensor. If the illumination spectral output in watts per unit wavelength and the sensor's response in microamperes photocurrent per watt per unit wavelength are given, then the resulting sensitivity can be scaled to any monochromatic wavelength of interest.

Once the sensor is described in radiometric terms on a "signal current out" for "illumination input" curve, the absolute internal gain can be calculated. The same curve also gives the saturation value of the sensor which is representative of the total storage capability of the sensor target (or the safe photocurrent which can be drawn from the photocathode for non-integrating sensors such as the image dissector).

Using these three values, the saturation current, the internal current gain, and the photoresponse in amperes per watt per unit area illumination, the sensitivity of any sensor can be computed for any illumination and at any frame time, exposure time, and sensor size. The results, shown in figures 4-1 through 4-6, are derived for the photoheliograph program using the television parameters of paragraph 4.1 and the net illumination to the sensor from table 2-4. Sensors must be compared on each curve since the spectral sensitivity of the sensors differs considerably. The first and last curves are the fixed frequency cameras at 2200Å in the ultraviolet and at 6563Å for the Hydrogen Alpha camera. The remaining four curves are two Fraunhofer lines and two places on the continuum for the tunable filter camera. The 4046Å line is the least illumination level within the range of the photoheliograph.

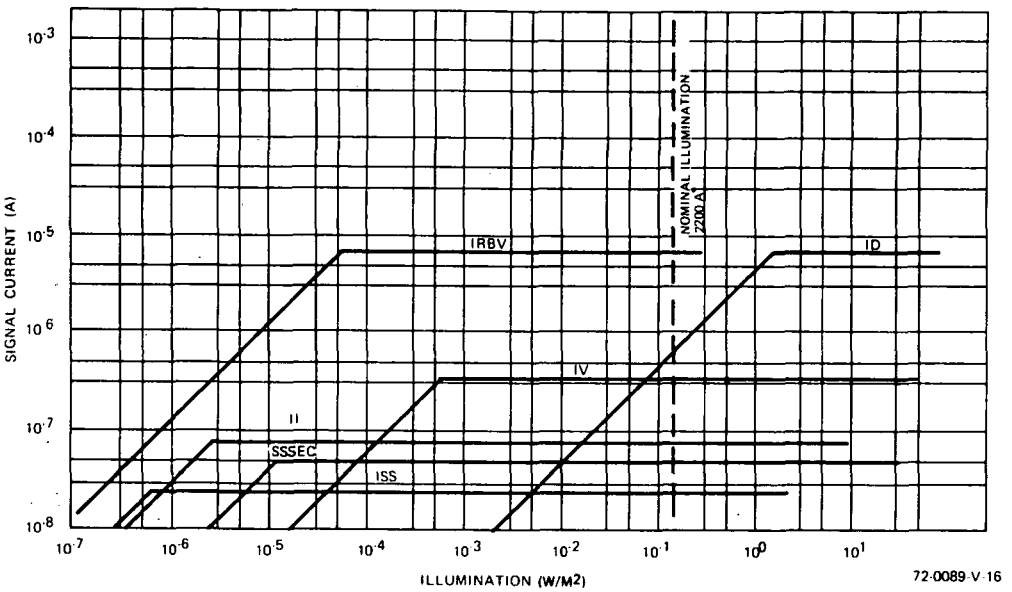

Figure 4-1. EIS Sensitivity to Ultraviolet at 2200 Å

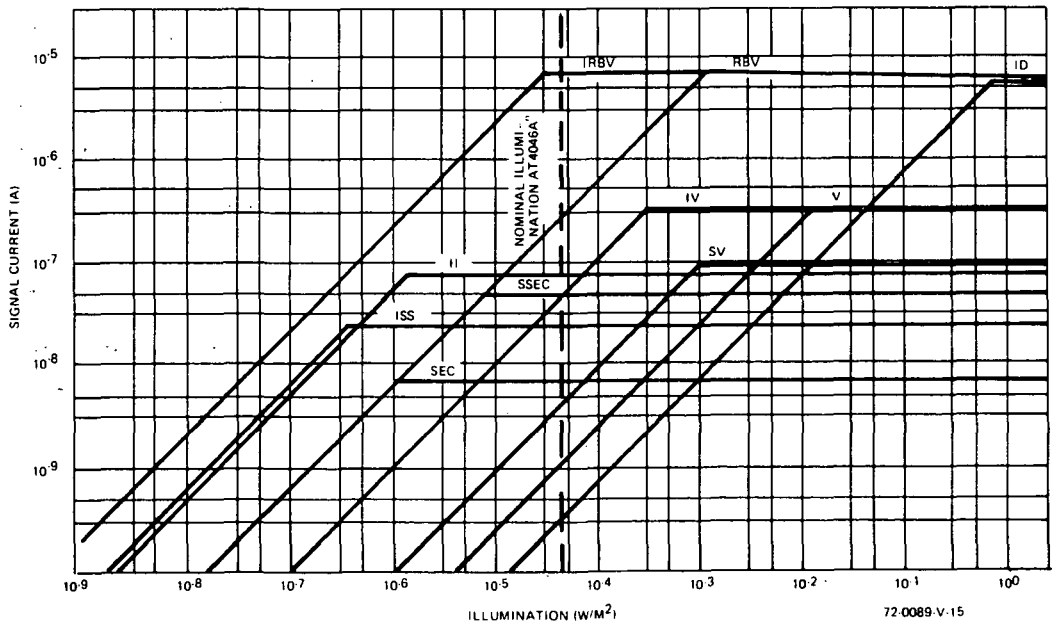

Figure 4-2. EIS Sensitivity to Minimum Visible at 2046 Å

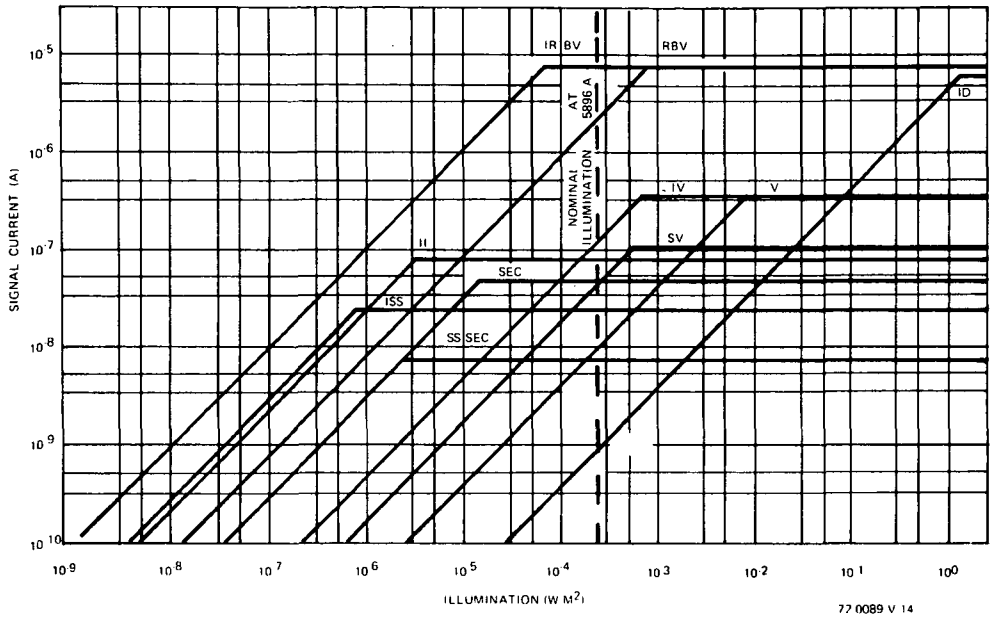

Figure 4-3. EIS Sensitivity to Visible at 5896 Å

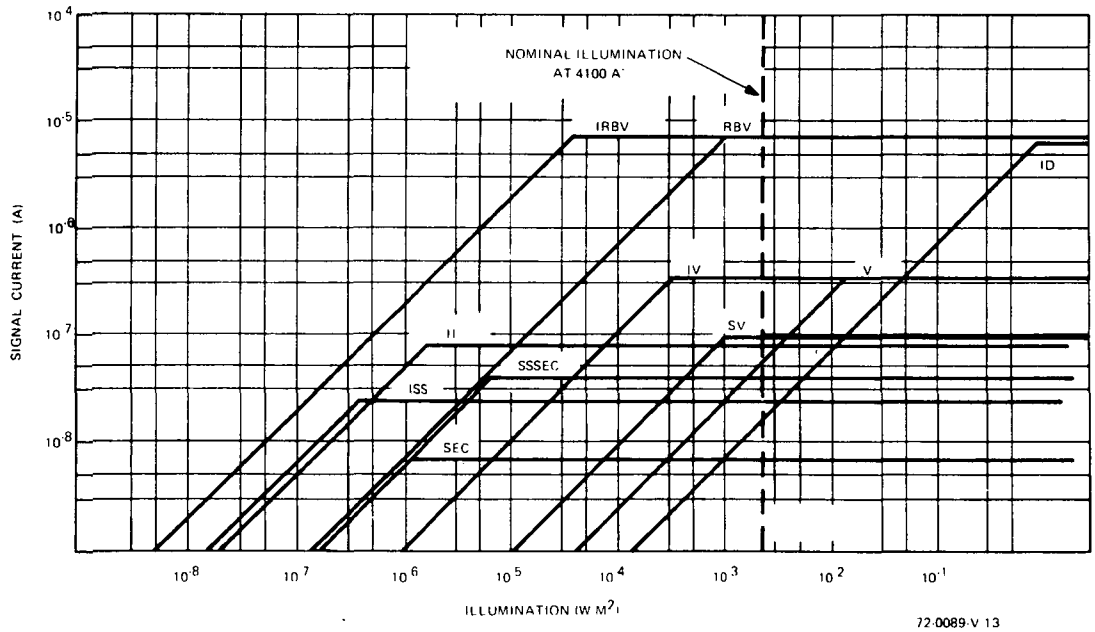

Figure 4-4. EIS Sensitivity to Visible Continuum at 4100 Å

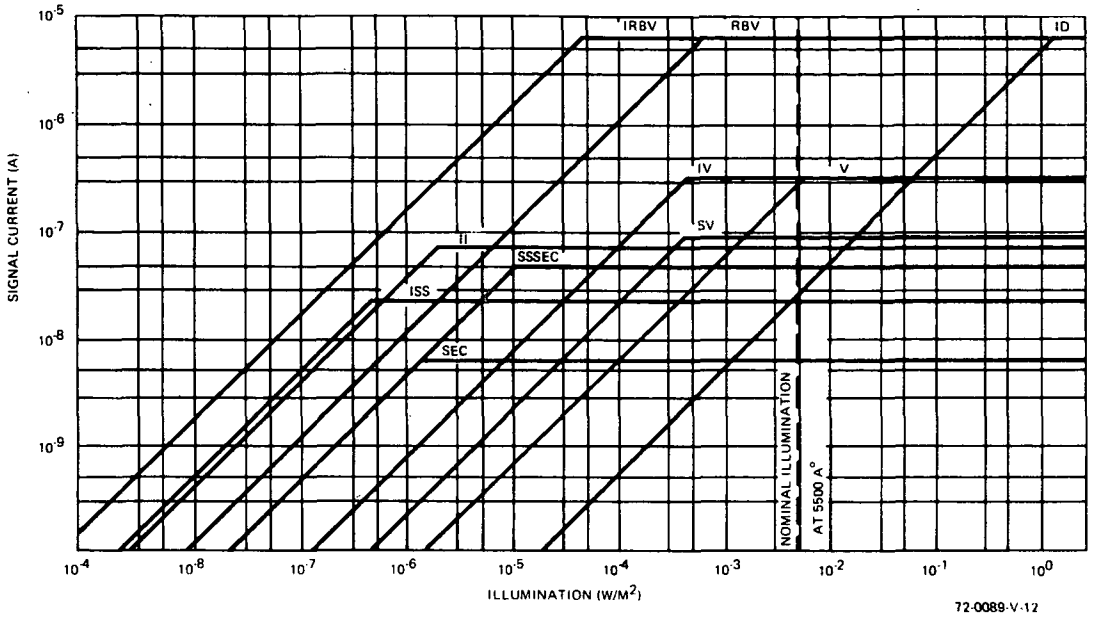

Figure 4-5. EIS Sensitivity to Visible Continuum at 5500 Å

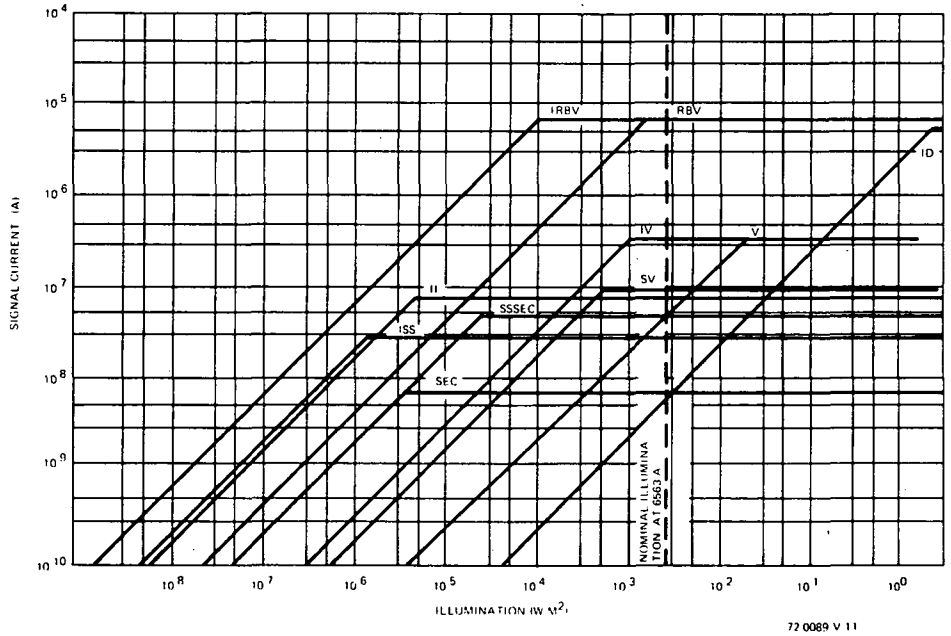

Figure 4-6. EIS Sensitivity to Hydrogen Alpha Line at 6563 Å

The curve for each sensor is the maximum internal gain so the break-point occurs at the minimum illumination for that sensor and is the best operating point for the sensor. This point can be maintained at higher illumination by means of neutral density filters, lens aperture, decreased exposure time, and internal sensor gain reductions. Operation at lower light levels follows the sloping curve and is accompanied by decreasing signal-to-noise ratio. All photoemissive surfaces and storage targets considered in this study have a unity gamma.

Figure 4-1 shows the sensor's response with the ultraviolet input. The silicon vidicon, vidicon, and the return beam vidicon are not shown since these photoconductors have no response at this wavelength. The illumination level through the photoheliograph is the greatest of any considered for the experiment and all sensors except the image dissector have sufficient energy to allow reduced exposure times if required.

Figures 4-2, 4-3, 4-4 and 4-5 include the two extremes and two intermediate illuminations which occur through the tunable filter. The 4046Å illumination combines the maximum attenuation Fraunhofer line with the narrowest bandwidth of the tunable filter and thus provides the minimum illumination value seen by the photoheliograph. Only the intensified return beam vidicon, the image isocon, the intensified silicon sensor, and the secondary electron conduction maintain their maximum operating point below this level while the intensified vidicon maintains a reduced but still satisfactory operating point. The 5896Å curve is another Fraunhofer line at the upper end of the tunable filter range and 4100Å and 5500Å represent two points on the solar continuum. The five sensors above satisfy the requirements of all of these illuminations, the image dissector meets none and the return beam vidicon, vidicon, silicon vidicon meet some but not all.

Figure 4-6 has the sensitivities of the sensors for the 6563Å Hydrogen Alpha camera. The illumination at this wavelength is sufficient for all sensors except the vidicon and image dissector. The return beam vidicon and the silicon vidicon both improve relative to the other sensors at this wavelength due to their extended red responses.

The image isocon, intensified silicon sensor, secondary electron conduction and intensified return beam vidicon have sufficient sensitivity

to operate at their respective optimum operating points for all illuminations of interest. The intensified vidicon is sufficient for all but the minimum level where it is slightly degraded in sensitivity. The image dissector does not have sufficient sensitivity for any illumination of interest and the remaining sensors have partial ability only.

4.4 SIGNAL-TO-NOISE RATIO

A figure of merit more important than sensitivity to sensor evaluation is the signal-to-noise ratio versus illumination. The values are more dependent on the overall television system characteristics and, therefore, are not as often included in the data sheet for a given sensor. However, when the electronic system constraints are set as in this case, the signal-to-noise ratios are a better way to compare sensors than by the signal currents versus illumination curves of paragraph 4.3.

4.4.1 Sources of Noise

The two general forms of noise in television systems are thermionic emission within the sensor and the thermal noise of the first stages of electronic amplification external to the sensor. Most sensors considered in this study are limited by one of those depending on whether or not they have an internal photomultiplier. However, both types of noise have various subforms which affect different sensors in different ways. Each of these forms has been included in the computer program and the appropriate computation made for the particular sensor being evaluated. A brief discussion of these types and how they predominate in various sensors is included here for clarity.

4.4.1.1 Thermionic Emission

Thermionic emission noise arises from several sources but it can always be described by the following equation.

$$I_{noise} = \sqrt{2e\,GK\,I_{sig}\,\Delta f} \quad \text{in amperes} \tag{4-1}$$

where $e = 1.6 \times 10^{-19}$ coulombs per electron

G = electron gain

K = noise multiplication

I_{sig} = signal current at source or beam current

Δf = noise bandwidth

There are several possible ways in which this noise current can arise within a given sensor and which can best be described by reference to a hypothetical sensor containing all possible sources. This sensor, shown in figure 4-7, is representative of an image orthicon, but each of the sensors considered here has only parts of the total. In the image intensifier section, photons are converted to photoelectrons which are given energy via a electrostatic or magnetic field so that they generate secondary electrons in the storage target causing gain in the section. Here the signal current is the photoelectrons per unit time for a given illumination, the gain is the secondaries generated per primary photoelectron, K is unity, and Δf is the frequency of the television frame time (1 Hz for this system) since the target is an integrating device. Due to the very low Δf, this source of noise rarely predominates in any sensor, but it does become noticeable at the very high gain of the intensified silicon sensor.

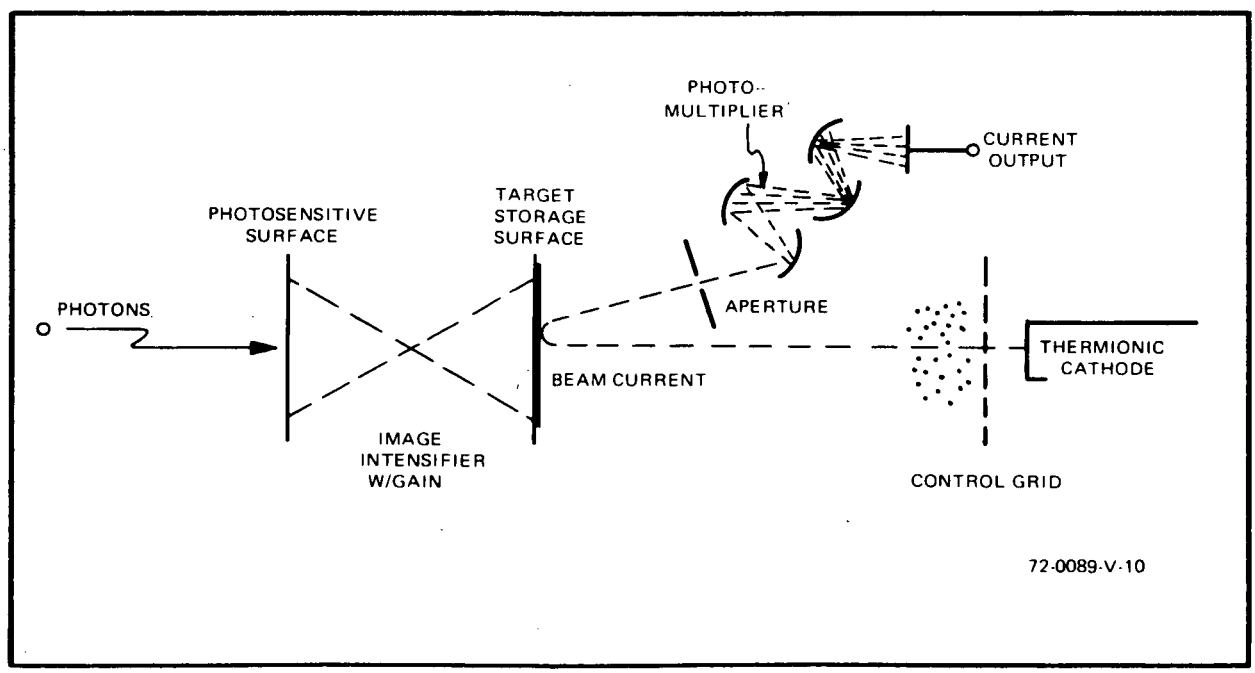

Figure 4-7. Hypothetical Sensor

The next source is the beam noise caused by nonuniform emission from the sensor cathode. Here the gain is unity, the signal current is the total beam current reaching the target, K ranges from unity for a grounded G1 to something well less than unity for more negative values of G1 due to the integrating effect of the space charge near the negative grid, and Δf is the video amplifier bandwidth or the MTF curve of the sensor whichever is limiting. This noise source exists for all sensors except the image dissector but is difficult to compute exactly. It is obvious, however, that G1 should be as negative (minimum bean current and maximum space charge) as is possible consistent with the requirement of discharging peak signal current and sensor dark current if present.

Secondary emission noise again has the form of equation 4-1. It is due to the emission of secondary electrons from the storage target and in each of the photomultiplier elements. Here, the signal current is the electrons per unit time through the photomultiplier defining aperture, G is the total gain of the photomultiplier or unity if read directly from the target, and Δf is the television video bandwidth or the sensor's MTF whichever is limiting. It can be shown that if the gain of each photomultiplier element is high, the initial signal-to-noise ratio is little decreased by the photomultiplier secondary emission noise. This condition sets K as a function of each sensor but 1.5 is a typical value and is used for all sensors herein.

4.4.1.2 Video Amplifier (Resistor Thermal Noise) Noise

The output signal current from a sensor must be developed across a load resistance for meaningful application. However any current flow through a resistive element causes thermal agitation as an additional source of noise which can be computed from equation 4-2, (reference 13).

$$\overline{E}_N^2 = 4\,kT \int_{f_1}^{f_2} R\,df \qquad (4\text{-}2)$$

where $k = 1.38 \times 10^{23}$ joules/^{o}K (Boltzman's constant)

T = temperature in degrees Kelvin

f_1, f_2 = frequency limits of video amplifier

R = resistor value in ohms.

The equation above, while theoretically true, has been modified to more simply compute the noise current found in typical, low-noise, solid-state television video preamplifier. Equation 4-3 makes the following assumptions all of which are consistent with state-of-the-art television preamplifier design.

a. The first amplification stage has sufficient power gain to ensure that it is the predominant noise source.

b. The first amplifier is a field effect transistor. Regular transistors, vacuum tubes, and unijunction transistors modify the equation somewhat and usually result in higher noise.

c. The combination of the sensor's target distributed capacity and the load resistor causes a frequency lag well within the video amplifier bandwidth which is compensated by a lead network in the preamplifier.

d. The net frequency response out of the preamplifier is flat out to the desired bandwidth.

With the assumptions above, equation 4-3 can be used by compute anticipated noise currents.

$$\overline{i}^2_{noise} = 4\,kT\,\Delta f\left(\frac{1}{R_L} + \frac{R_{eqv}}{R_L^2} + \pi^2\,R_{eqv}\,C_T^2\,\Delta f^2\right) \qquad (4\text{-}3)$$

where $k = 1.38 \times 10^{-23}$ joules/^oK (Boltzman's Constant)

T = temperature in degrees Kelvin

Δf = net video amplifier bandwidth

R_L = load resistor at sensor output

R_{eqv} = equivalent input impedance of FET first stage amplifier $\approx 1/g_m$ at the operating point.

C_T = sensor and distributed capacity at R_L

Figure 4-8 illustrates the independent effects of the first and last terms of equation 4-3 for values typical of present television systems. Note that for the values used, the middle term $\left(R_{eqv}/R_L^2\right)$ can be neglected. It is obvious, from the figure, that for the bandwidth of interest in this

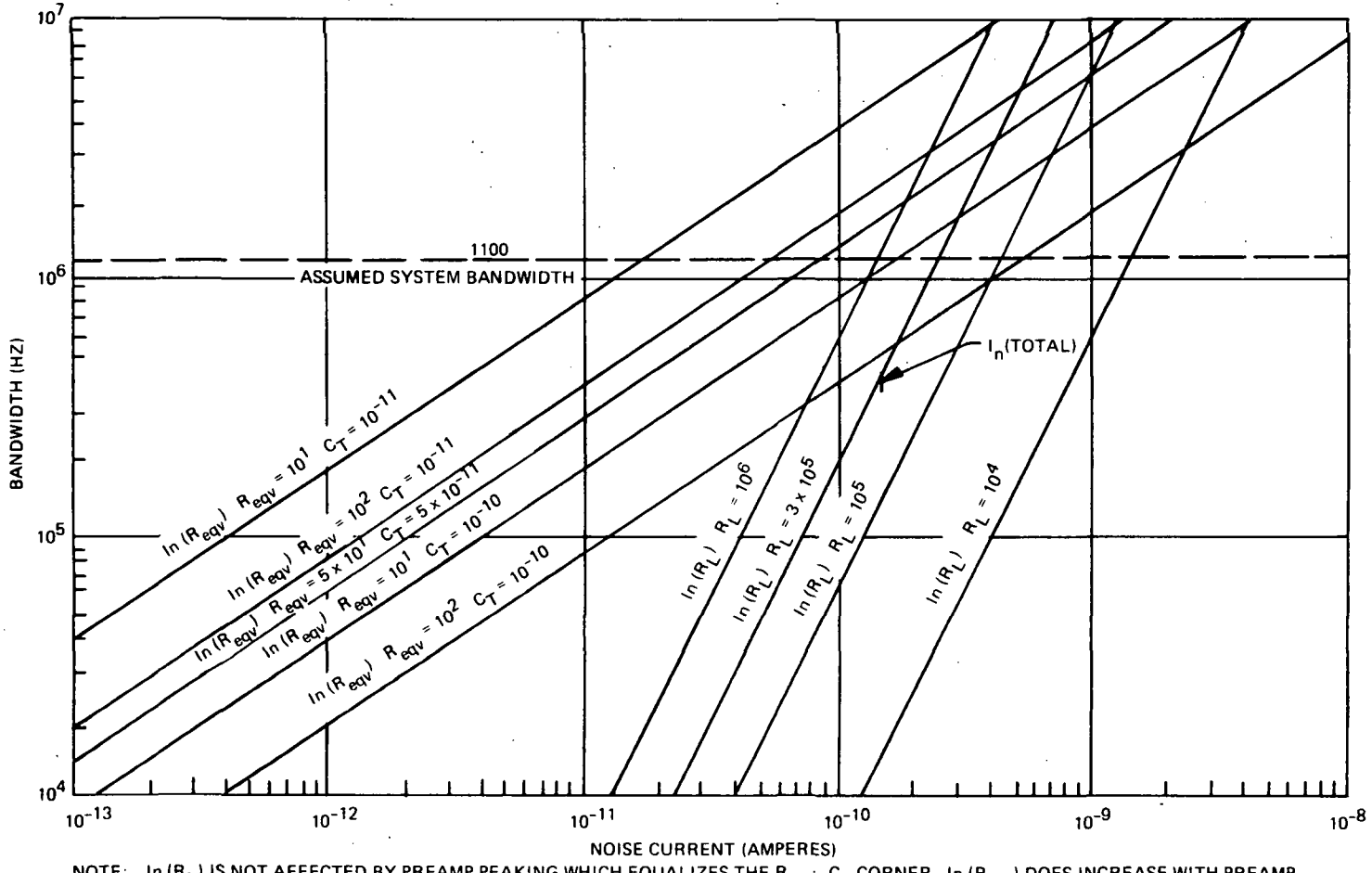

NOTE: $\ln(R_L)$ IS NOT AFFECTED BY PREAMP PEAKING WHICH EQUALIZES THE $R_L \cdot C_T$ CORNER. $\ln(R_{eqv})$ DOES INCREASE WITH PREAMP PEAKING.

71-1038-VB-8-1

Figure 4-8. TV System Noise Versus System Bandwidth

study, R_L noise predominates. Also, equation 4-3 shows that signal current increases directly and noise current only as a square root function as R_L increases. Thus, good design maximizes R_L consistent with external interference and the ability of the preamplifier lead network to compensate for the $C_T R_L$ lag. The combination chosen as design criteria on the figure represent obtainable values which allow the possibility of slight improvement.

4.4.2 Noise Characteristics of Sensor

Basically, sensors with photomultipliers are noise limited within the sensors while those without are video amplifier limited. The first class include the image isocon, image dissector, and return beam vidicon while the others fall in the second category. Each in the second category depend only on their signal current compared to the noise current obtained in the preamplifier and thus improved signal-to-noise ratio depends entirely on increased signal current. However, each of the three sensors in the first category has different noise sources predominating and must be considered separately.

The image dissector has no thermionic cathode and no storage target so that its noise source is the photoemission noise at full video bandwidth and multiplied by the K factor in the photomultiplier. Since this sensor does not have the integrating effect of a storage target, it has very poor sensitivity and low signal-to-noise ratio at most useful light levels.

The return beam vidicon has a combination of the photoemissive noise plus the thermionic noise caused by the read beam, and the RMS sum is then also multiplied by the K factor of the photomultiplier. In practical operation, the beam current is seen through the photomultiplier and this noise source predominates. Noise can be minimized by control of the beam current over temperature and illumination to maintain the beam at a just sufficient level to discharge the target without increasing lag. This, however, is difficult to maintain and often fixed beam currents are used with resulting loss in signal-to-noise ratio. Another problem with the RBV is that the output signal is maximum in black and minimum in whites so that signal-to-noise ratio is worst in highlight regions.

The image isocon operates the same as the return beam vidicon with one important exception which benefits its signal-to-noise characteristics.

This is obtained by changing the aperture from a pinhole admitting the total beam current to a ring aperture which reflects the primary beam and admits the current scattered from the main beam by the collision with the target. This scattered signal is also proportional to illumination but is opposite in polarity and thus has maximum signal-to-noise ratio in high lights. Also, since the main beam current is eliminated, the predominating noise becomes the secondary emission of the target. However, in spite of these improvements, the II still has a relatively low signal-to-noise ratio for the requirements of this study since the II target is a relatively low-storage capability device which is not maximized for the required slow scan operation.

4.4.3 Computed Sensor Signal-to-Noise

Using the foregoing noise deviations with the computer program (see Appendix C), the anticipated signal-to-noise ratio for each sensor was found for each illumination. The peak value is determined by the maximum storage capability as defined in paragraph 4.3. This is a constant for each sensor, but the location of the breakpoint is a function of the illumination. Sensors which are preamplifier limited have a fixed-noise source and the curve below the breakpoint is determined by the sensor's gamma which is unity for all sensors considered. The image isocon, image dissector, and return beam vidicon all depend on a square root noise factor of thermionic emission noise, and, thus, signal-to-noise ratio does not decrease as rapidly with decreasing illumination as with the other sensors.

Figures 4-9 through 4-14 show the resulting signal-to-noise ratio. In each case, there is an illumination level in which each of the image isocon, intensified silicon sensor, slow scan secondary electron conduction or the intensified vidicon is the maximum signal-to-noise ratio. However, on each figure is the illumination anticipated in the photoheliograph experiment, and, at this point, the IV gives the maximum signal-to-noise ratio in every case including the minimum illumination case at 4046Å. Here the IV is operating below its peak operating point, but its large target storage capability and initially high signal-to-noise ratio still maintains a satisfactory value.

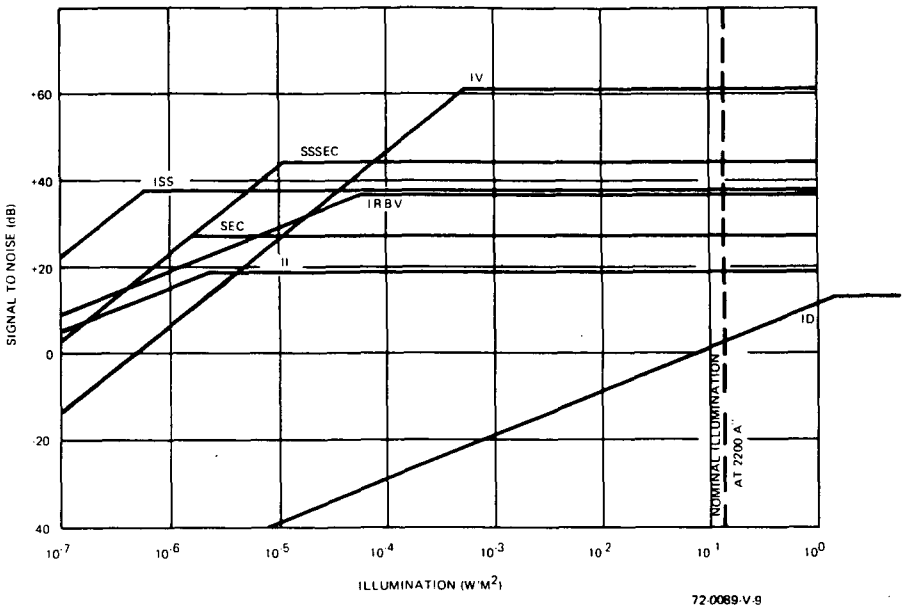

Figure 4-9. EIS Signal to Noise from Ultraviolet at 2200Å

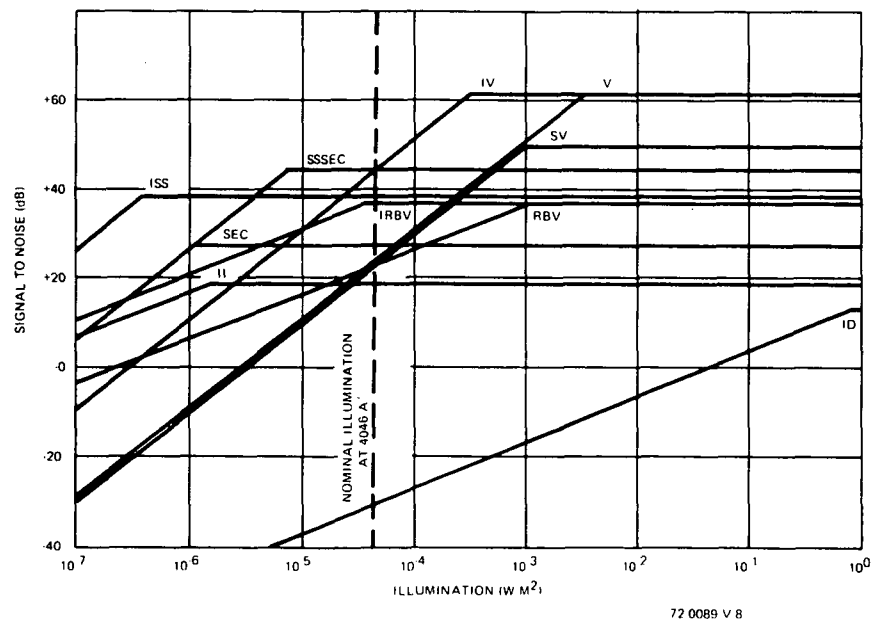

Figure 4-10. EIS Signal to Noise from Minimum Visible Continuum at 4046Å

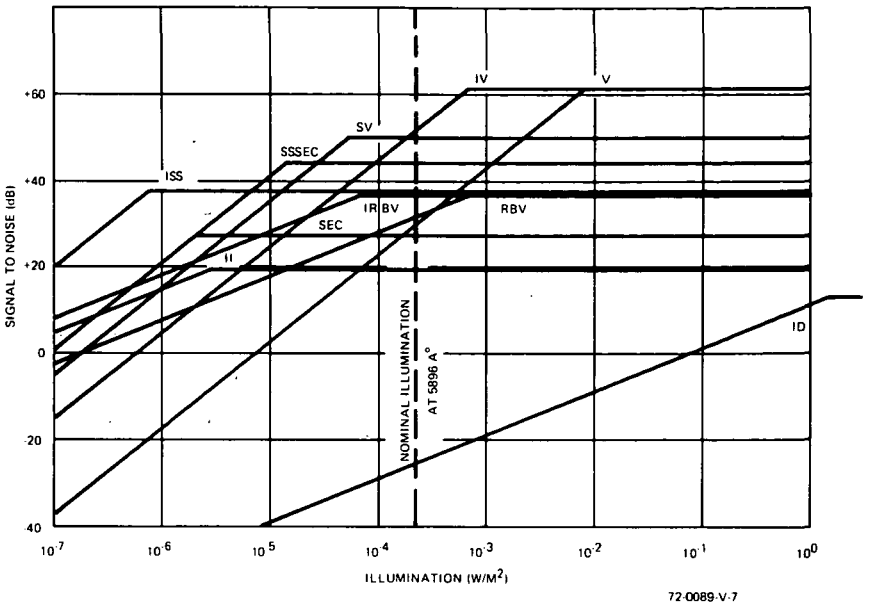

Figure 4-11. EIS Signal to Noise from Visible Continuum at 5896Å

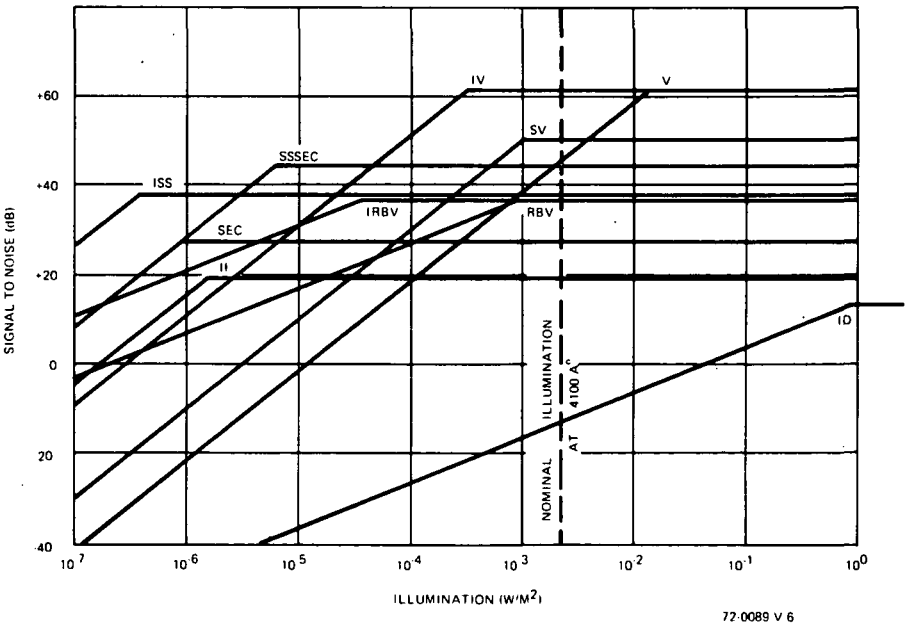

Figure 4-12. EIS Signal to Noise from Visible Continuum at 4100Å

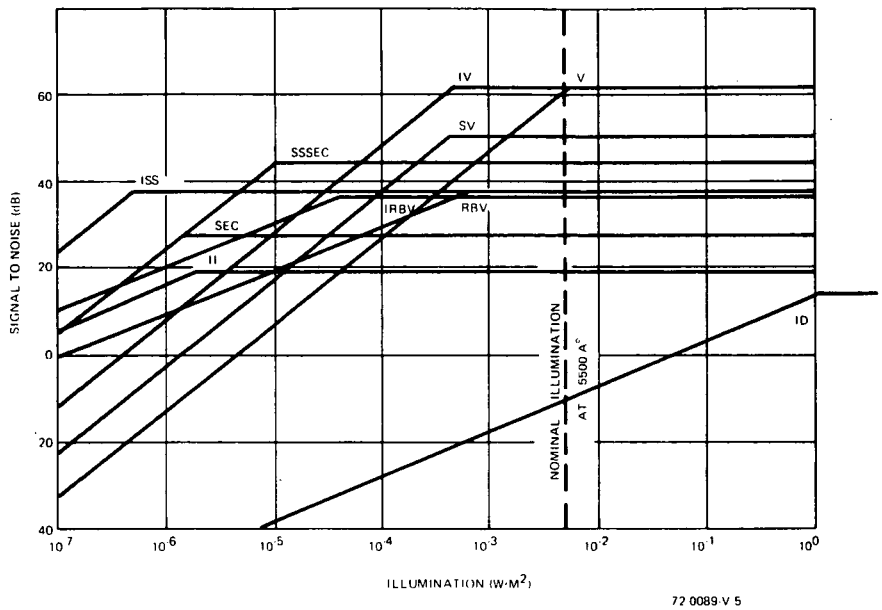

Figure 4-13. EIS Signal to Noise from Visible Continuum at 5500Å

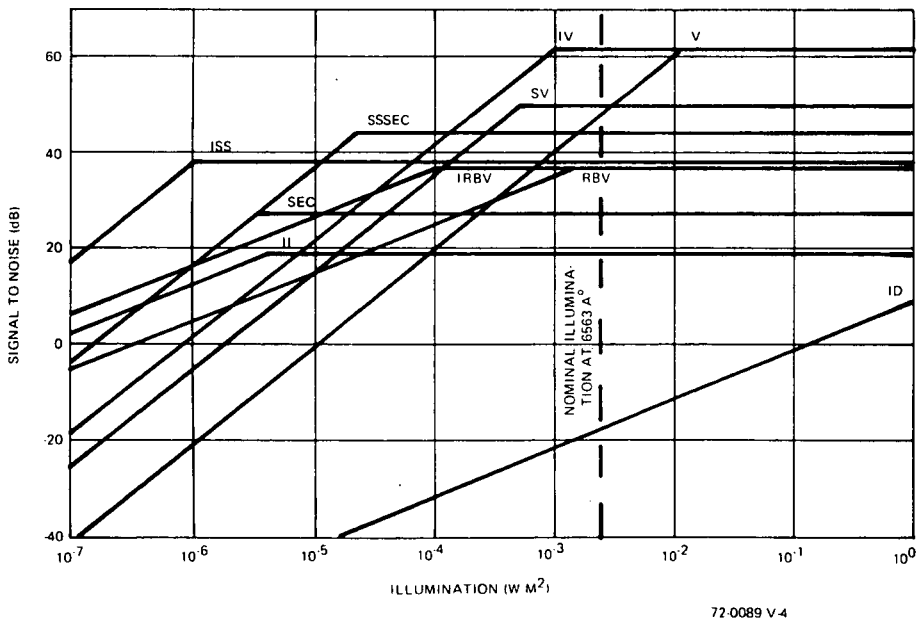

Figure 4-14. EIS Signal to Noise from Hydrogen Alpha Line at 6563Å

4.5 SPECTRAL RESPONSE

Every sensor discussed except for the silicon vidicon and the return beam vidicon have many possible photosensitive surfaces. Figure 4-15 shows the responses of the two above, a typical slow scan photoconductive surface for a vidicon and an S20 photocathode on fiber optics such as used on secondary electron conduction, intensified silicon sensor, image dissector, or image isocon. The photoconductive surfaces have typically higher quantum efficiencies than the photoemissive surfaces but the five shown will all satisfy the spectral requirements of the photoheliograph experiment except the UV portion. Both the lead oxide of the plumbicon and the selenium sulfide of the GEC slow-scan Mariner type vidicons fail to meet the above requirements and any others do not perform as well as these, so any sensor considered will be considered with one of the five above photosensitive surfaces.

The 2000- to 3000-Å UV requirement is a more difficult problem, primarily due to few requirements for this spectral response. Most of the manufacturers of sensors considered in this study have the technology to build the required front end and have, in fact, built some form of the UV sensitive device but the particular sensor would be a custom sensor. The primary difficulty is that the usual faceplate glasses are opaque in this region, and special faceplates such as sapphire, fused quartz or silicia, magnesium fluoride, or lithium fluoride are required. Each of these has special processing requirements and represents a change in the photosensitive material deposition technique, but again, it has been done successfully. Figure 4-16 illustrates four possible combinations which could be used. The cesium telluride/quartz is sensitive only in a narrow-band bracketing the desired 2000- to 3000-Å region. This would then act as a high-pass filter on the main solar output and reduce the filtering requirements on the photoheliograph. This advantage, however, creates a calibration difficulty which would require special light sources and special test equipment. The bialkali/quartz and the UV vidicon cover from 2000 to 6000Å at a relatively good quantum efficiency and still filters out the solar IR output but would not provide operation with the Hydrogen alpha camera. The final curve is S20/sapphire and has the double advantage of being a very familiar

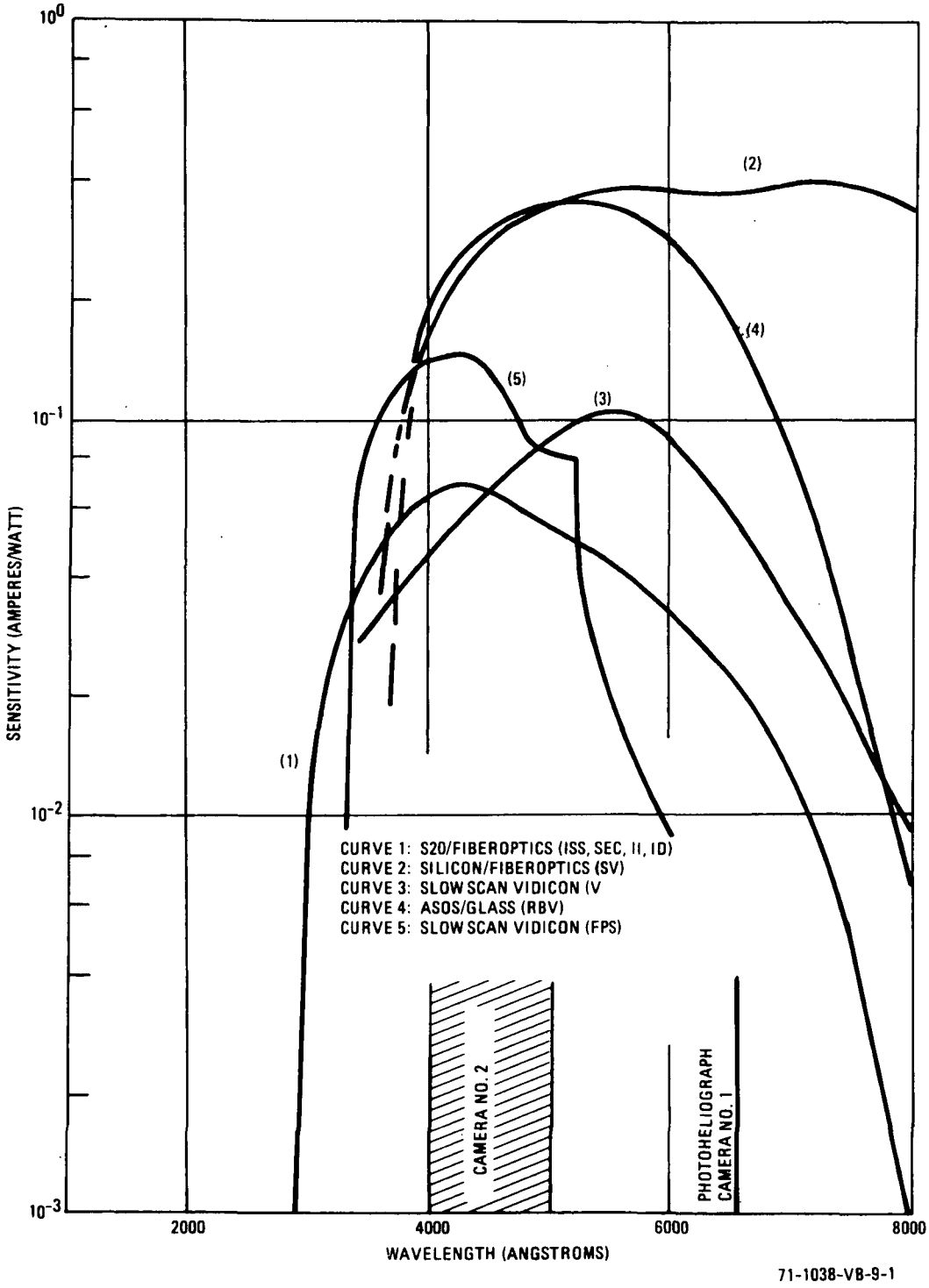

Figure 4-15. Spectral Response of Selected Photocathodes

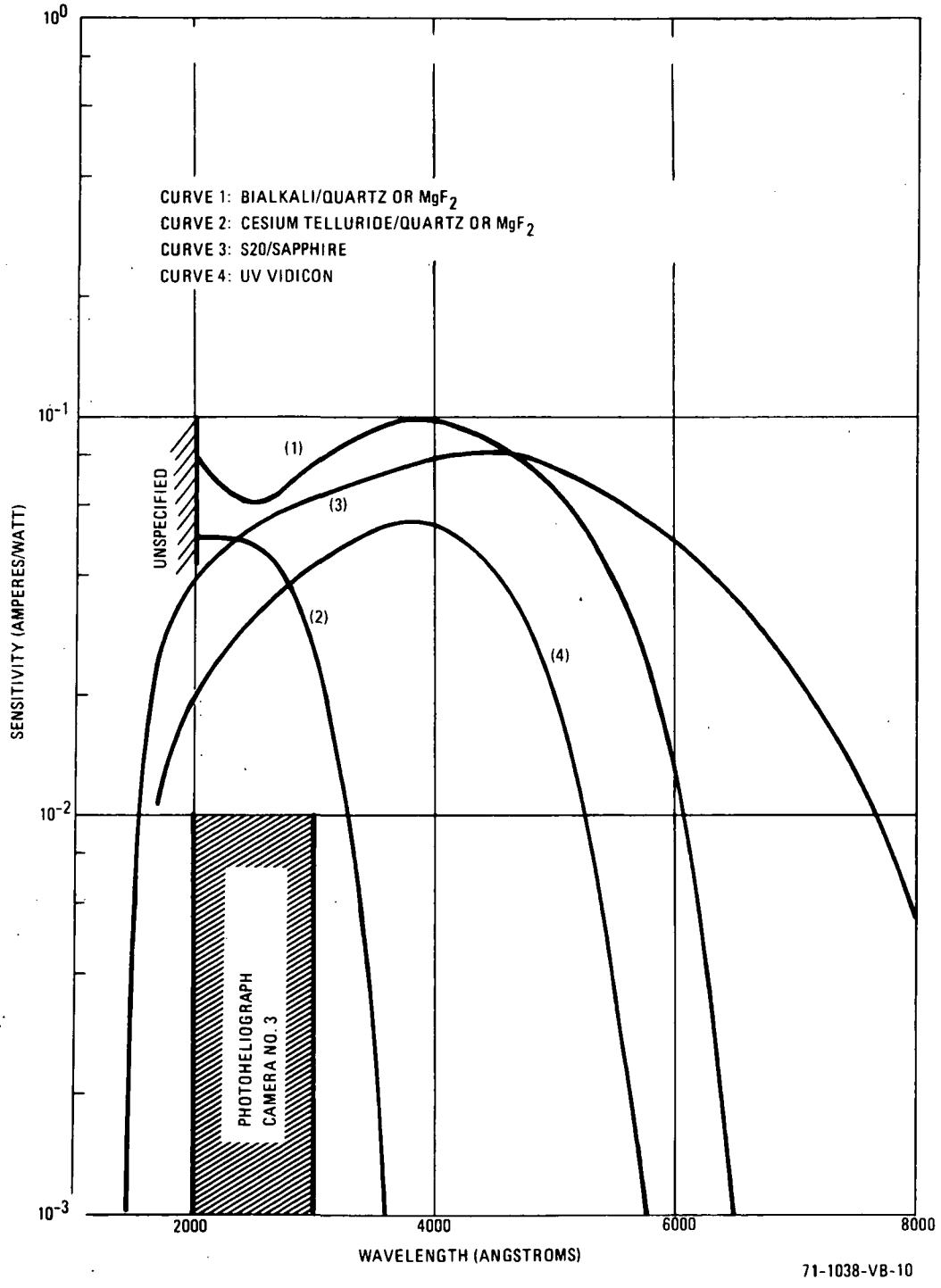

Figure 4-16. Ultraviolet Sensitive Photocathodes

photosensitive material of excellent characteristics and also a single sensor could cover the entire spectral requirements of the photoheliograph experiment.

Of the UV photosensitive surfaces, the bialkali, cesium telluride, and S-20 are photoemissive surfaces and can be used with several sensors including the II, ID, ISS, SEC, or I. The UV vidicon surface is photoconductive and can be used only with the unintensified vidicon. However, the illumination intensity at the 2200 Å UV band is great enough so that this is a possible choice if stability requirements do not require too short a exposure time.

A problem area with all the UV type sensors is the lack of a fiber optics coupling which would allow a flat surface input to mate with a curved surface photocathode. This would prevent the use of most electrostatic lens in the image section of intensifiers, SEC's, ISS's, and II's. This can be solved by use of either optics which give a curved focus plane matching the photocathode shape (see Appendix A) or a magnetic lens which does not have controlled gain but which can focus one flat field onto a second flat field.

One additional consideration is that a Gregorian telescope generates a convex focus field and might thus be able to match directly to a properly curved photocathode on UV glass. This would require a more complex matching of sensor to the photoheliograph but offers some distinct advantages.

There are flat input face, electrostatically focussed, intensifiers which will be considered but most present versions have insufficient resolution.

The spectral characteristics shown in the previous figures have all been stored in the computer program and are used to compute the sensitivities obtained at each of the illuminations of interest. The S-20 photocathode is used in all computations except those in the vidicon, return beam vidicon, and silicon vidicon. The other photosensitive surfaces could be scaled by comparison or computed directly if they would be considered for use. At present, only the cesium telluride/quartz would be likely to have an advantage over S-20 and this would be due to its ability to filter out the peak solar intensity and thus reduce the requirements of the UV spectral filter of the photoheliograph.

4.6 SENSOR MTF

The photoheliograph itself provides a limiting resolution which should not be degraded further by the remainder of the system including the television cameras, the onboard data handling equipment, the downlink, and the data retrieval and analysis. Perfect operation is always impossible, but to make the entire experiment feasible, the system resolution must be the primary design constraint.

The photoheliograph is defined to have a diffraction limited resolution with a 65-centimeter primary mirror and an 0.2 central obscuration. This limiting resolution is the radius between the central bright area and the first null obtained from a point source imaged through an ideal lens. This radius can be computed by the equation:

$$y = 1.22 \lambda f\#$$

where λ = wavelength of illumination

f# = f# of telescope system

y = distance corresponding to one line pair.

The computation gives a value of 33 line pairs per millimeter at 0.5 μm for the 65-centimeter photoheliograph and 78 line pair per millimeter for the 1.5-meter photoheliograph.

The effects of central obscuration are more difficult to compute but increasing obscuration has the effect of maintaining constant limiting resolution, decreasing total sensitivity, decreasing the MTF at lower spacial frequencies while increasing the MTF at higher spacial frequencies. Figure 4-17 illustrates this effect and also indicates that the 0.2 obscuration of the photoehliograph has little effect.

The comparative resolution of the various sensors is shown in figure 4-18. Each of the sensors considered in this study has had its MTF curve modified to a line pairs per millimeter value for the abscissa so that they can be compared to each other and also be translated into the resolution obtained using the 21- by 21-millimeter format of the photoheliograph. Each sensor is the highest resolution sensor available in its generic type consistent with the other photoheliograph considerations. All of the conditions discussed in paragraph 4.1 are used with the illumination levels found in

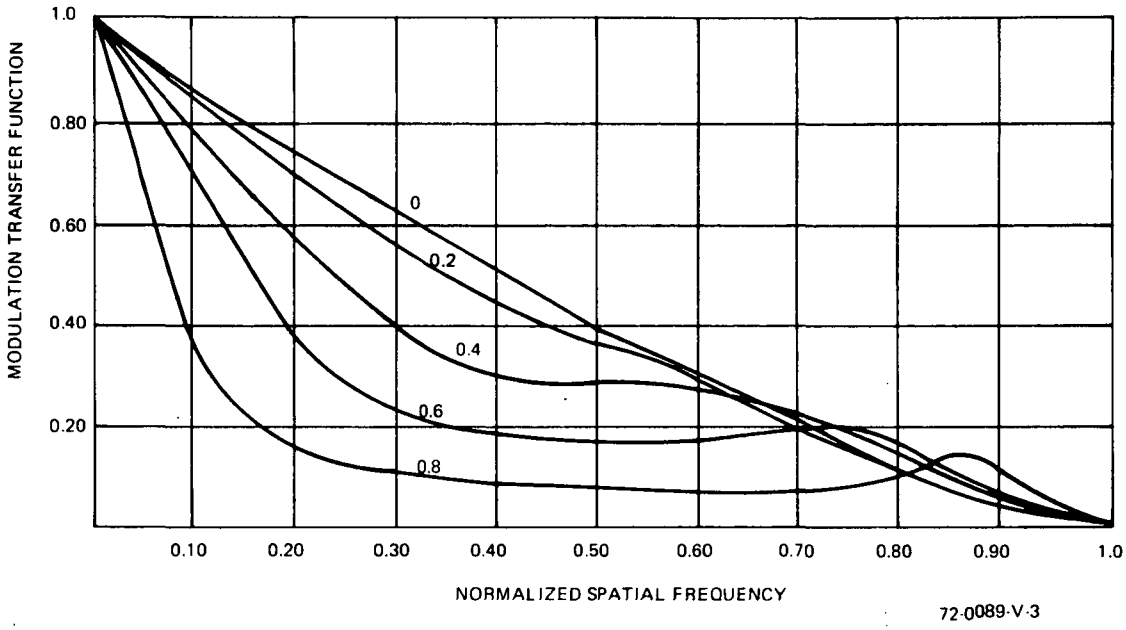

Figure 4-17. Modulation Transfer Function for a Perfect Lens With a Central, Circular Obscuration

paragraph 4.3 Resolution is little effected by the illumination although reference 14 does indicate a slight loss of resolution for decreasing wavelength for photoemissive devices such as the SEC, ISS, II, and ID. This is caused by the higher energy acquired by the photoelectrons which causes a larger dispersion before being acquired by the electric or magnetic field of the intensifier. However, this effect is not sufficient to modify figure 4-18.

Referring again to figure 4-18, the photoheliograph diffraction limit is shown at 33 line pairs per millimeter and the stated design goal of a satisfactory would be to have an MTF greater than 70 percent at this value. At this value, the return beam vidicon is the only electronic imagery tube which has the required MTF, and it actually exceeds the high resolution SO-392 film for the useful range of the photoheliograph. The image isocon has no capability at 33 lp/mm and the secondary electron conduction, intensified silicon sensor, or silicon vidicon are under 10 percent which is

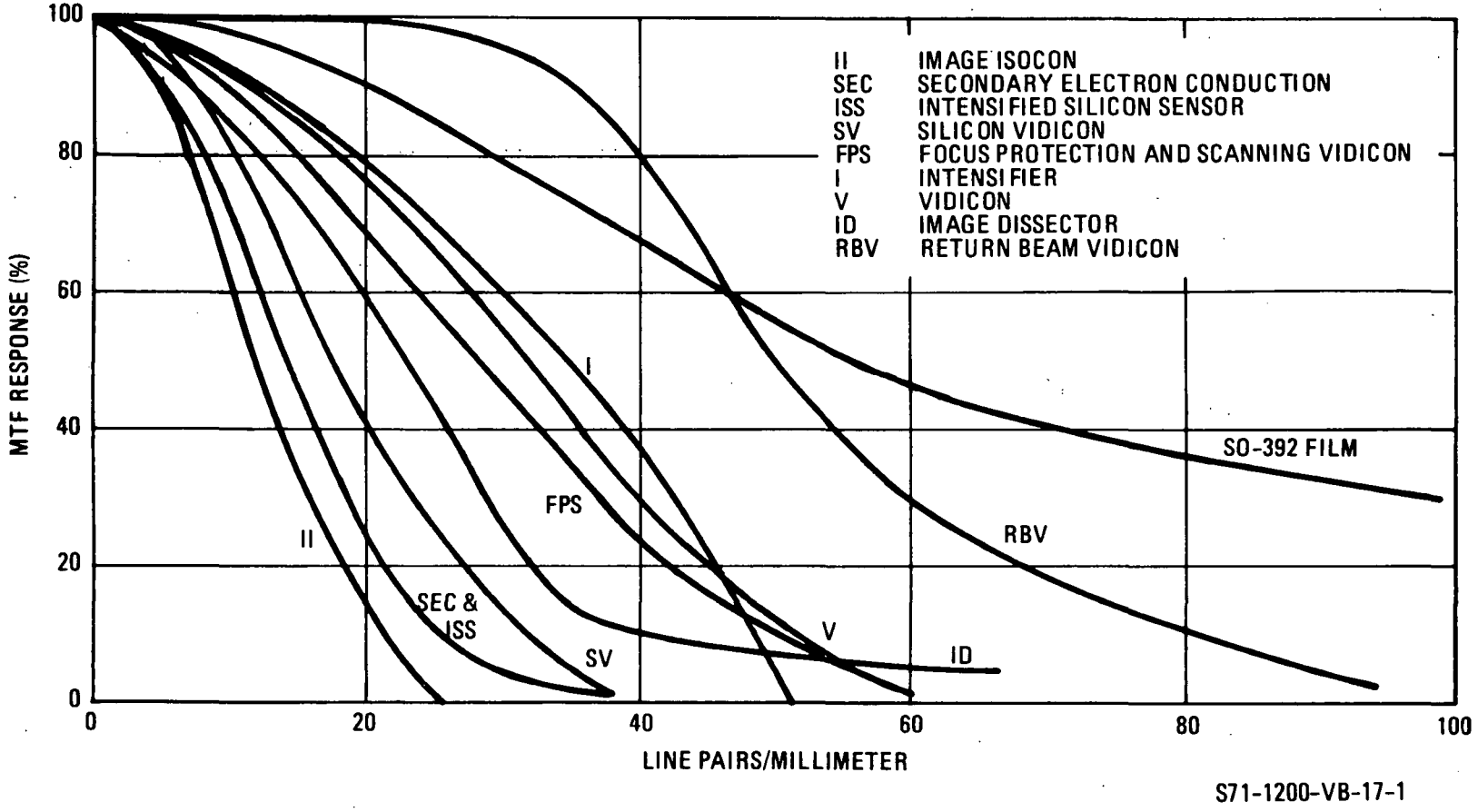

Figure 4-18. Comparative Sensor MTF

an unacceptable level. The image dissector has significant but low MTF and has been disqualified previously due to low sensitivity. Finally the intensifier, focus projection and scanning, and vidicon have MTF's in the 40 to 60 percent range at 33 lp/mm and thus are amendable to electronic image enhancement to achieve the desired 70 percent MTF within the EIS.

Returning to paragraph 4.3, the intensified vidicon was the optimum sensor for the important signal-to-noise characteristic at all illuminations and the intensified return beam vidicon also has sufficient but lower values. Figure 4-19 shows the effect on MTF when an intensifier is mated to either a vidicon or a return beam vidicon. The result for both is a value below the desired 70 percent MTF but still one which provides a reasonable value to use with electronic image enhancement. Theoretically, electronic signal enhancement can provide a square MTF curve which is 100 percent out to the limiting resolution of the sensor at a cost in signal-to-noise ratio. In practice, the decrease in signal-to-noise ratio approximates the peak increase in MTF so that a 2:1 increase in MTF would cause a 6-dB decrease in signal to noise ratio. Thus, an increase to 100 percent from 25 to 50 percent MTF would often be feasible while increases from 10 or 20 percent to 100 percent would be lost unless the original signal-to-noise ratio was

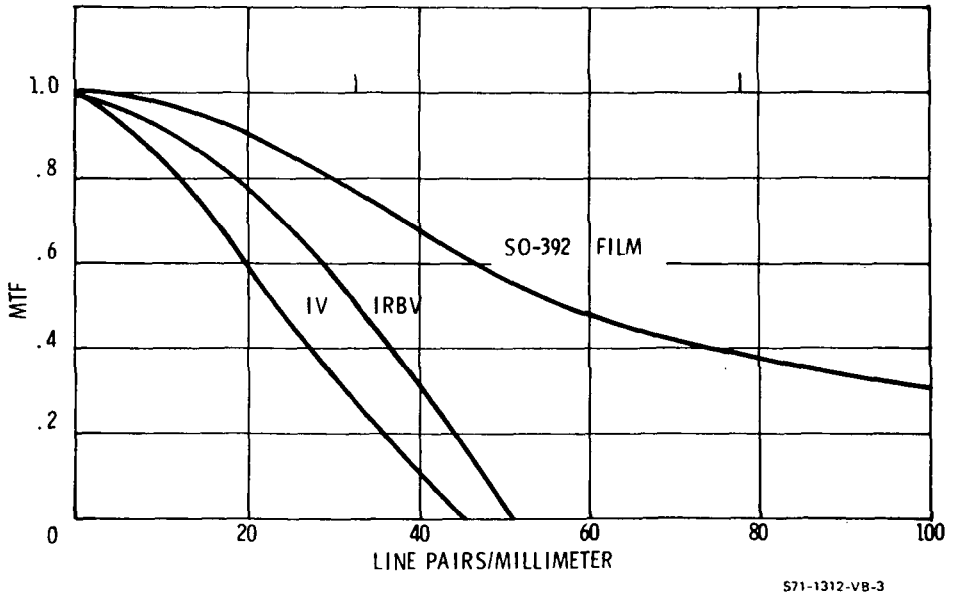

Figure 4-19. Effect of Intensifiers on MTF

extremely high. Here the 60-dB signal-to-noise ratio of the IV allows a 4:1 aperture correction at a cost of some 12-dB signal-to-noise ratio so that the final value of 48 dB is still quite acceptable. The IRBV, on the other hand, has less than 40 dB signal-to-noise ratio to start, and even a 6-dB loss in signal-to-noise ratio to achieve a 2:1 increase in MTF may be undesirable.

Horizontal aperture correction is simply done within the electronics of the television camera itself by use of a no-phase shift peaking of the video amplifier chain. Vertical aperture correction is more difficult and must be done during data reduction. The usual technique uses two delay lines each with a delay equal to one TV line time. The t + 1 line is compared to the t - 1 line in an add circuit. This signal is then subtracted from the t_o line, and, finally, the difference signal is summed with the original t_o line and displayed. This form of signal enhancement has neither the range nor the linearity of horizontal aperture correction, but the results do enhance the system MTF, are measurable, and are repeatable.

The difficulty in the obvious choice of the RBV or the vidicon is their lack of sensitivity if image motion compensation cannot be obtained or if IMC is only good for a limited time. Sensitivity sufficient for the UV camera is obtained by use of a single vidicon. The IV, shown in figure 4-19 indicates some deterioration, but is still sufficient MTF for the remainder of the requirements. The double and triple intensifiers, required to use the RBV and vidicon with the universal filters at shorter exposures, would degrade the MTF below that of the ISS and SEC besides adding other side effects.

4.7 ELECTRONIC GAIN VARIATIONS

Since television cameras in space must operate with none or a minimum of adjustments, it is important that the camera be adaptable to changes in the environment. One of the most important and also probably the most likely to change characteristics is the illumination. This occurs due to changes in the solar output, initial tolerances, and aging in the telescopes mirrors, the filters, and the television sensor. Thus, it is important that the television cameras be able to operate at maximum operating points throughout several orders of magnitude of change. This can be acomplished

all or in part by mechanically adjustable apertures or shutter speeds, but it is likely that the variations encountered will require additional range from the sensor. This can be obtained by electronic gating and/or variations in internal gain of the sensor.

Each of the sensors has some capability, both by shuttering or by gain change, but by different modes. The vidicon, FPS vidicon, and silicon vidicon can be changed only be variations in their target voltage which create changes in quantum efficiency and storage capability. This allows a change of 5:1 or less before storage reduction, dark current, or lag causes serious side effects. Generally, shuttering of the target can be used at times down to milliseconds with no problem. Sensors such as the image isocon, return beam vidicon, and the image dissector contain photomultipliers behind the target. Gain variations of 100 can be obtained by varying the voltages on the dynodes of the photomultiplier. Although most control is obtained by the variation of just one or two dynodes, the balance of the voltages across the multiple dynodes can make it difficult to maintain constant resolution over the entire range. Gating is obtained only in the photocathode of the RBV. The II, however, has a photocathode emitting photoelectrons which are electronically focused onto a target material. In this case, either the photocathode or the target is capable of being shuttered. Some electron gain occurs in the target as a function of the photoelectron energy but gain control is not recommended.

The SEC and ISS have a photocathode and target similar to the II and can be shuttered at either point. In addition, versions of both sensors have been built with triode image sections which allow shuttering at lower voltages and faster rates. Gain control is obtained by varying the photocathode voltage. This voltage determines the energy acquired by each photoelectron which in turn determines the secondaries obtained in the target material. Gain variations of 100:1 are readily obtainable from either sensor with no loss in other characteristics.

The IV and IRBV can obtain the gain control range mentioned above by varying the target voltage. In addition, the intensifier considered for the EIS has a nominal gain of 50 which can be decreased electronically by an order of magnitude. It also has a triode image section which allows fine

focussing and shuttering of the image. The shutter control gives gain cut offs of greater than 10^5 and should be capable of any shutter speeds anticipated for the EIS.

4.8 OTHER SENSOR CONSIDERATIONS

4.8.1 Lag

Lag has several physical causes, but the result is an incomplete read-out of the charge image on the sensor in a single frame. In a slow scan operation, this requires additional erasure time, besides the desired read-out, to eliminate any charge on the target before the next exposure. It also reduces signal to noise in the desired readout frame.

The cause of lag is primarily the beam acceptance or the time/beam energy required to transfer the information contained in the storage target electron distribution to either the video amplifier in a direct target read sensor or to the reflected beam. Also, if a separate intensifier is used, a small amount of storage occurs in the exit phosphor.

For most standard scan systems and especially for the slow-scan requirements of the EIS, the first cause contributes the major portion of the lag associated with a given sensor. The exact-mechanisms causing this effect are outside the interest of this study, but a concept can be established by reference to figure 4-20. The front of the target is usually aluminum or some conductive coating which is charged to uniform positive voltage from an external source. This lead is also the signal current output point for direct read sensors such as the ISS, V, FPS, and SEC. The rest of the material is the storage target itself which acts just like a capacitor whose rear side has been placed to ground potential by the read beam. When this occurs, the beam does not land on the target but returns to G2 or through the photomultiplier depending on the type of sensor. When the illumination is turned on, the photons or photoelectrons pierce the conductive surface and cause a temporary redistribution in the target material so that the rear side of the target moves positive toward the front target voltage. The read beam then sees a positive voltage and impinges on the target to restore the ground level thus causing a electron flow into B^+ and a reduction in the return beam.

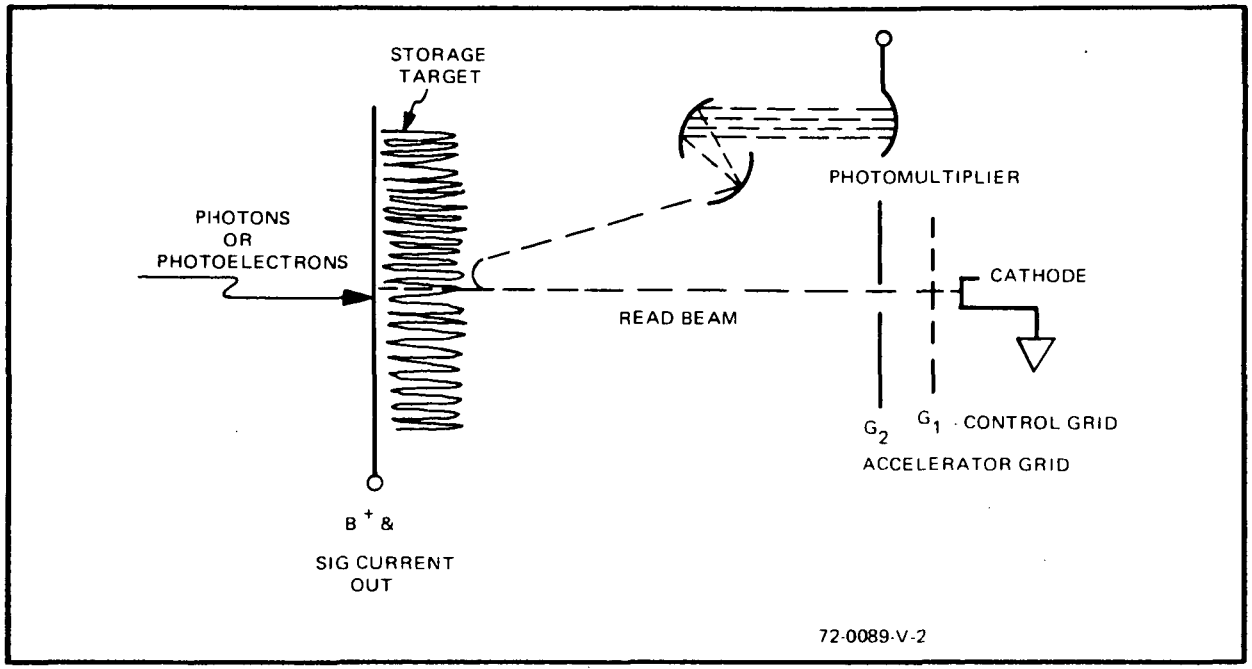

Figure 4-20. Typical Storage Target Diagram

The lag itself occurs as a function of the bulk capacity of the target, the internal series resistance of the target, and the stiffness or amperes per unit area of the beam. The first two depend on the type of target material used and may be selected due to additional criteria. The capacity is, of course, a function of the dielectric constant of the material and sets the total number of electrons which can be stored before readout or essentially the saturation current of the sensor. However, the dielectric constant only sets the maximum charge storage, but other considerations determine the amount of charge actually available for current redistribution so that two targets of equal capacitance may have different values of saturation current and lag. Increase in B^+ voltage also increases the total charge storage and decreases lag since conduction is eased by the higher electric field. The limit here is the dielectric breakdown of the target material or excessive leakage (dark current) which masks the true signal. The density of the beam current is usually adjustable for each sensor, and since the beam is never a point source a value must be chosen that reasonably

discharges the maximum current distribution expected while not spreading so wide as to deteriorate the resolution.

Table 4-1 shows the bulk capacity of several sensors and the lag which occurs when tested at the standard scan rate test which measure the residual signal in the third field after illumination. The dependence on capacity is obvious ranging from practically no lag in the ID which has no storage target to very significant values for the RBV and FPS. The difference between the FPS and RBV must be in the internal resistance and the beam current used since their bulk capacity is equivalent. The V bulk capacity was not available but its sensitivity values indicate sufficient storage ability, and the lag is more than satisfactory.

TABLE 4-1
COMPARATIVE SENSOR CAPACITY AND LAG

	Target Capacity (pF/cm^2)	Lag in 3rd Field (50 msec)
Image Dissector	0	0
Image Isocon	6.5	3 percent
SEC	150	5 percent
Plumbicon	190	6 percent
Silicon Vidicon	2,000	7 percent
Intensified Silicon Sensor	2,000	7 percent
Slow Scan Vidicon	Not Available	< 10 percent
FPS Slow Scan Vidicon	16,000	10 to 30 percent
RBV Vidicon	16,000	50 percent

There is additionally a finite charge time required to charge the target following exposure before a signal can be read out. This is usually a very small time and is not significant for slow scan operations except for the return beam vidicon.

Other characteristics, however, must be taken into consideration when reviewing sensors for single exposure operation. Such things as redistribution and charge buildup favor the IO and II sensors when continuous exposure, fast scan is used. This allows buildup to occur in the target over

several frames until equilibrium is reached, and results in test data which is correct only for this type generation. Therefore, data taken in standard scan, continuous exposure cannot be used for comparison of sensors to be operated in a single frame, slow-scan mode unless special care is taken with the data.

4.8.2 Slow-Scan Capability

The requirements of a slow-scan sensor are not always compatible with those of standard scan systems. Generally, any sensor can be optimized for one or the other, but the standard design is either a compromise or biased toward standard television operation. The limitation on operation is invariably in the storage or integrating target material. Thus, the image dissector, which has no storage capability, can operate over a broad range of scan rates.

A given target material has a bulk capacitance and also a percentage of the total coulombs of charge which are free to move in a given sensor. This value of total per electrons per unit area nominal to the electron beam determines the maximum number of electrons available for signal current flow in the sensor. However, a slow-scan, high-resolution sensor scans the beam more slowly over a smaller pixel than occurs with a standard scan rate, medium resolution system. Thus, for a given target, the slow-scan, high-resolution sensor would generate less coulombs of charge due to the smaller pixel and would do it more slowly due to the slow scan rate. This results in a much smaller signal current for the sensor. Therefore, the slow-scan sensor usually has a higher capacity target or perhaps the same target material built more thickly so as to allow a satisfactory current flow at the target's saturation level. The ideal target then would have the maximum free electron/capacitance ratio and a thickness which would give the maximum electron storage while still maintaining the lag low enough so that the target could be discharged at the desired scan rate.

Referring to figures 4-1 through 4-7 and 4-9 through 4-14, the signal currents and signal-to-noise ratios shown are obtained from available sensors. Of the sensors shown, the RBV is normally usable only as a slow-scan sensor while the vidicon and FPS vidicon values are from vidicons designed for slow-scan operation. The SEC and II both have excellent

slow-scan capabilities except for a limited signal current. Development work on SEC's increased signal current by a factor of 3 with no side effects except a slight increase in lag. Increase of 5 or more is feasible at slow-scan rates and is shown in the figures as the SSSEC.

The silicon vidicon and the ISS sensors have an additional problem at slow scan caused by their inherent dark current. This current is essentially the back bias leakage current of the silicon diodes and as such follows the rule of doubling the current every 10°C. This dark current is a dc value and can be biased out within the ability of the beam current to discharge the sum of the dark current and the signal current. However, since the total target storage capability is constant and the bulk leakage continuous; as the scan rate decreases, the dark current becomes as large or larger than the signal current itself and small variations in individual diode leakage would manifest itself as signal modulation. Therefore, in slow-scan operation, it would be essential to operate either of these sensors using passive cooling to maintain the target region from -10 to -25°C where the dark current would not be significant compared to the signal current at the anticipated scan rates.

4.8.3 Form Factor

There are few available sensors which meet the exact photoheliograph format of 30-mm diagonal and a 21- by 21-millimeter square format. However, table 4-2 gives the parameters for several sensors which approach the requirement sufficiently close to serve as a guideline. The volume is the least variation between sensors at a change of about 4:1. The SEC and the ISS obtain their signal gain by energy acquired by the photoelectrons and have very high voltage electrostatic lens sections compared to the photomultiplier and photoconductive target sensors. On the other hand, the photomultiplier sensors have several more dc levels required for the multiple dynodes in the photomultiplier section. All the sensors except for the FPS vidicon are magnetic deflection and magnetic focus in the reading gun section. This represents the majority of the power used in the sensor. The amount is determined by the field strength required, the sensor dimensions, the coil L/DCR ratio, and other factors. Typically, for a slow-scan system, this might be 2 to 6 watts for the ID's 22 gauss focus field to 50 watts or more for the shaped high-intensity field required by the RBV. The

TABLE 4-2

SENSOR SIZE AND COMPLEXITY COMPARISON

Sensor	Input Diagonal (mm)	Length (in.)	Diameter (in.)	No. of Voltages*	Maximum Voltage (kV)	Deflect	Focus
II	40	17	3.06	18	1.7	Mag	Mag (70 gauss)
ISS	40	13.5	4.0	9	10	Mag	Mag (30g)
ID	35	12.75	2.25	15	1.5	Mag	Mag (22g)
P	40	12.25	2.25	9	2	Mag	Mag (40g)
V	28	8.9	1.75	8	1.5	Mag	Mag (40g)
SV	Not available						
FPS	60	21.5	3.155	9	3	Elect.	Mag (20g)
RBV	30	7.8	2.34	15	2.5	Mag	Mag (125g)
SEC	40	13.5	4.0	9	10	Mag	Mag (30g)
I	28	4.1	3.3	2	16	-	Elect.

*Included are all grids, dynodes, targets, focus and deflection voltages.

electrostatically deflected FPS vidicon is the most efficient sensor, requiring only about 2 watts for its focus field.

The IV combination is the smallest and requires less voltages than any other candidate shown and quite closely matches the photoheliograph input size requirements. The present version would clip off each corner due to the less than 30-min diagonal, but it is hoped that this increase could be obtained in the same physical size. If not, a 36-mm diagonal version exists without the slow-scan phosphor, and this could be adapted to later versions if required.

4.8.4 Television System Complexity

All of the sensors considered would use a similar block diagram for the primary video chain with variations in the peripheral circuitry. Most of the additional circuitry is the fixed dc required by the image sections or photomultiplier sections of particular sensors. All but the RBV sensor would use a continuous scan system with either continuous exposure or shuttering during a "no beam" frame. The RBV sensor has lag values which

normally do not decay on a continuous scan basis within the recycle time of the photoheliograph equipment. Therefore, a special erase/prepare cycle would increase the complexity and power consumption of a system using this sensor.

4.8.5 Sensor Qualifications in Space

Every sensor considered except for the RBV has been qualified in a space hardened version and then successfully used in a space system. The RBV is being built in a space-hardened version, of proper dimensions for the photoheliograph experiment, and it is scheduled for a launch in the Earth Resources Technology Satellite. Therefore, while system complexity, sensor size and fragility, and/or power consumption may be a strong factor against the use of a particular sensor, none can be rejected as unusable for space. The RBV in its present design, however, does not have the capability of erase/prime in a sufficiently fast time to allow 3 seconds between frames. Work is in progress to reduce the time required for erasure and may be obtained successfully by the time period of the photoheliograph.

The recommended IV combination has been designed for use as a slow-scan, high-resolution sensor for the JPL Viking Orbiter program. Although this particular sensor has not had a actual space mission, it follows on the success of many vidicons in space and has successfully passed stringent environmental tests to qualify for its purpose.

4.9 CONCLUSIONS

Based on the results shown in this section, the intensified vidicon (IV) is selected as the optimum sensor for use with the 65-centimeter photoheliograph. It rates the highest in signal-to-noise ratio and has simplicity of design and external system requirements. Its resolution is exceeded only by the RBV, and this difference decreases if the intensifier is used with both; the intensifier is required for the visible camera and possibly for the Hydrogen Alpha camera. The RBV, however, requires complex electronic circuitry, higher power, and still cannot meet the frame times and recycle times required by this program. The IV has marginal worst case sensitivity if the spacecraft stability requires short

exposure times but it gives overall best operation available from the present state of the art in electronic imaging. Film sensitivity is also marginal, at least at fast shutter speeds. Thus the success of the mission requires a certain minimum level of spacecraft stability or IMC within the photoheliograph.

Finally, the availability of the IV, as a space-qualified sensor for a program comparable in its slow-scan, high-resolution requirements, makes it available now for an actual EIS to demonstrate its compatibility with the photoheliograph.

5. ELECTRONIC IMAGING SYSTEM

5.1 INTRODUCTION

Previous sections of this report have defined the solar input to be studied by the experiment: The photoheliograph, which serves as the primary instrument for the experiment; typical spacecraft, which might carry the experiment; the data link, which stores and conveys the experiment results; and the basic electronic sensor, which converts the photoheliograph output into electronic information. This section is devoted to first defining a television subsystem which will allow the selected sensor to form the electronic image. The second portion is the full Electronic Imaging System (EIS), data recorders to store data, a data line for transmission, and finally the data-link interface. The EIS then allows information to be transmitted and the storage space made available for additional electronic images.

Once the initial criteria are determined by the Principal Investigator for the photoheliograph experiment, the television subsystem can be accurately defined with minimum consideration to the vehicle which will carry it. Thus, the resulting system will be adaptable to different vehicles with little modification required.

The full EIS interfaces directly with the vehicle and downlink equipment, and certain considerations cannot be totally defined until the total program is defined. However, much effort has been done to define a Skylab B/ATM B mission, and the planning can be utilized on programs that may evolve in the future. Therefore, the EIS defined here optimizes the information output of the photoheliograph television subsystem as interfaced with the oboard storage/downlink telemetry/on-ground tracking and storage capability planned for the Skylab B/ATM B space vehicle.

5.2 TELEVISION SUBSYSTEM

5.2.1 General

The photoheliograph program requires three separate television cameras to record occurrences on the sun in a simultaneous or near-simultaneous exposure. Although each of the cameras record information from a different wavelength of light, the majority of the separating conditions are similar. Since this is the case, it is desirable to design the cameras so that they are nearly identical. The visible camera and the Hydrogen Alpha camera will be identical and interchangeable with adjustments in neutral density filters and/or gain changes to adapt to the different levels in intensity of illumination. The ultraviolet camera will have the identical electronic package and a similar sensor, but the short wavelength requires a change in photocathodes. This change and its results are discussed in paragraph 5.2.3, but all other discussion in this section applies to all three cameras.

5.2.2 System Description

Two possible modes of operation will be described with their advantages and disadvantages. Both concepts can be described with the same block diagram shown in figure 5-1 since the only differences between the two occur in the synchronizing generator and the final output format. It should be recognized that this diagram differs little from many normal television cameras. The extra blocks and the changes within standard blocks required to change the normal concept into a slow-scan, high-resolution scientific recording camera will be discussed in detail. Figure 5-2 describes the basic internal timing diagram for the approach which presently appears most satisfactory.

5.2.2.1 Video Chain

This portion of the camera consists of the preamplifier, postamplifier, horizontal aperture correction, video clamp, video mixer, and the video output stages. It is primarily an analog amplifier whose purpose is to give voltage and power gain to the signal current from the vidicon. The basic

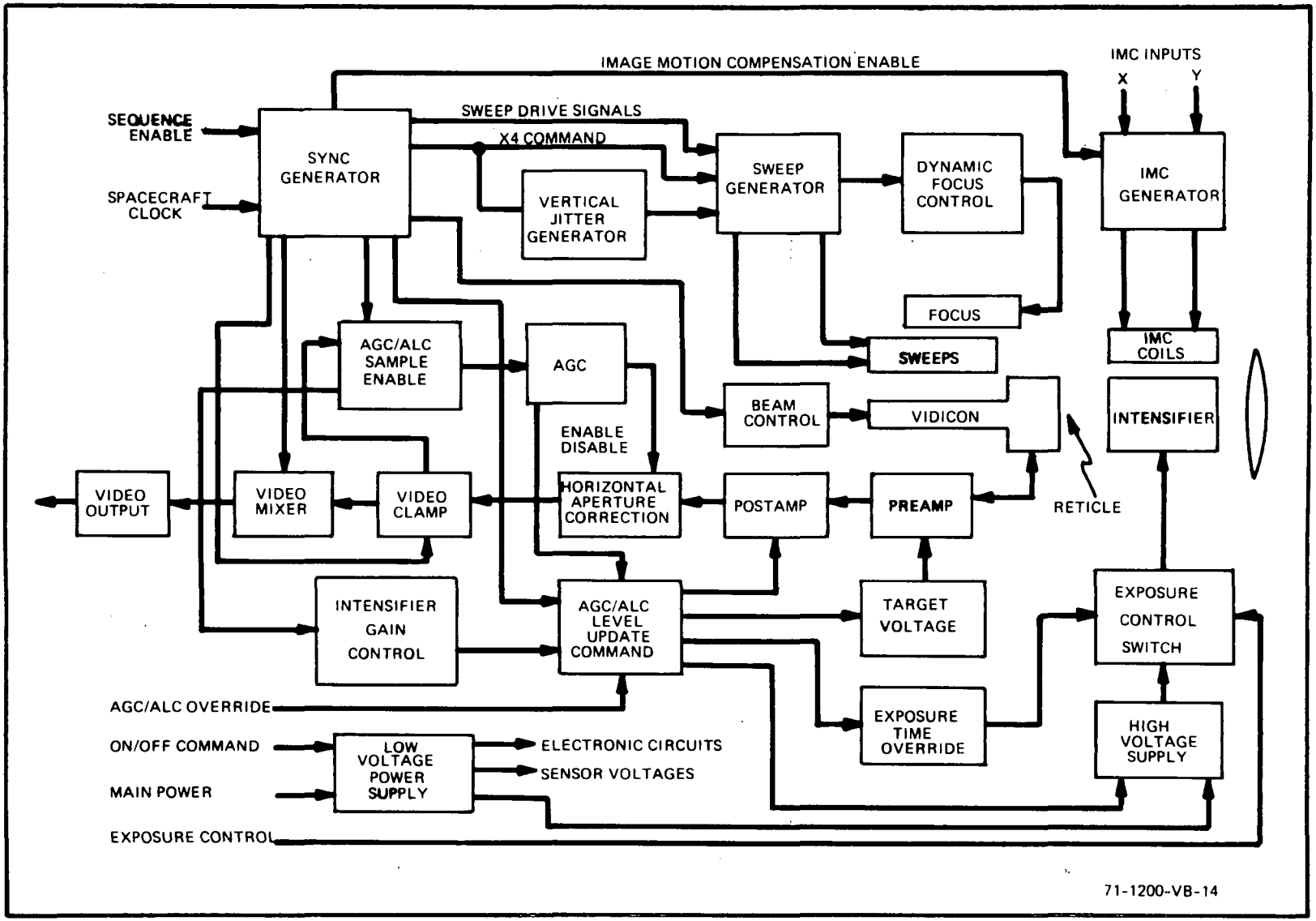

Figure 5-1. Single Photoheliograph Television Camera Block Diagram

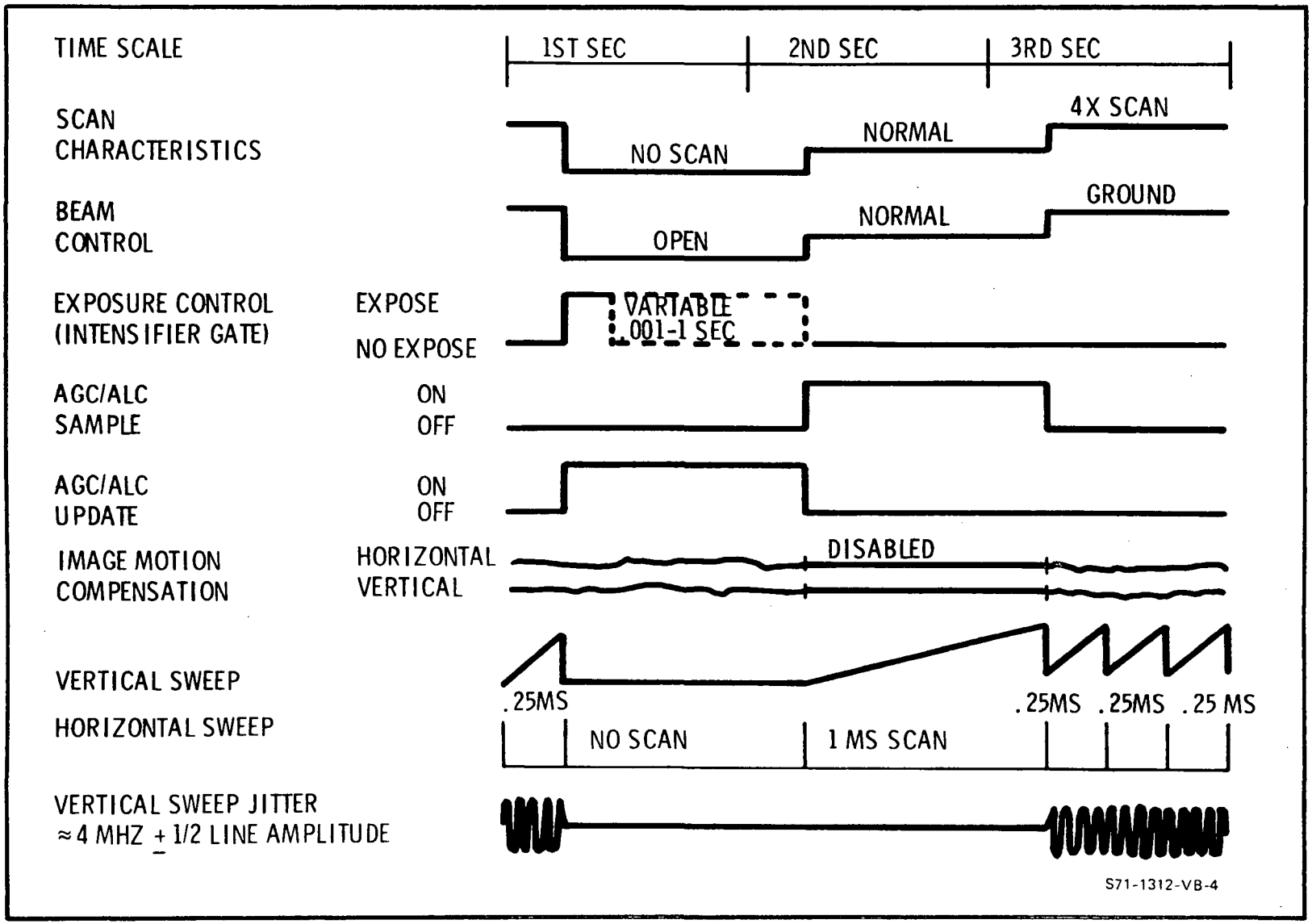

Figure 5-2. Single Photoheliograph Camera Interval Timing Diagram

criteria for a low-noise preamplifier was discussed in Section 4 and must be adhered to for optimum signal-to-noise ratio. The overall gain must have a flat frequency response with any phase shift constant over frequency so as to not distort the vidicon signal current. Note that individual lead and lag corners are acceptable as long as the output gain is constant with frequency and is achieved with linear correction. Normally, the sensor distributed capacity and the preamplifier lead resistor make a low-frequency lag which is corrected by a lead in the preamplifier. Often, an additional lead is inserted in the postamplifier to compensate for lags in the video output driver.

The horizontal aperture correction circuit introduces a gain variation into the video to compensate for reduced high-frequency response of the sensor itself. Figure 5-3 is an MTF curve of the intensifier, video, and IV combination described earlier. In addition, the video bandpass is shown when modified with the maximum value of aperture correction usually available. The final video output MTF is shown after the initial sensor output is operated on

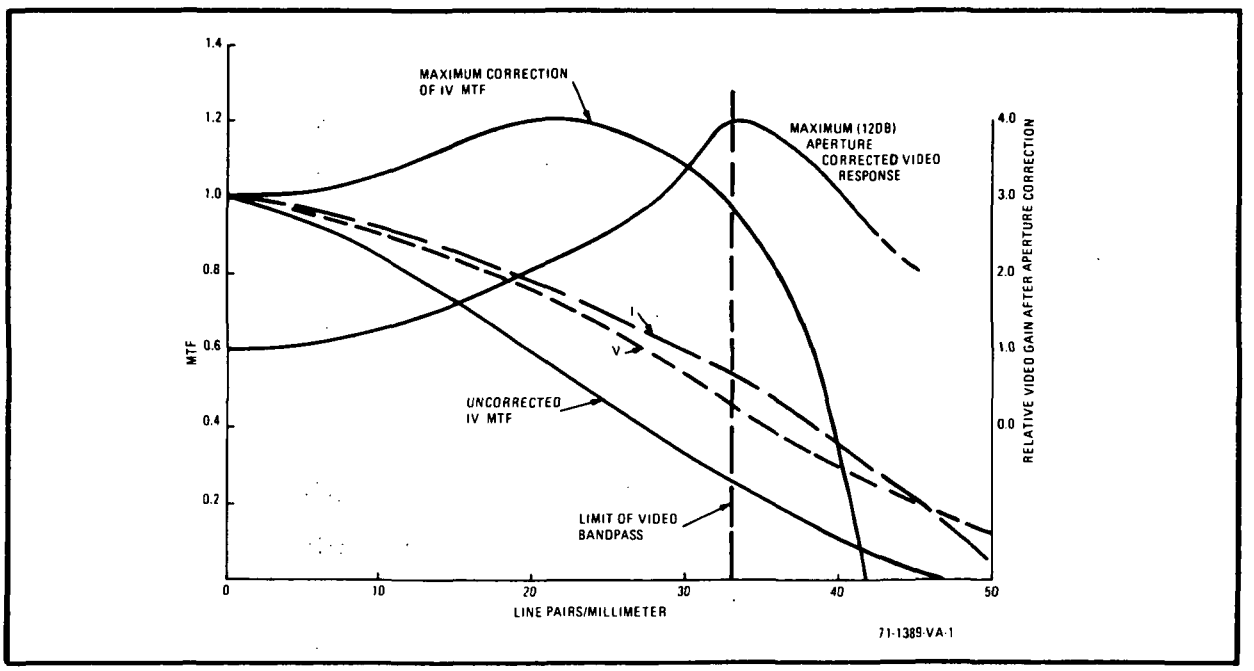

Figure 5-3. Individual and Composite MTF's

by the aperture correction circuit. The maximum value shown is in excess of that usually desired and would be adjusted down until the peak is near 100 percent at 20 lp/mm and some 70 to 75 percent at 33 lp/mm. The center of the aperture correction is a fixed value which should be selected based on the typical sensor's MTF and the video bandpass used. However, the maximum gain of the correction network can be made variable to best approximate the desired MTF for each individual sensor.

It can be shown (reference 13) that a dissipationless delay line has the following characteristics:

Impedance $Z_o = \sqrt{L/C}$

Propagation Velocity $\nu = \frac{1}{\sqrt{LC}}$

Propagation Delay $T_d = X\sqrt{LC}$

Since the above equations are independent of frequency, the time delay is a function of delay line length only and is independent of frequency. Thus, if a circuit is built such as is shown in figure 5-4, its input/output equation can be written

$$e_{out}/e_{in}G_2 = \left(1 - \frac{G_1}{G_2} \cos \beta \ell\right) e^{-j\beta\ell}$$

and the resulting gain versus frequency response is shown in figure 5-4b.

The video clamp circuit is essentially a dc restorer circuit to reset the proper black level of the video which will shift in the ac coupled video chain with various signals or change with temperature becuase of the sensor's dark current. The clamp should be operated on a line-to-line basis.

The video mixer adds the digital format required to operate the video monitors and maintain a proper time sequence of events. Any internal test signals would also be inserted into the video by this circuit.

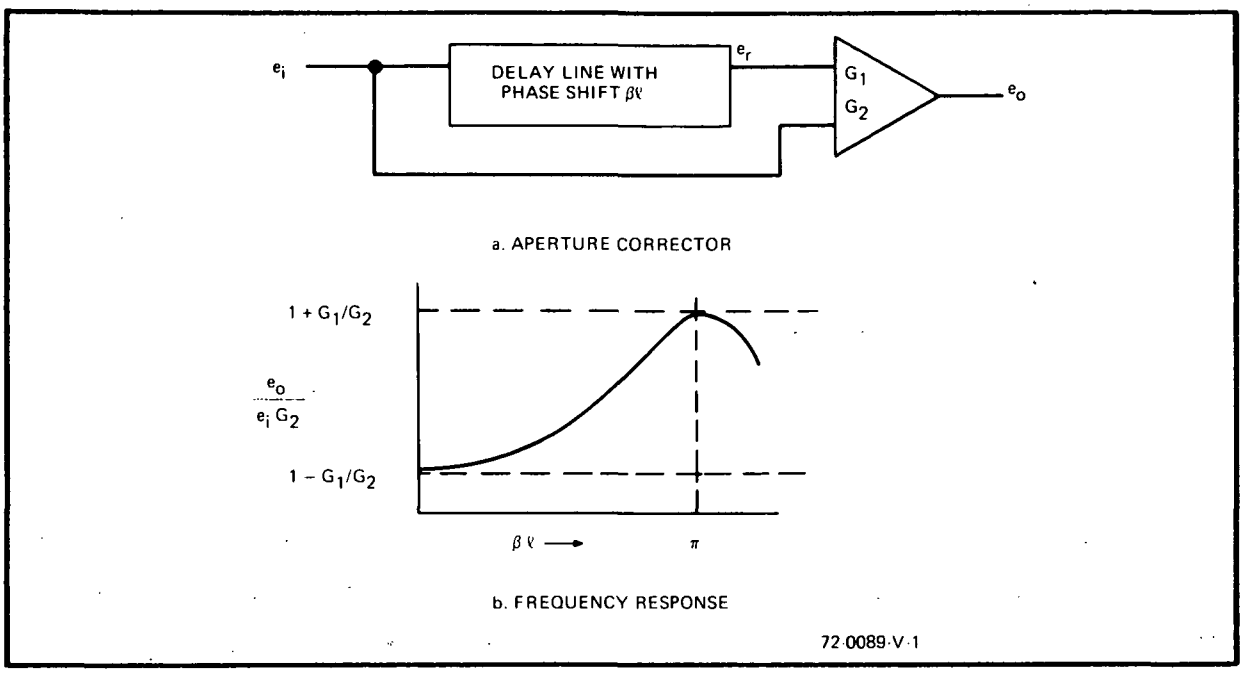

Figure 5-4. Characteristics of Aperture Correction with a Dissipationless Delay Line

One deviation in this particular video chain is its bandwidth and cutoff characteristics. The television subsystem's bandwidth must be flat to the diffraction limit of the photoheliograph. Then, to minimize noise and to reduce telemetry and tape recorder bandwidth, the cutoff must be extremely sharp. Since the overall MTF is high at the cutoff frequency, the phase shift caused by the sharp cutoff must be corrected by phase correction circuits.

A question that may arise is what happens to the overall MTF of a sensor if it is limited by the video bandpass. First, the cutoff has no effect on any sinusoidal information less than the cutoff limit of 33 lp/mm. Secondly, the MTF curve, which is based on a square wave target will be reduced by the information which is lost due to the sharp cutoff. A square wave can be represented by a series of the form:

$$4/\pi \left(\sin x - \frac{\sin 3x}{3} + \frac{\sin 5x}{5} - \ldots \frac{\sin nx}{n}\right)$$

Thus, the net MTF of a square wave is the value of the harmonic in the series times the response of the sensor at that resolution. Referring to figure 5-3, it can be seen that the third and fifth harmonic values contribute little to the result and can be neglected.

Finally, it must be remembered that the photoheliograph itself has reduced the MTF to its diffraction limit at 33 lp/mm and thus there is little chance of the input illumination being a square wave in the actual EIS.

5.2.2.2 Deflection, Focus, and Sensor Controls

A vidicon is basically simple to operate with all but the control grid voltage maintained at a constant dc volts for all operation after initial adjustment. The sensor cathode is switched between two fixed voltages: ground for normal scan time when the video information is being read from the target and a voltage which is positive with respect to the storage target during line-to-line retrace.

The beam control grid is operated at those different levels as shown in figure 5-2. First, during the full exposure cycle, the beam is open so that no information is lost. Next, the beam is switched to the level found to give sufficient discharge of the target and maximum resolution during the single frame readout cycle. Last, the beam is grounded to give maximum discharge current for the four erase frames to minimize any residual signal.

The sweep deflection circuits are magnetic, and both should be driven type with feedback to provide maximum stability and resolution. It is not anticipated that any nonlinearities will be introduced by the sensor or the surrounding components so that if the sweep drive is linear and a high-quality deflection yoke is used, there will be no need for any special linearity correction circuitry.

Dynamic focus control is likely to be required due to modifications to the beam energy by the deflection field and thus slight changes in the beam landing characteristics. Since most of this error is caused by the deflection

circuits and is symmetrical to the sensor, a satisfactory dynamic correction is obtained by using a portion of the deflection circuit, changing the shape of one-half to make a triangular waveform, performing an integration to smooth the waveform, and then add the result into the dc focus field to obtain best overall focus.

5.2.2.3 Synchronizer

The circuit shall consist of all digital microcircuitry for both accuracy and reliability. It would receive its basic input from the spacecraft clock and would be controlled by external command sequences yet to be established. Its output signals would control all the functions shown in figure 5-1 plus all the subtiming required by that circuitry. It is also anticipated that a space-qualified television subsystem would contain a variety of internal monitoring signals which would be keyed by the synchronizer into the video format automatically. The synchronizer will generate and insert into the video all signals required to give necessary timing information to the recorders, telemetry, and, finally, the information analysis equipment so that a known sequence of events is maintained.

5.2.2.4 Automatic Illumination Controls

The illumination seen by the EIS will vary as much as two or three orders of magnitude over the experiment and it will be important to both maintain the video level constant and to record accurately the change in illumination. This control is primarily obtained by changing the intensifier gain or by exposure time variations. Secondary controls of automatic gain control and vidicon target voltage control can provide additional range at the cost of certain side effects. Finally, it is equally important to place in the video output signals representing the gain changes so that the absolute illumination can be found. A calibrated source such as a light-emitting diode would be commanded into the field of view for internal gain calibration at appropriate times such as at the beginning and end of each active EIS time.

The exposure control is obtained by gating the focus grid of the triode intensifier. This gate width can readily be operated from less than 1 millisecond out of the full exposure time of 1 second. Use of maximum exposure time will probably be limited by the spacecraft stability or the full range of automatic control could be obtained by this mode of operations.

The second gain control method is to control the high-voltage cathode of the intersifier. A reduction in this voltage can reduce the intensifier gain from its maximum value of 50 to 5 or less with little effect on resolution.

Automatic gain control (AGC) within the video chain is a third way of maintaining video output constant, but it is obtained at a cost of signal-to-noise ratio. However, consider that the total noise consists of the noise in the television subsystem plus that in the data recorder, telemetry, and the ground recorder. Thus, if the illumination falls below a level where the exposure control and intensifier gain can increase it at the desired level, it would be desirable to increase the video amplifier gain at a reduction in signal-to-noise ratio within the television subsystem to prevent a much greater loss in signal to noise external to the television subsystem.

Finally, the photon conversion efficiency of thevidicon is a function of the applied target voltage. However, the increase in gain with an increase in target voltage also produces an increase in dark current which often shows as a shading effect on the video and also causes an increase in lag or residual signal. A decrease in target voltage reduces gain but also reduces storage ability which results in a loss of contrast. Thus, this method of gain control is essentially an emergency override in the case of an extreme solar event or some unanticipated deterioration in the overall system capability and it would not be used in any form of normal operation.

The method by which these gain controls are determined and then used is a problem considerably different from the normal television camera and it depends on large part on the use of the particular camera on a frame-to-frame basis. Consider the difference between a standard television camera

which scans continuously at a rate usually much faster than the rate of change of the scene under observation as opposed to the photoheliograph television camera which has video only 33 percent of the time and whose video may change considerably on a frame-to-frame basis.

The first assumption that must be made if the scene changes between two successive frames, then control must either be from a predetermined fixed setting or from astronant command. It would not be possible to have control within a single frame since that control would itself modulate the video output. If there are multiple frames of the same or similar illuminated scenes, then it is important to move from either saturation or noise level as quickly as possible to minimize any loss of information. The method which seems optimum would have a sample and hold circuit to store a single frame of video. This signal would be compared by a double threshold; one at about 70 percent of saturation and the other at about 30 percent of saturation. Then, the AGC/ACC step size would be determined by the amount of deviation and the dynamic range within the video. Since the dynamic range in the video wall be 40 dB or more, a scene which exceeds either threshold for 100 percent of a frame would necessitate a 20 dB or larger step between frames. Lesser differences would cause successively smaller steps until the differential weighting requirement is satisfied.

The exposure control has the largest range and would make any large steps with fine control obtained from the intensifier high-voltage control. It is assumed that the other gain controls discussed will not normally be used, but, if the situation arises, the target voltage would be reduced for illumination above the range of other controls while the video AGC would be used to increase amplifier gain for very low illuminations.

The values described here are anticipated to be in excess of the actual requirements since the solar energy and photoheliograph are reasonably well defined and most extreme changes can be anticipated so that the video gains will be changed by command. However, it seems mandatory on a

mission of this expense and importance, to maximize the capabilities of the instrumentation where possible.

5.2.2.5 Image Motion Compensation

Figure 5-1 shows an image motion compensation circuit which would allow a certain amount of correction to the photoelectrons in the intensifier section. Although the capability has been demonstrated for the recommended intensifier, the accuracy and range have not been evaluated. It is likely that correction of more than a few percent would not be feasible, and since the correction is at the television subsystem, the photoheliograph must not shift sufficiently to move the format more than a few percent of the format width. Finally, the entire concept depends on an external sensor to determine and generate the error inputs to the television subsystem.

5.2.2.6 Secondary Approach

The timing diagram of figure 5-2 maximizes the data storage capability since the output of the three cameras occurs one after the other. However, the exposure times of the three cameras are not simultaneous, but instead each camera is exposed sequentially over the 3-second total cycle time. It has been presumed so far that the change in solar activity or the motion of the photoheliograph does not sufficiently change the scene in a 3-second period as to disallow comparision of the three cameras. It is also assumed that the improved data storage would be desirable.

The alternate solution would not change any of the previous discussion, although it has a relatively strong impact on the synchronizer design for the television subsystem and requires a few additional considerations from the system. Basically, the change consists of having a exposure frame during which all three cameras are exposed simultaneously. After this has occurred, the full sequence previously described would occur. This change would cause two difficulties. First, there would be an immediate loss of 33 1/3 percent of data handling capability since the data is recorded on video tape and cannot be turned on or off at these rates. It is possible that this

dead time could be utilized by other experiments or housekeeping information so that the time is not lost. The second problem is that the simultaneous exposure requires that the information stored on the sensor's storage target will be there for an average of 1/2 second for one camera, 1 1/2 seconds for the second camera, and 2 1/2 seconds for the third camera. The particular vidicon recommended for the mission meets or surpasses a requirement of more than 80 percent of stored information remaining after 10 seconds so the problem does not exist for this sensor but it remains a consideration for the decision.

5.2.3 Ultraviolet Television Subsystem

The wavelength of illumination to be viewed with the ultraviolet camera necessitates special considerations for this camera. The combination of fiber optics/S-20 photocathode used with the other two cameras will not operate at the 2200-Å wavelength. As can be seen in figure 4-16, it is the fiber optics and not the S-20 photocathode which cannot meet the requirement. However, the fiber optics are used to make the normal curved surface of the photocathode of an intensifier appear as a flat face to the photoheliograph focus field. This would not be obtained with the sapphire/S-20 combination, and, to be usable, the intensifier would have to be lengthened to decrease the curvature required of the photocathode.

A second and more feasible alternate is to use the vidicon without an intensifier and with the ultraviolet photoconductive surface shown in figure 4-15. This is possible because the comparatively wide (100-Å) filter gives more illumination to the ultraviolet camera than the other cameras. Also, the width and the fixed nature of the filter make the illumination more constant thereby allowing the loss of the gain range obtainable by varying the intensifier gain.

Thus, the only significant change for the ultraviolet television subsystem is a change in the photosensitive surface of the sensor and a possible omission of the intensifier.

5.3 SYSTEM CONSIDERATIONS

5.3.1 Introduction

The electronic imaging system includes the television subsystem, the astronaut/ground control system, the data storage devices, and the downlink telemetry interfaces. In general, only portions of the total system will be part of the photoheliograph program, and the rest will be included in the spacecraft data management subsystem. Therefore, the system described here is not recommended as a final system but only as a representative system which would satisfactorily record the output data from the photoheliograph experiment.

5.3.2 System Description

Figure 5-5 illustrates the block diagram, and figure 5-6 shows the two possible timing sequences likely to be used to record and telemeter data.

The left side of the block diagram contains the three television subsystems and the timing inputs necessary to obtain the operation described previously. The camera control unit can be controlled by the astronaut or ground control to generate outputs every 3 (continuous), 32, 256, 2048 seconds, etc. The circuit should also contain an automatic output for any time the sun moves out of the format. Figure 5-6 shows the continuous and a 32-second cycle timing diagram. The START and STOP sequences are those anticipated for the ERTS analog recorder, and these times obviously affect the total data storage capability of the system since start and stop times do not have any data stored. Actually for redundancy and to allow time for automatic gain control corrections, it might be more desirable to record two or three full sequences of information per recorder On time rather than the single sequence illustrated. Since the full START/RECORD/STOP sequence takes 16 seconds for one full sequence of the three cameras and only 22 seconds for three full sequences of the three cameras, the above possibility should be considered.

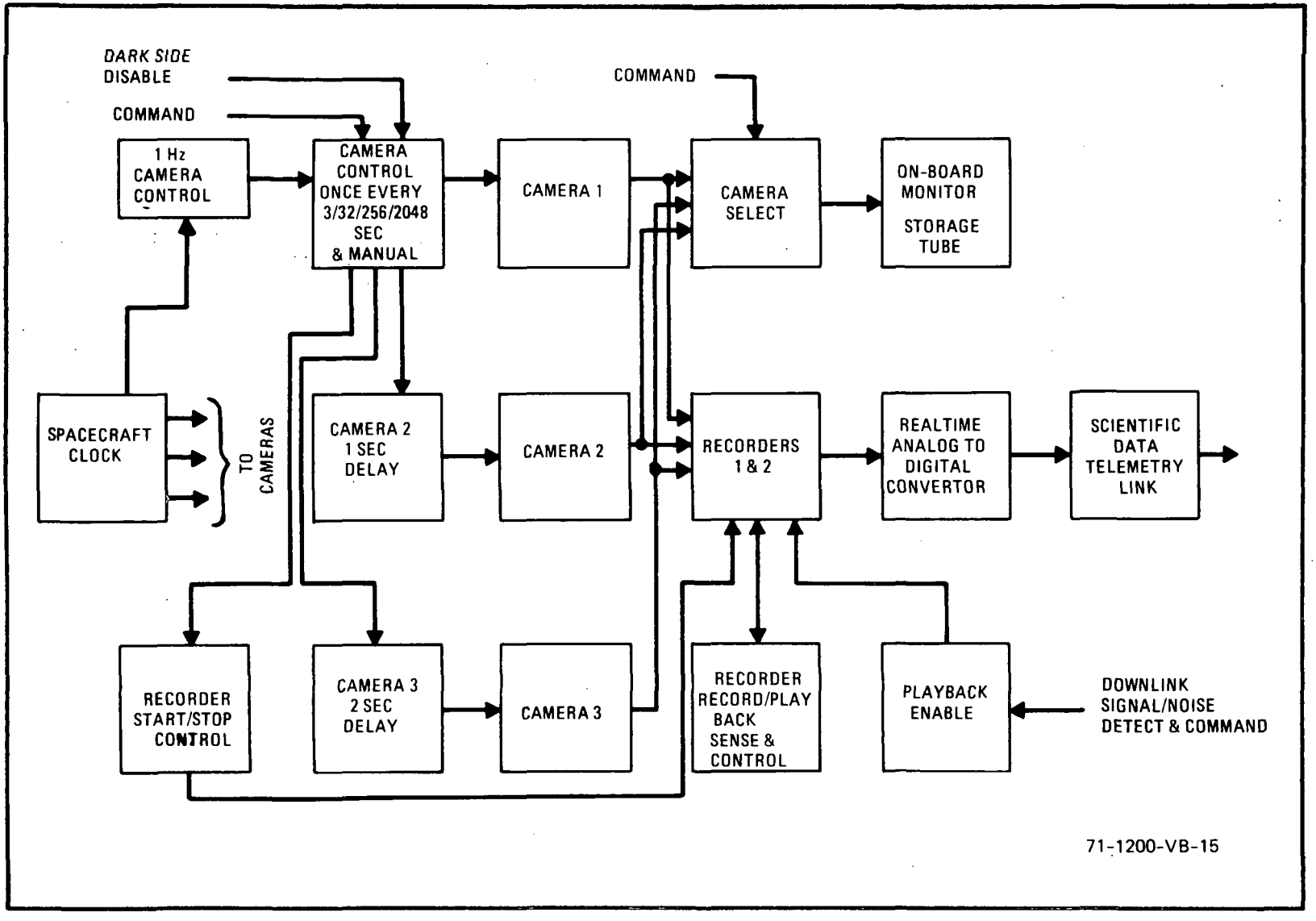

Figure 5-5. Photoheliograph Electro-Optical Sensor System

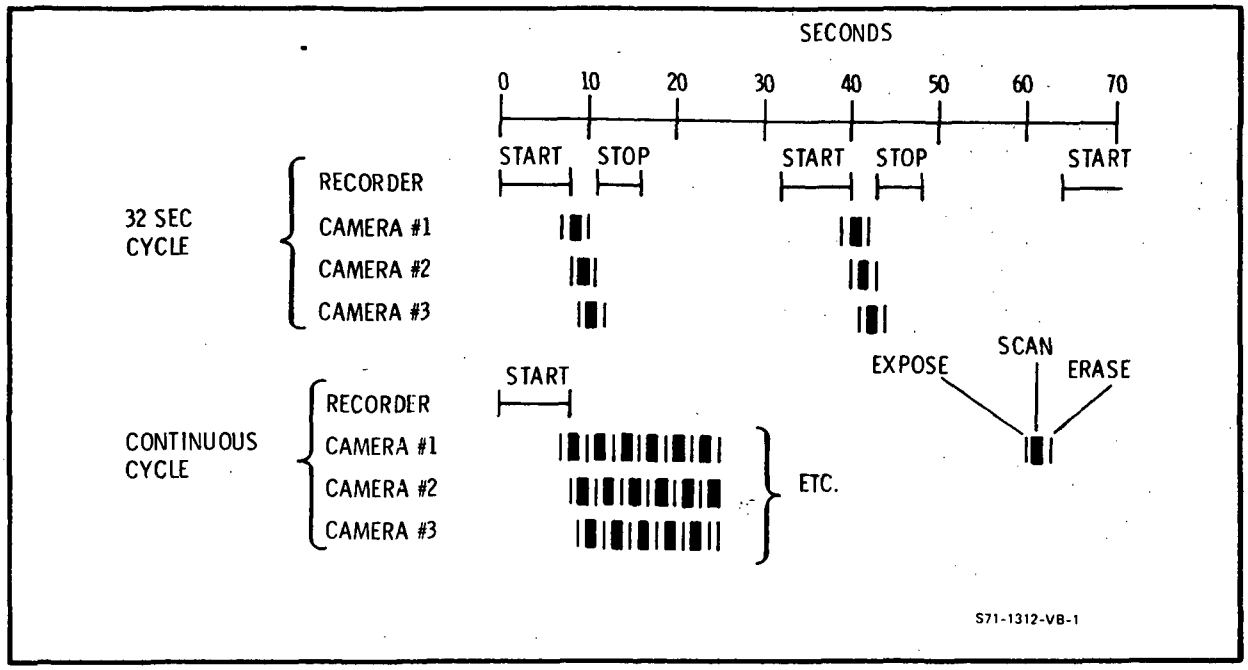

Figure 5-6. Timing Diagram for Photoheliograph Electro-Optical Sensor System

The lower right blocks include the data storage, telemetry interface, and the playback/record sensing and switching controls. This general system has been previously described in paragraph 3.1.3 and will not be repeated except that the basic requirement is that the system contains two recorders so that record and playback can be obtained simultaneously when required.

The remaining component of the EIS is the astronaut's onboard monitor. Since the television subsystem is a slow-scan system which is difficult to read directly, a direct view storage tube monitor provides a display which is readily readable and should satisfy the pointing and control requirements of the monitor. The camera select unit would allow the astronaut to first determine which of the three cameras he wanted to view. Then he could select the update time for the monitor from no update to updating every repeated frame of information. The resolution capability anticipated for this unit would be less than the EIS capability but should be more than sufficient for pointing and focus control.

6. CONCLUSIONS AND RECOMMENDATIONS

6.1 CONCLUSIONS

The net result of Sections 4 and 5 of the study is that an electronic imaging sensor is available for the present photoheliograph program and that an electronic imaging system can be built to meet the objectives of the photoheliograph program. A second result is that a sensor and system improvement must occur to be fully compatible with the objectives of the 1.5- and 3.0-meter photoheliographs. Part of this growth would be obtained in sensor development. Appendix A describes an overall system consideration distinctly advantageous for the electronic imaging system and large-scale telescopes. The greater storage and telemetry requirements of future telescopes are compatible with anticipated volume and power growth factors of future space vehicles. Thus, it is concluded that electronic imaging systems are now and will be available for the anticipated requirements of high-resolution, visible space telescopes.

Returning to the present system, the details of the television subsystem are summarized in table 6-1. The information contained in the table applies to each one of the three television subsystems except for slight changes in the ultraviolet camera due to the change in photosensitive surface on the intensifier. The form factor values listed under Mechanical Characteristics are conservative but are not necessarily final values. The actual values would be modified to some extent to meet the photoheliograph detail form factor values.

The characteristics of the other portions of the electronic imaging system, such as the astronauts' monitor, the recorders, telemetry, and television control circuitry, cannot be accurately described until the exact space

TABLE 6-1

DETAILED PARAMETERS
ELECTRONIC CHARACTERISTICS

Intensifier	
Generic Type	Electrostatic/Gated
Photocathode Type	S-20/Fiber-optics
Photocathode Sensitivity	See figure 4-15 (curve 1)
Photocathode Size	28 mm Dia
Magnification	0.94 to 1.0
Gain	50 watts/watt max.
Output Phosphor	P11/Fiber-optics
MTF at 33 lp/mm	54%
Sensor	
Type	Fiber-optic input, slow-scan Vidicon
Deflection	Magnetic
Focus	Magnetic
Photoconductor Size	30 mm Dia
Photoconductor Sensitivity	See figure 4-15 (curve 3)
Gamma	0.9 to 1.1
Storage Ability	>95% at 9 seconds
Signal Current (Saturation)	3.3×10^{-7} A
MTF at 33 lp/mm	47%
System	
Frame Time	1 second
Line Time	666.67 μsec
Number of Lines	1,500
Vertical Duty Cycle	98%
Horizontal Duty Cycle	95%
Video Bandwidth	1.1 MHz

TABLE 6-1 (Continued)

Aperture Correction (adjustable) AGC/ALC Range	12 dB max at 1.1 MHz
Intensifier Exposure Control	0.001 to 1 second (60 dB)
Intensifier Gain Range	20 dB
Vidicon Target Gain Range	6 dB
Postamplifier Gain Range	20 dB
Noise current (no aperture correction)	3×10^{-10} A
Noise current (max aperture correction)	1.2×10^{-9} A
Signal to Noise (no aperture correction)	60 dB
Signal to Noise (max aperture correction)	48 dB
Net MTF at 33 lp/mm (no aperture correction)	26%
Net MTF at 33 lp/mm (aperture correction)	>70%

MECHANICAL CHARACTERISTICS

Volume (per television camera)

Length	18 inches
Width	6 inches
Height	6 inches

Weight (per television camera)

Approximately 30 pounds

Power (per television camera)

Approximately 40 watts

vehicle is specified since much of the circuitry will be shared with other systems. However, every consideration contained in Section 5 would be compatible with any space vehicle capable of utilizing the photoheliograph. The definitions used on this study were based on NASA studies for the Skylab B/ATM B system and, as such, match most projected programs.

6.2 RECOMMENDATIONS

The study has concluded that an electronic imaging system (EIS) can be built to meet the requirements of the photoheliograph program. Although the major assumptions used in the study are conservative, the reduction from theory to hardware always presents interface problems which are best found and eliminated at the feasibility model level. Furthermore, actual test results between film cameras and the EIS with the photoheliograph may resolve some of the questions which exist on the comparative value of the two methods.

Thus, it is recommended that a single EIS be built which would contain a single camera capable of full operation as either the visible camera or the Hydrogen Alpha camera. Since the study has indicated that all three cameras could be similar, most of the interface problems could be solved by this method. The ultraviolet camera has not only the sensor modification discussed in the study, but, in addition, the 2200-Å solar value would not be visible on Earth and a calibration source would have to be operated in a vacuum to prevent absorption by the air. To be useful, a high-resolution monitor would also be built to allow direct viewing of the results obtained from the special scan system. Finally, a modified video tape recorder should be obtained which would have the capacity to record at least several frames of video. This would allow testing of telemetry equipment, ground data handling equipment, and the data correlation computers for data analysis.

The initial testing of the EIS should be with calibrated sources to determine range and capabilities of internal functions such as signal-to-noise ratio, sensitivity, automatic exposure, and gain controls. At the conclusion of this test series, the recommended EIS would be capable of being mated with the feasibility photcheliograph already under test at California Institute of Technology's Big Bear Observatory. This series of tests should fully determine the correctness of the computations set forth

in this study and allow any changes required to build a space-qualified EIS for use with the 65-centimeter photoheliograph. At this point, the original EIS would be available for upgrading to the requirements of larger space telescopes.

A second recommendation is for the initiation of additional study on the actual values of spacecraft stability which will occur. Part of this study should specify the requirements of image motion compensation (IMC) within the photoheliograph, its reference, the accuracy required, the recycle time, and the total control time. An additional part should consider the lack of IMC and determine the imaging system's exposure times which would reduce the deterioration from spacecraft jitter to acceptable levels.

A third recommendation is the initiation of a study program which would directly compare film versus electronic imaging from an overall viewpoint including the spacecraft portion through data analysis and interpretation. The study should at minimum include comparable signal-to-noise ratio, sensitivity, resolution, total volume required of film camera plus film storage versus television camera and video recorders, on-ground data storage requirements, comparative data analysis and interpretation techniques.

APPENDIX A
SPECIAL OPTICS CONSIDERATIONS

Two characteristics of the possible television systems for the photoheliograph could require special optical systems within the television camera system. A decision on the necessity or desirability of either of these techniques will depend on the final configuration of the photoheliograph and the particular television system selected.

A. 1 ULTRAVIOLET CAMERA FLAT FIELD REQUIREMENT

The first system would apply to the ultraviolet television camera only and is based on the shape of the photosensitive surface of the television sensor. The difficulty is the unavailability of UV sensitive fiber optics which can couple a flat field format to whatever shape photosensitive surface is used by the sensor. Most photoconductive sensors such as the RBV, FPS vidicon, and other vidicons use flat photosensitive surfaces and present no problem when modified to UV sensitive glass. Magnetic intensifiers and imaging sensors also operate in a flat-to-flat focus plane and present no problem to the optics. However, if IMC is not used with the photoheliograph, the available illumination may be too low to use vidicons without intensification and the magnetic fields required by magnetic intensifiers or image sections require large amounts of power and also tend to interact with the deflection and focus fields of the sensor thus creating distortion and resolution problems.

The illumination levels found in the study for the 2200-Å camera indicate that a certain amount of reduced exposure time is obtainable with the selected vidicon with no intensifier but with the sapphire/ultraviolet photoconductor combination added. This is the optimum camera for the UV if the stability will permit its use.

The possibility of using an electrostatic intensifier or an ISS or SEC type sensor with an electrostatic image section must also be considered. This capability is slightly enhanced when a Gregorian telescope is used since its best focus field is convex and an intensifier of proper length could be designed to have a similar curvature for its photosensitive surface and still maintain high internal resolution. The increase in size to obtain an approximate flat field to flat field image in electrostatic intensifiers has already been developed by the EMI Corp of Britain but the quality is not sufficient for this program.

A reflective relay system could be implemented using a simple refractive element near the photocathode surface to provide field curvature as shown in figure A-1. The central obscuration of the relay system should be designed to match the obscuration of the primary telescope. This type of system would be rather large since the camera body must be smaller than the projection of the obscuration of the secondary mirror in the plane of the tube.

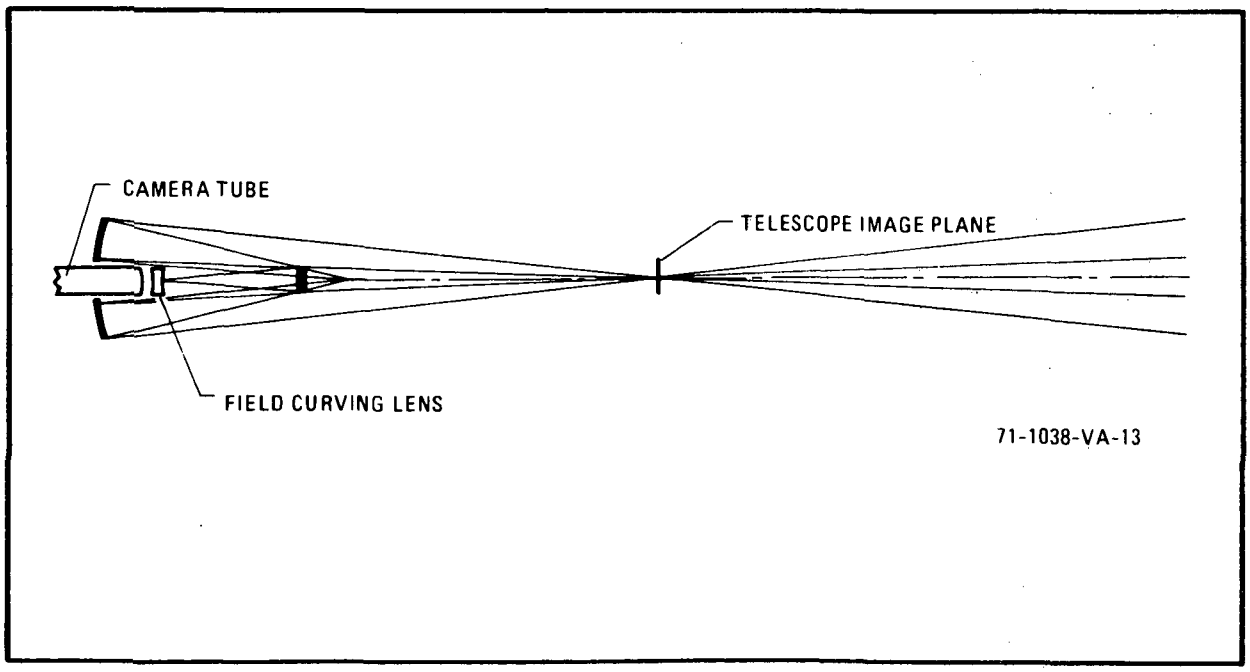

Figure A-1. Focus Plane Shaping System

A refractive relay optical system could also be used to perform this task and would have to be made of silica or perhaps calcium fluoride.

A. 2 INCREASED FORMAT OPTICS

The second optical consideration is a scheme to increase the effective resolution of the television systems and is applicable to all three cameras. Essentially, the idea is based on the fact that the resolution in line pairs per millimeter value is limited on most television sensors when compared to film, but the television sensor uses the same image plane rather than the large bulk required by larger film frames. Thus, it is suggested that the 21 by 21mm format be optically enlarged to a size compatible with the largest sensors made. Since 60mm diagonal sensors are not uncommon, a 2:1 increase in format could be used to obtain a 2:1 increase in the MTF versus line pairs per millimeter of figure 4-18. For purposes of using the existing configuration of the telescope with a TV camera of a 42 by 42mm format, a negative lens system such as the Barlow type could be used to expand the telescope format of 21 by 21mm to the 42 by 42mm format. This is graphically illustrated in figure A-2a. An alternative way of accomplishing this is by using a positive relay lens as shown in figure A-2b.

Both methods result in an increase in system focal length and an increase in geometric f/# by a ratio of 42/21 if the same FOV is maintained. The design of the lens system could provide for a flat image plane.

This study has indicated that a feasible electronic imaging system can be built within the constraints of the present 65-cm photoheliograph, so that the change to an increased format would be of little advantage and perhaps would decrease resolution by creating a more difficult focusing problem for the overall high f/# system. However, the study has also shown that electronic sensor growth is required to meet the objectives of the projected 1. 5- and 3-meter telescopes. Since the systems will be lower f/# systems, there will be additional illumination, and the increased format size will be of significant benefit to the electronic imaging system which is used with these instruments.

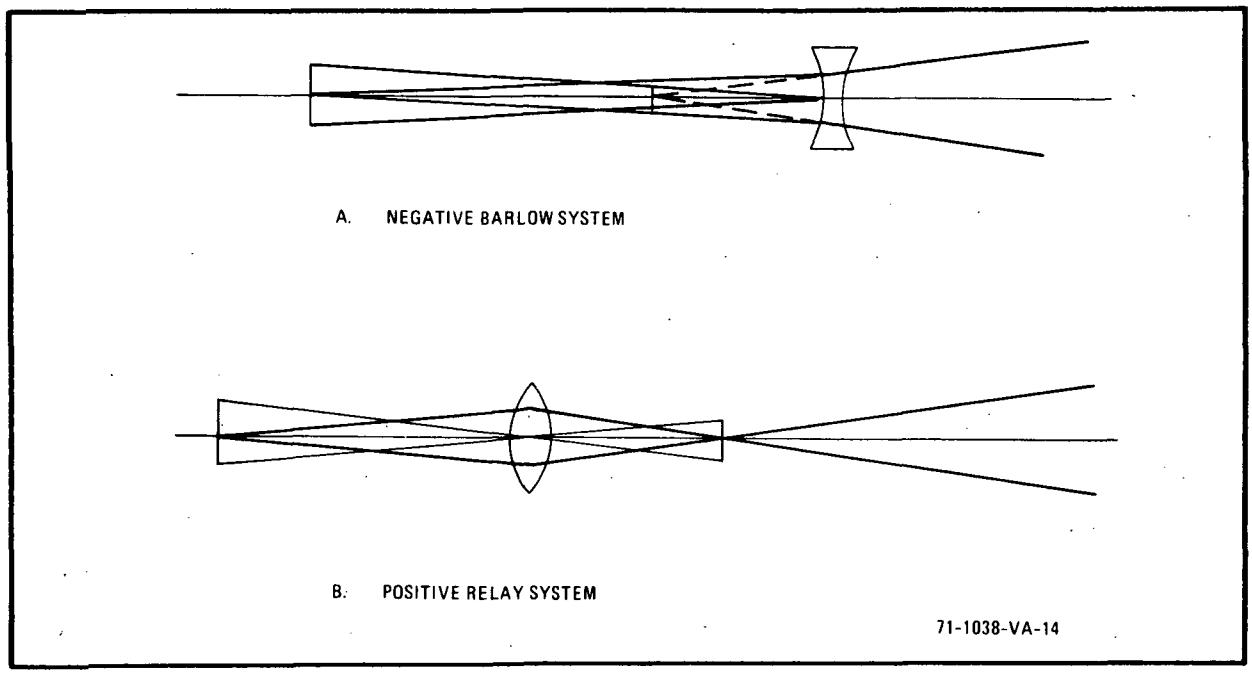

Figure A-2. Format Increasing Optics

APPENDIX B
FILM

A complete comparison of the merits of using television or film for recording images from the photoheliograph is outside the scope of this report, but a few important aspects will be reviewed.

B.1 SPECTRAL SENSITIVITY

Figure B-1 illustrates the spectral responses of Kodak film types 3400 and SO-392. Both curves have been transcribed from Kodak data sheets with the ordinate converted into watt · second/meter^2 to be compatible with the sensor data in this study. Type SO-392 is described as "Solar Flare Patrol" film and is optimized to be used with the Hydrogen Alpha band at 6563A, and as such would be used in the Hydrogen Alpha camera. Type 3400 is a Panchromatic film and as such would be used for the visible camera of the photoheliograph.

Both films above were plotted only to 4000 Å as this was the limit on the supplied data sheets. A special film, SO-212, is available for use down to the 2200-Å region and below and could be used for the ultraviolet camera with the photoheliograph. SO-212 is essentially the 3400 film but without a gelatin backing because the gelatin is UV absorptive and prevents the emulsion from being exposed. This gelatin removal, however, has the side effects of producing a brittle, hard to handle film which is highly susceptible to exposure by electrostatic discharge. Both of these difficulties are being investigated, but no information was available for this report.

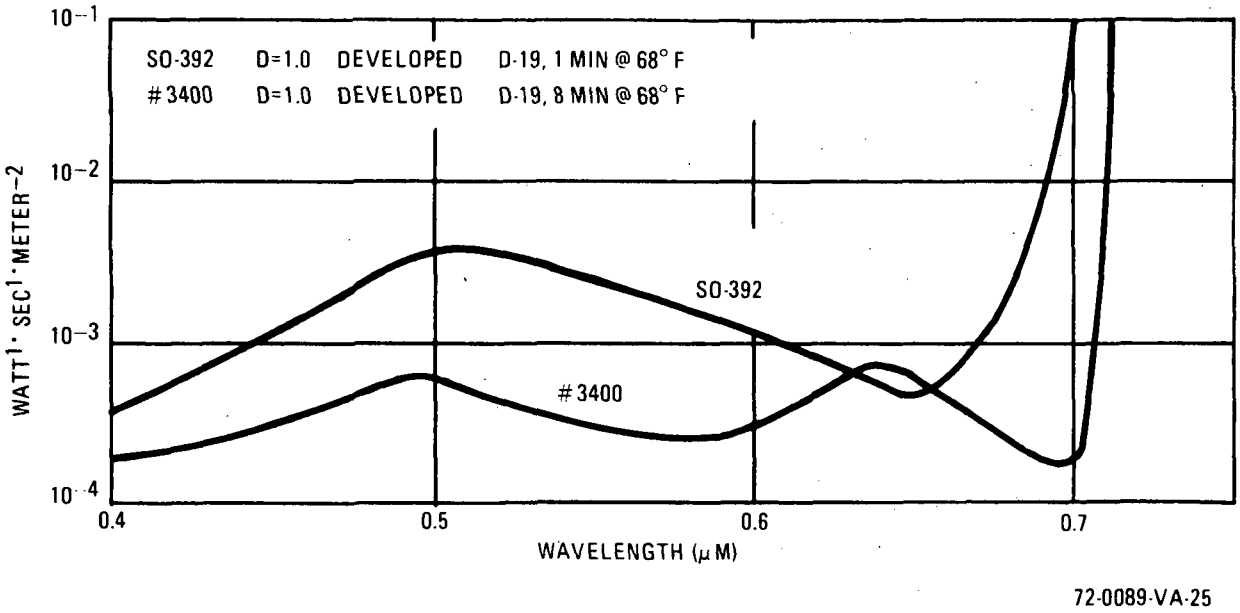

Figure B-1. Film Spectral Sensitivity Curves

B.2 ABSOLUTE SENSITIVITY

The purpose of this paragraph is to obtain an understanding of the comparable sensitivities of the electronic imaging sensors considered in this study with film. It is difficult to compare electronic imaging with film since many of the definitions differ. However, an attempt has been made by comparing the sensor's signal-to-noise ratio versus illumination curves with film density versus illumination. This comparison should be exact along the abscissa for a given film development criteria and the ordinate would be accurate for a low-base fog value. With this in mind, the ordinate of figure B-2 was computed in watt^{1} . second^{1} . meter^{-2} which is watt^{1} . meter^{-2} for a 1-second exposure. Figure B-2 then shows the signal-to-noise ratio of the electronic imaging sensors for a 1-second exposure to 5000-Å illumination. Since figure B-2 is for a film density of 1.0 and an exposure time of 1 second, this point can be transcribed to figure B-2 at

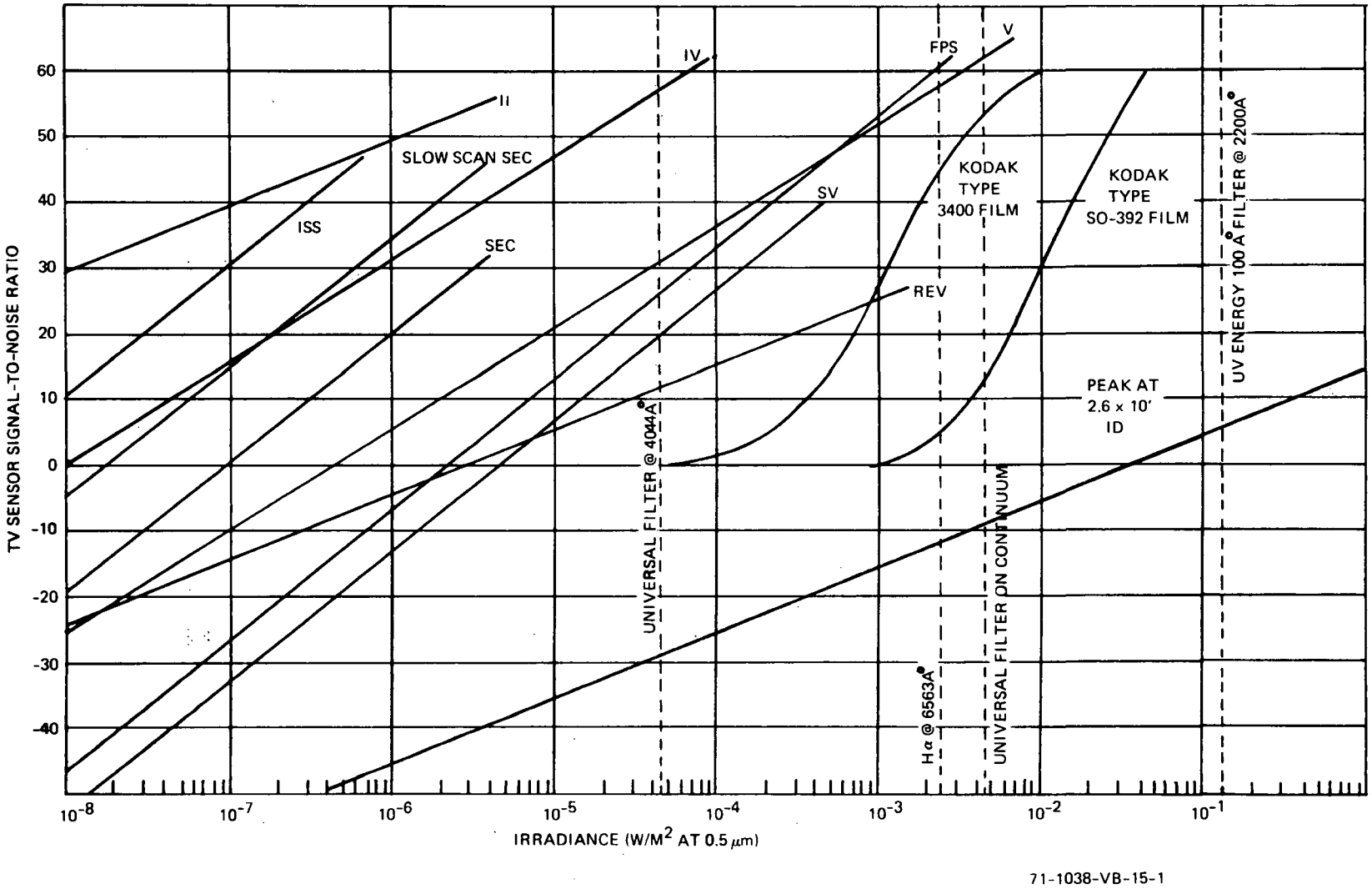

Figure B-2. Sensor Comparison by Signal/Noise for Photoheliograph, 1-sec Frame Rate, 1,000 TV Lines, 400-kHz Bandwidth

an ordinate value of 20 dB or slightly less for low-base fog values. The slopes of the curves are then determined from the film data sheet characteristic curves at the specified development time. Each of the results is for 5000 Å only, but by selecting the desired wavelength from figure B-1, the film curve can be shifted along the abscissa to the correct value. For instance, if the SO-392 film sensitivity at 6563 Å was desired, the curve would be shifted to the value of 7×10^{-4} watt^{1} . meter^{-2} obtained from figure B-1 at a density of 1.0. It could then be compared to the illumination line shown for 6563 Å on figure B-2.

The results in figure B-2 indicate that the selected films are just sufficiently sensitive to operate with the anticipated illumination at a 1-second exposure and a density near 1.0. Thus, if the spacecraft stability is as indicated to date, the resolution advantage of the film will partially be lost due to image motion during the exposure time.

The aforementioned values are based on Kodak nominal data for the specified films. Special processing techniques used at California Institute of Technology for their solar telescope at the Big Bear Observatory increase the sensitivity of SO-392 by approximately a factor of 50. This much improves the short exposure capability of the film, but the results cannot be shown here since the spectral sensitivity and characteristic curves were not available.

B.3 RADIATION SHIELDING

Since all films "fog" when radiated, some form of shielding is necessary to preserve a satisfactory base density level when stored in space. Figure B-3, extracted from reference 17, shows the amount of aluminum necessary to limit the fog density of Panatomic X film to any desired amount for a typical ATM of 210 nmi with a 25-degree inclination.

Reference 18 discusses the problem under the NASA plan to bring up all film at first launch and return exposed portions during each return trip.

The conclusion is that the amount of shielding necessary to prevent fogging for the 252-day total mission is not feasible. The report therefore assumes a maximum mission and assumes prefogging of all other film to a computed level which will cause the same 0.2 level of density regardless of mission length. This prefogging requires complex computation and exposure procedures before launch. Then the prelaunch handling and on-board storage must be carefully planned to ensure that the astronauts use the correctly fogged films for each part of the mission. In addition, this level of prefogging has an important effect on the dynamic range on a particular frame.

Even with the above precautions, figure B-3 shows that moderately heavy shielding will be required, probably in the level of 10 to 50 grams per square centimeter of surface area of the storage container. Since the planned mission is for some 150,000 frames of film, this is a considerable weight penalty.

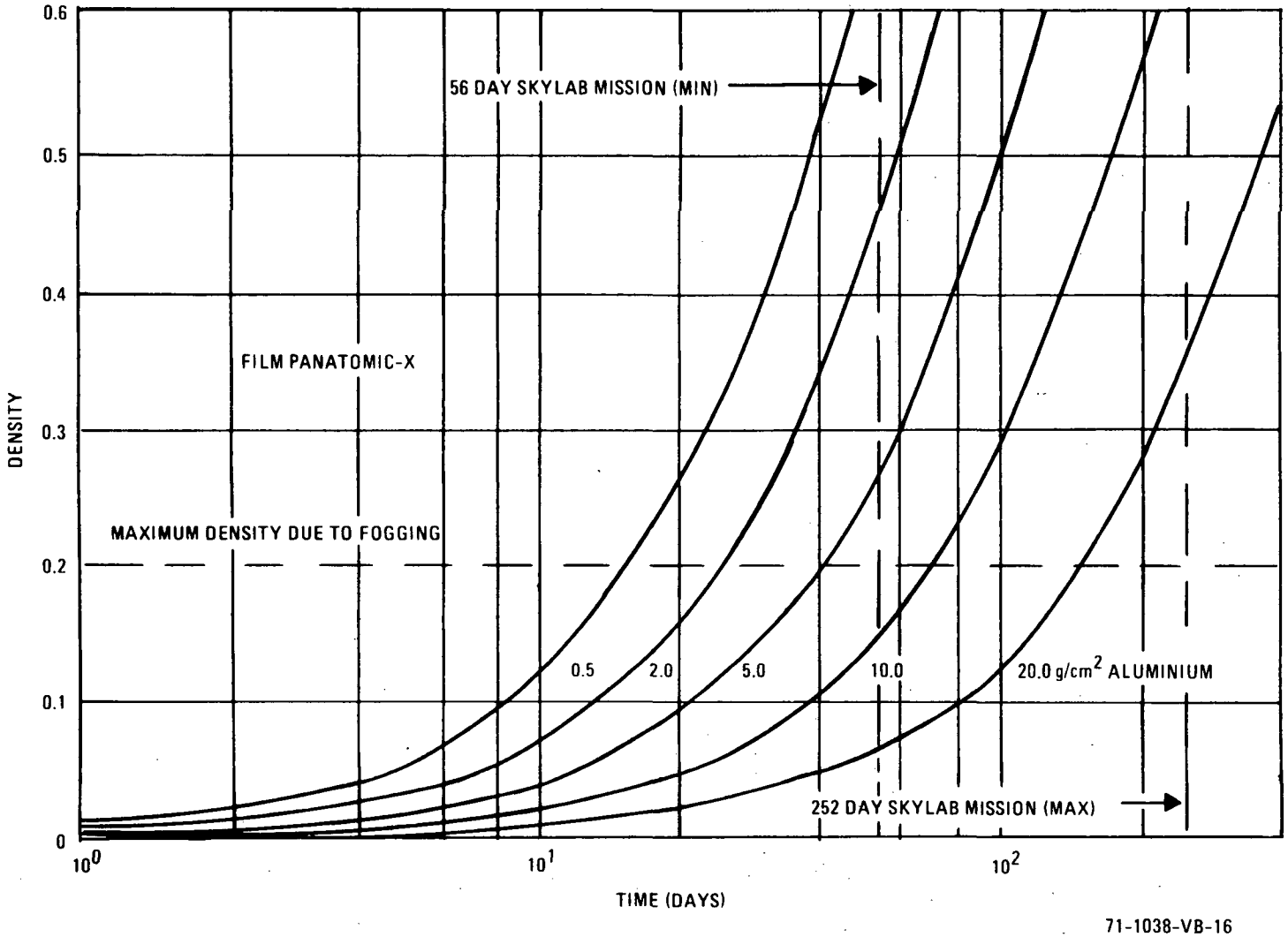

Figure B-3. Film Density Due to Radiation Exposure Versus Time in Orbit for the Film Panatomic-X

APPENDIX C

TELEVISION SYSTEM ANALYSIS COMPUTER PROGRAM

The radiometric analysis of various TV sensors to determine the amount of signal current, noise current, and signal-to-noise ratio has been accomplished with the aid of a general purpose computer. Three separate Fortran IV programs have been written for the Control Data Corporation 6400 computer.

Program FOTOCUR convolves the photocathode spectral response with a given illumination spectrum through a given optics subsystem and over a prescribed filter band to calculate the current density and the photon current density of the photocathode.

Program SIG2NOZ calculates the exposure current, signal current, noise current, and signal-to-noise ratio for various camera tube-photocathode combinations, using the output current densities of Program FOTOCUR as input data.

Program SIG2NZ1 calculates the noise current and the signal-to-noise ratio for various camera tube-photocathode combinations using a given signal current as input.

A simple block diagram of Program FOTOCUR is given in figure C-1, and figure C-2 is a block diagram of Program SIG2NOZ. The block diagram of Program SIG2NZ1 is practically the same as SIG2NOZ, except that the saturation signal current of the tube of interest is supplied, rather than a tape of current densities. Exposure current, noise current, and signal-to-noise ratio are the outputs of SIG2NZ1.

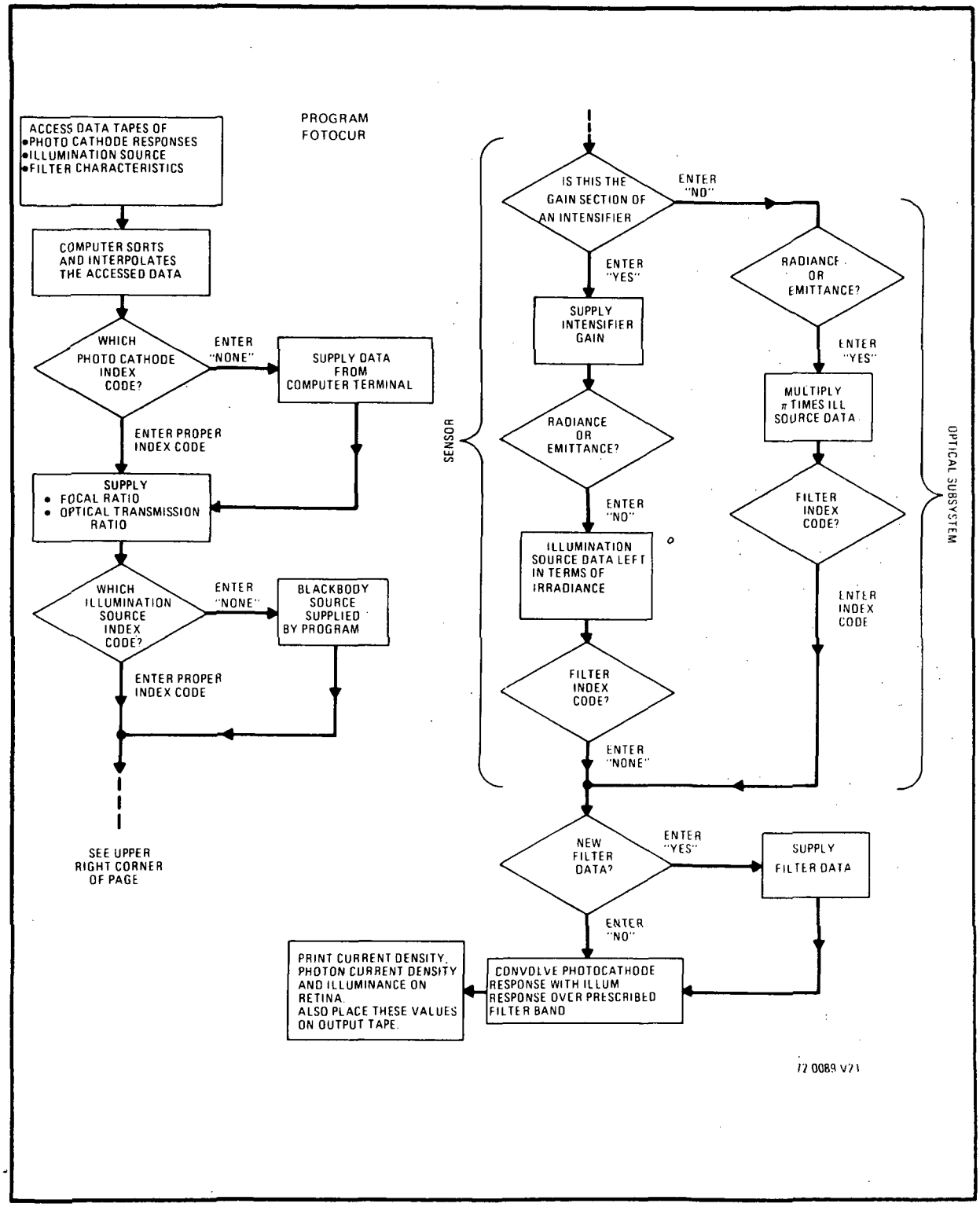

Figure C-1. Block Diagram of Program FOTOCUR

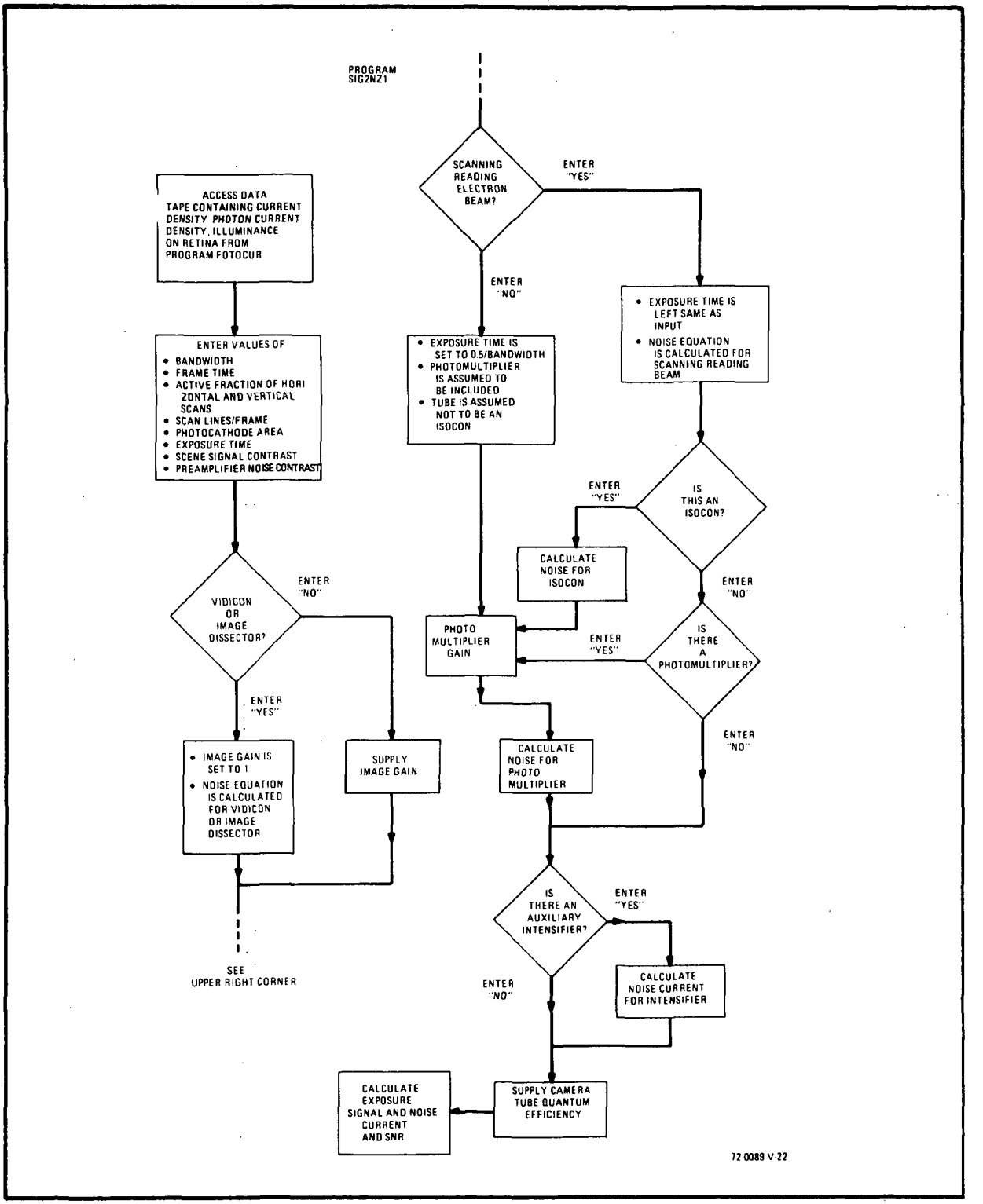

Figure C-2. Block Diagram of Program SIG2NOZ

C.1 INPUT DATA TAPES (PROGRAM FOTOCUR)

TAPE 1 is a data tape containing spectral responses, in milliamperes per watt per micrometer, of photocathodes of interest (see figure C-3 for the contents of TAPE 1). TAPE 2 is a data tape containing spectral characteristics, in watts$\cdot$cm$^{-2}\cdot$ Ster$^{-1}\cdot\mu$m^{-1} (see figure C-4 for the contents of TAPE 2). TAPE 3 is a data tape containing the filter transmission characteristics (percent transmission) over the spectral bandwidth of the filter (see figure C-5 for the contents of TAPE 3).

The common characteristics of the three data tapes are outlined in the following subparagraphs.

a. Data Entry Into Program FOTOCUR

All the data which the particular application is likely to require may be placed into each of the three data tapes. The proper data for a particular photocathode, illumination source, or filter is read into the program from each of the larger three files. The program has the ability to search through a particular data file for a code word indicating where data reading is to commence and a code number where the data reading is to stop. Thus, the responses of all the photocathodes may all be placed on the same data tape, and the program uses only the portion of data between the given code words. A separate data tape containing all the illumination sources may also be constructed under the same principle (explained in paragraph C.1.1b). Similarly, one data tape can contain all the various filter characteristics. Before Program FOTOCUR is run, the separate data files are called by

```
GET, TAPE 1 = FLSIN1
GET, TAPE 2 = FLSIN2
GET, TAPE 3 = FLSIN3
```

b. Data Format

Tapes 1, 2, and 3 all have the same format. The first line of each subfile is the index code of the photocathode (such as, PC3); the

illumination source (such as, SOURCE 2); or the filter (such as 4045.8, bandcenter of the filter). The second line of the subfile is a descriptive phrase of the photocathode (such as SLOW SCAN VIDICON), the illumination source(such as SOLAR ABSOLUTE DATA) or the filter (such as 1/8 ANGSTROM FILTER - 5 PERCENT TRANSMISSION).

The data from each file are entered in pairs, the first element of which is wavelength in micrometers. The second element of the pair is one of the following depending on the data file:

- photocathode sensitivity (mA/watt)
- source spectral power (watt$\cdot$ster$^{-1}\cdot\mu$m$^{-1}\cdot$cm^{-2})
- filter percent transmission (as a decimal).

The SOURCE 2 data shall be used as an example of the way the data must be placed in any of the data files.

SOURCE 2
SOLAR ABSOLUTE DATA

.200000	3.9100E+01
.205000	6.9500E+01
.	.
.	.
.	.
1.0E-32	0.

- The first line has a maximum of 10 characters
- The second line has a maximum of 60 characters.
- Each first column data value, beginning with line three, must be preceded by three blank spaces.
- Each first column number must be a six significant figure number less than one.
- Five blank spaces must be placed between the data columns.
- Each second column number must be a five significant figure number between 1 and 10 followed by the letter E, the symbol + (or -), and two digits (zeroes included) indicating the power of 10.
- The number 1.0E-32 must be in the last column of the first line of column 1. This indicates the end of the subfile; thus, no more

data is read from the particular tape. The second column of the last line is an arbitrary number, since the program does not enter any data when 1.0E-32 is encountered.

- The data of a particular subfile on the tape may have any order; for example, the data need not be placed on the file sequentially with respect to wavelength. Program FOTOCUR contains a sorting routine which places the data in the proper order.
- Any two data points may be separated by an arbitrary interval. Program FOTOCUR has a quadratic interpolation routine to supply arbitrary data points over the data array.

C.2 OUTPUT DATA TAPE - PROGRAM FOTOCUR

The focal ratio, optical transmission ratio, current density, photon current density, and illuminance on the retina of Program FOTOCUR are output onto TAPE 4 of the program. This data file becomes TAPE 1 of Program SIG2NOZ. TAPE 4 can be saved for further use by immediately typing

SAVE, TAPE 4 = SNRINPT

after the run is complete (SNRINPT is an arbitrary seven character name used as an example file name).

C.3 PROGRAM FOTOCUR PRINTOUT ANALYSIS

a. Unintensified Camera Sensor

A typical run for a camera sensor without an intensifier is given in figure C-6. The entire program is given in figure C-6. The lines which do not begin with a question mark indicate the printout which the internal program controls after the initial run statement has been given. The lines which do begin with a question mark indicate that data is to be typed into the machine from the on-line terminal.

If the response NONE is given to the photocathode index code, the data is to be input from the terminal in the same format as TAPE 1. The focal ratio and optical transmission ratio may be entered as two numbers separated by a space or a comma.

The index code for the source has been SOURCE 2 (solar absolute data file) for all front-end photocathodes. However, if the answer is NONE, a blackbody source is assumed and a blackbody temperature is then requested.

The "gain section intensifier?" answer is always NO and the "radiance--emittance?" answer is always YES or radiance for an unintensified tube. The YES answer allows the input solar spectral powers to be multiplied by π.

The "filter index code?" answer is the center frequency, in angstroms, of the filter band. If the entire illumination is to be admitted then the answer is NONE.

If NEW is typed in response to "new data ready on tape," other filter data, to be entered at the terminal, are requested. If NO is typed to "print spectrum?", the next six lines of printout are skipped and just the spectral band, current density, irradiance on retina, photon current density, and "new data" are printed.

b. Intensified Camera Sensor

Typical runs for a camera sensor with an intensifier are given in figure C-7a and C-7b. Two separate runs of Program FOTOCUR are required to determine the current density of the intensified tube. The first run (figure C-7a) converts the photocurrent from the combination of the illumination and the intensifier photocathode into a new illumination from the output phosphor of the intensifier with the proper gain value. The format is similar to that of the run of figure C-6. The second run (figure C-7b) determines the output current density of the photocathode of the camera sensor to the phosphor illumination, which in this example is the slow scan vidicon. The spectral response of the vidicon (given as SOURCE 3) modifies the input current density from the intensifier to give the output current density of the intensified camera sensor.

The answers to the questions of the second run shall be explained. This focal ratio and optical transmission ratio are 0.89 and 1. The 0.89 cancels the $(\pi/4)^{1/2}$ term in the irradiance equation, effectively making the focal ratio 1 since there are no optics here. The index code for the source is SOURCE 3, which is the P-20 spectral response in watt$\cdot$cm$^{-2}\cdot$ $\cdot$milliampere$^{-1}\cdot\mu$m^{-1}. The power density at the photocathode is the output of the intensifier phosphor of the first run. This number is multiplied by the intensifier gain (≈ 50) and the SOURCE 3 spectral response. A NO answer to the radiance-emittance question allows the data to remain as is; i.e., without the π multiplying factor. The index code for the filter is NONE, since the filter operates on the input power to the intensifier. The remaining portion of the second run (figure C-7a) is similar to the preceding examples.

C.4 SENSOR SIGNAL-TO-NOISE RATIO-PROGRAM SIG2NOZ

Two programs have been devised to calculate the sensor signal-to--noise ratio; one program (SIG2NOZ) uses output current density data of Program 1 to calculate the exposure current, signal current, noise current, and SNR. The other program (SIG2NZ1) has the signal current as an input with the same outputs.

a. Program SIG2NOZ

Figure C-8 gives sample outputs for various sensors used for this program. An input data tape is required for this output. The data tape is accessed by

GET, TAPE 1 = SNRINPT.

This is explained in paragraph C.2. The first eight questions simply require the proper data values. A YES answer to "Is this either a vidicon or an image dissector? YES?" sets the current gain equal to 1; a NO answer sets up the question "current gain of the image section?," whereupon the proper value is entered. A NO answer to "Is there a scanning reading electron beam?" sets the exposure time to 0.5/bandwidth,

ISOCON to NO and multiplier to YES. A YES answer sets up the question "Is this an ISOCON." YES to this question assumes photomultiplier output, setting up the question "multiplier gain?," whereupon the data is entered. A NO answer causes the question "Is there an electron multiplier output?" to be asked. A NO answer sets the gain of the photomultiplier equal to 1; a YES answer causes the computer to ask "multiplier gain?" to which one responds with the data value. A NO to "Is there an auxiliary image intensifier?" sets the intensifier gain to 1. The YES option is not used in the signal-to-noise program since during this study the calculation of signal current of the intensified tube have been moved from Program 2 (SIG2NOZ) to Program 1, as described in paragraph C.3b. Not considering the intensifier in the noise current calculation contributes a small error. However, for a single intensifier of gain 50, all sensors, except the ISS, are considered preamplifier limited.

b. Program SIG2NZ2

Figure C-9 gives sample outputs for various sensors used in this program. This program differs from Program SIG2NOZ in that the saturation signal current of each tube is the input, rather than the current densities of the data tape from Program FOTOCUR.

C.5 DATA TAPES FOR PROGRAM SIG2NOZ

Figure C-10 is a list of the signal-to-noise data tapes that have been generated from Program 1 for use in Program SIG2NOZ. Each data tape consists of five lines: a photocathode identifier, an illumination source identifier, a filter center band, bandwidth and transmission ratio identifier, a row of data containing the focal ratio and optical transmission ratio, and a row of data containing beam current density, photon current density and irradiance on the retina.

At present, this complete data list is on one tape. To use a particular five-line data file as TAPE 1 in Program SIG2NOZ, it is necessary to delete (by proper editing in the computer) portions of the large data file to extract the file of interest. The program does not, at present, contain a subroutine that can search for the desired signal-to-noise input data.

C.6 LISTINGS OF COMPUTER PROGRAMS

Listings of the computer programs are given in the event the recipient of this study wishes to verify the data or place the program on his own computer. Program FOTOCUR is listed in figure C-11, Program SIG2-NOZ in figure C-12 and Program SIG2NZ1 in figure C-13.

```
PC1
JEDEC-S20(ISS,SEC,II,ID)
    .400000       6.5000E+01
    .300000       6.0000E+00
    .350000       4.5000E+01
    .450000       6.1000E+01
  * .500000       5.2000E+01
    .550000       4.2000E+01
    .600000       3.4000E+01
    .650000       2.4000E+01
    .700000       1.3000E+01
    .750000       6.0000E+00
    .800000       1.5000E+00
  * .850000            0.
    1.0E-32            0.
PC2
BENDIX S20-3 (RED RESPONSE)
    .400000       1.7000E+01
    .300000       1.0000E+00 -
    .350000       1.0000E+01
  * .450000       4.6000E+01
    .500000       5.3000E+01
    .550000       6.5000E+01
    .600000       6.5000E+01
    .650000       6.4000E+01
    .700000       6.0000E+01
    .750000       5.3000E+01
    .800000       5.5000E+01
    .850000       3.2000E+01
    .900000            0.
    1.0E-32            0.
```

Figure C-3

PC3
SLOW SCAN VIDICON

.300000	1.9000E+01
.350000	3.0000E+01
.400000	4.6000E+01
.450000	6.8000E+01
.500000	9.4000E+01
.550000	1.1000E+02
.600000	8.4000E+01
.650000	6.0000E+01
.700000	3.7000E+01
.750000	1.9000E+01
.800000	9.6000E+00
.850000	3.0000E+00
.900000	0.
1.0E-32	0.

PC4
RETURN BEAM VIDICON

.300000	0.
.350000	1.0000E+00
.400000	2.0000E+02
.450000	3.0000E+02
.500000	3.4000E+02
.550000	3.4000E+02
.600000	2.9000E+02
.650000	1.7000E+02
.700000	7.8000E+01
.750000	2.5000E+01
.800000	6.8000E+00
1.0E-32	0.

PC2A
SILICON VIDICON

.300000	2.0000E-01
.350000	1.6000E+01
.400000	1.7000E+02
.450000	2.7000E+02
.500000	3.4000E+02
.550000	3.8000E+02
.600000	3.8000E+02
.650000	3.8000E+02
.700000	3.9000E+02
.750000	3.9000E+02
.800000	3.4000E+02
1.0E-32	0.

Figure C-3 (Continued)

```
PC5
CESIUM TELLURIDE/QUARTZ (VIDICON)
    .200000       4.9000E+01
    .210000       4.9000E+01
    .220000       4.9000E+01
    .230000       4.9000E+01
    .240000       4.9000E+01
    1.0E-32            0.
PC6 -
S/20 SAPPHIRE (ULTRAVIOLET RESPONSE)
    .200000       4.0000E+01
    .210000       4.2000E+01
    .220000       4.4000E+01
   *.230000       4.7000E+01 -
    .240000       4.8000E+01
    1.0E-32            0.
PC7
WESTINGHOUSE UV SENSITIVE VIDICON P.C.
    .170000       5.0000E+00
    .180000       1.3000E+01
    .190000       1.8000E+01
    .200000       2.1000E+01
    .210000       2.4000E+01
    .220000       2.7000E+01
    .230000       2.9000E+01
    .240000       3.2000E+01
    .250000       3.4000E+01
    .300000       4.3000E+01
    .350000       5.1000E+01
   *.370000       5.3000E+01
    .380000       5.4000E+01
    .390000       5.4000E+01
    .400000       5.3000E+01
    .430000       4.9000E+01
    .450000       4.4000E+01
    .470000       3.5000E+01
    .500000       2.2000E+01
    .530000       1.1000E+01
    .550000       5.0000E+00
    1.0E-32            0.
```

Figure C-3 (Continued)

```
SØURCE 3
P-20 SPECTRAL RESPØNSE
    .450000      1.9620E-03
    .460000      3.9240E-03
    .470000      9.8100E-03
    .480000      1.7660E-02
    .490000      3.3350E-02
    .500000      6.0820E-02
    .510000      1.0200E-01
    .520000      1.4130E-01
    .530000      1.7660E-01
    .540000      1.9030E-01
    .550000      1.9620E-01
    .560000      1.9620E-01
    .570000      1.9030E-01
    .580000      1.7270E-01
    .590000      1.5110E-01
    .600000      1.2560E-01
    .610000      1.0200E-01
    .620000      7.8480E-02
    .630000      5.8860E-02
    .640000      4.3160E-02
    .650000      3.3350E-02
    .660000      2.5510E-02
    .670000      1.9620E-02
    .680000      1.3730E-02
    .690000      9.8100E-03
    .700000      7.8480E-03
    .710000      5.8860E-03
    .720000      3.9240E-03
    .730000      1.9620E-03
   1.0E-32           0.
SØURCE 2
SØLAR ABSØLUTE DATA
    .200000      3.9100E+01
    .205000      6.9500E+01
    .210000      9.5500E+01
    .220000      1.4100E+02
    .230000      1.5600E+02
    .240000      1.9300E+02
    .250000      2.7000E+02
    .260000      3.9100E+02
    .270000      5.7800E+02
    .278430      7.8000E+02
    .278440      7.0400E+02
    .281330      7.0400E+02
    .281340      9.0000E+02
    .284400      9.7600E+02
    .284500      8.4000E+02
```

Figure C-4

.285500	8.4000E+02
.285600	1.0700E+03
.287970	1.1100E+03
.287980	9.2000E+02
.288240	9.2000E+02
.288250	1.1300E+03
.300000	1.6500E+03
.320000	2.2400E+03
.340000	2.6800E+03
.358000	2.9600E+03
.358010	9.7600E+01
.358230	9.7600E+01
.358240	2.9600E+03
.373340	3.2600E+03
.373350	3.2400E+01
.373640	3.2400E+01
.373650	3.2600E+03
.381950	3.4000E+03
.381960	6.8000E+01
.382140	6.8000E+01
.382150	3.4000E+03
.392410	3.5600E+03
.392420	2.1200E+02
.394330	2.1200E+03
.394340	3.5600E+03
.396120	3.6000E+03
.396130	2.1400E+02
.397570	2.1400E+02
.397580	3.6000E+03
.404510	3.7100E+03
.404520	7.8000E+01
.404640	7.8000E+01
.404650	3.7100E+03
.410000	3.8200E+03
.410020	8.2000E+02
.410320	8.2000E+02
.410330	3.8200E+03
.420000	3.9000E+03
.422600	3.9000E+03
.422610	7.8000E+01
.422750	7.8000E+01
.422760	3.9000E+03
.430000	3.9100E+03
.433910	3.9100E+03
.433920	6.2500E+02
.434190	6.2500E+02
.434200	3.9100E+03
.438310	3.9000E+03
.438320	1.1700E+02

Figure C-4 (Continued)

.438420	1.1700E+02
.438430	3.9000E+03
.450000	3.8700E+03
.460000	3.8200E+03
.485940	3.6700E+03
.485950	5.4700E+02
.486320	5.4700E+02
.486330	3.6700E+03
.500000	3.5700E+03
.516680	3.5200E+03
.516690	4.4500E+02
.516780	4.4500E+02
.516790	3.5200E+03
.517210	3.5200E+03
.517220	3.4200E+02
.517330	3.4200E+02
.517340	3.5200E+03
.518280	3.5200E+03
.518290	3.0900E+02
.518440	3.0900E+02
.518450	3.5200E+03
.550000	3.2500E+03
.588960	2.9300E+03
.588970	1.1700E+02
.589050	1.1700E+02
.589060	2.9300E+03
.589560	2.9300E+03
.589570	1.4400E+02
.589630	1.4400E+02
.589640	2.9300E+03
.600000	2.8600E+03
.656080	2.5400E+03
.656090	3.9000E+02
.656500	3.9000E+02
.656510	2.5400E+03
.700000	2.2500E+03
.750000	1.9300E+03
.800000	1.7300E+03
.900000	1.3500E+03
1.000000	1.1100E+03
1.200000	7.4000E+02
1.600000	3.3000E+02
2.000000	1.5000E+02
3.000000	3.9000E+01
4.000000	1.3700E+01
1.0E-32	0.

Figure C-4 (Continued)

```
4045.8
1/8 ANGSTROM FILTER-5 PERCENT TRANSMISSION
   .404574      5.0000E-02 -
   .404587      5.0000E-02
   1.0E-32           0.
5890
1/4 ANGSTROM FILTER-5 PERCENT TRANSMISSION
   .588988      5.0000E-02
   .589013      5.0000E-02
   1.0E-32           0.
6562.8-
1/2 ANGSTROM FILTER-10 PERCENT TRANSMISSION
   .656255      1.0000E-01
   .656305      1.0000E-01
   1.0E-32           0.
2200
100 ANGSTROM FILTER-15 PERCENT TRANSMISSION
   .215000      1.5000E-01
   .225000      1.5000E-01
   1.0E-32           0.
5500
1/4 ANGSTROM FILTER-5 PERCENT TRANSMISSION
   .549988      5.0000E-02
   .550013      5.0000E-02
   1.0E-32           0.
4100
1/8 ANGSTROM FILTER-5 PERCENT TRANSMISSION-
   .409994      5.0000E-02
   .410007      5.0000E-02
   1.0E-32           0.
5395.9
1/4 ANGSTROM FILTER-5 PERCENT TRANSMISSION
   .589573      5.0000E-02
   .589603      5.0000E-02
   1.0E-32           0.
```

Figure C-5

```
WHICH INDEX CØDE FØR PHØTØCATHØDE ØR NØNE?
? PC3

PC3        SLØW SCAN VIDICØN

FØCAL RATIØ, AND ØPTICAL TRANSMISSIØN RATIØ?
? 81. 1.
WHICH INDEX CØDE FØR SØURCE        ØR NØNE?
? SØURCE 2

SØURCE 2  SØLAR ABSØLUTE DATA

IS THIS THE GAIN SECTIØN ØF AN INTENSIFIER?
? NØ
RADIANCE IN WATT/CM**2'MICRØN'STERADIAN
 ØR EMITTANCE IN WATT/CM**2*MICRØN?
? YES
WHICH INDEX CØDE FØR FILTER        ØR NØNE?
? 5895.9

5895.9     1/4 ANGSTRØM FILTER-5 PERCENT TRANSMISSIØN

WHAT NEW DATA IS READY ØN TAPE? ØR GØ.
? GØ
PRINT SPECTRUM?
? YES
SPECTRAL BAND:    .589578 TØ    .589603 MICRØMETER

WAVELENGTH EMITTANCE    IRRADIANCE  PHØTØRESP  CURRENT DENSITY
  MICRØN    W/CM**2*UM  W/CM**2*UM    MA/WATT     MA/CM**2*UM

   .589578  4.5239E+02  8.6139E-04  8.9254E+01  7.6928E-02
   .589603  4.5239E+02  8.6139E-04  8.9242E+01  7.6917E-02
SPECTRAL BAND:    .589578 TØ    .589603 MICRØMETER
CURRENT DENSITY= 1.92305E-06 MILLIAMPERE/CM**2
IRRADIANCE ØN RETINA: 2.15473E-08 WATT/CM**2
PHØTØN CURRENT DENSITY= 6.39620E+10 PHØTØN/S*CM**2
WHAT NEW DATA IS READY ØN TAPE? ØR GØ.
? NØNE
 STØP.
```

Figure C-6

```
WHICH INDEX CODE FOR PHOTOCATHODE OR NONE?
? PC6

PC6          S/20 SAPPHIRE (ULTRAVIOLET RESPONSE)

FOCAL RATIO, AND OPTICAL TRANSMISSION RATIO?
? 111.1.
WHICH INDEX CODE FOR SOURCE       OR NONE?
? SOURCE 2

SOURCE 2   SOLAR ABSOLUTE DATA

IS THIS THE GAIN SECTION OF AN INTENSIFIER?
? NO
RADIANCE IN WATT/CM**2'MICRON'STERADIAN
 OR EMITTANCE IN WATT/CM**2*MICRON?
? YES
WHICH INDEX CODE FOR FILTER       OR NONE?
? 2200

2200          100 ANGSTROM FILTER-15 PERCENT TRANSMISSION

WHAT NEW DATA IS READY ON TAPE? OR GO.
? GO
PRINT SPECTRUM?
? YES
SPECTRAL BAND:    .215000 TO    .225000 MICROMETER

WAVELENGTH EMITTANCE   IRRADIANCE  PHOTORESP  CURRENT DENSITY
  MICRON   W/CM**2*UM  W/CM**2*UM   MA/WATT    MA/CM**2*UM

    .215000  3.8347E+02  1.1671E-03  4.2875E+01  5.0040E-02
    .220000  4.4296E+02  1.3482E-03  4.4000E+01  5.9321E-02
    .225000  4.5789E+02  1.3936E-03  4.5750E+01  6.3753E-02
SPECTRAL BAND:    .215000 TO    .225000 MICROMETER
CURRENT DENSITY= 5.35136E-04 MILLIAMPERE/CM**2
IRRADIANCE ON RETINA: 1.32559E-05 WATT/CM**2
PHOTON CURRENT DENSITY= 1.46924E+13 PHOTON/S*CM**2
WHAT NEW DATA IS READY ON TAPE? OR GO.
? NONE
 STOP.
```

72-0089-VB-23

Figure C-7a

```
WHICH INDEX CODE FOR PHOTOCATHODE OR NAME?
? PC4

PC4          RETURN BEAM VIDICON

FOCAL RATIO, AND OPTICAL TRANSMISSION RATIO?
? .89 1.
WHICH INDEX CODE FOR SOURCE          OR NONE?
? SOURCE 3

SOURCE 3   P-20 SPECTRAL RESPONSE

IS THIS THE GAIN SECTION OF AN INTENSIFIER?
? YES
GAIN OF INTENSIFIER?
? 50.
CURRENT DENSITY AT PHOTOCATHODE-MA/CM**2?
? 5.85136E-04
RADIANCE IN WATT/CM**2'MICRON'STERADIAN
 OR EMITTANCE IN WATT/CM**2*MICRON?
? NO
WHICH INDEX CODE FOR FILTER          OR NONE?
? 2=NONE
WHAT NEW DATA IS READY ON TAPE? OR GO.
? GO
PRINT SPECTRUM?
? NO
SPECTRAL BAND:    .450000 TO    .730000 MICROMETER
CURRENT DENSITY= 6.15678E-02 MILLIAMPERE/CM**2
IRRADIANCE ON RETINA: 2.00263E-04 WATT/CM**2
PHOTON CURRENT DENSITY= 5.71690E+14 PHOTON/S*CM**2
WHAT NEW DATA IS READY ON TAPE? OR GO.
? NONE
 STOP.
```

72-0089-VB-24

Figure C-7b

```
MAXIMUM HIGHLIGHT SIGNAL/NOISE FOR TV CAMERA.

BANDWIDTH IN KILOHERTZ?                                  Image Dissector
? 1100.
FRAME TIME IN SECONDS
? 1.
ACTIVE FRACTION OF HORIZONTAL AND VERTICAL SCANS?
? .95 .93
SCAN LINES/FRAME?
? 1500.
  1470 ACTIVE SCAN LINES.
  1393 SAMPLES PER HORIZONTAL LINE.
PHOTOCATHODE AREA IN CM**2?
? 4.4
EXPOSURE TIME IN SECONDS?
? 1.
SCENE SIGNAL CONTRAST?
? 1.
PREAMPLIFIER NOISE CURRENT IN NANOAMP?-
? .3
IS THIS EITHER A VIDICON OR AN IMAGE DISSECTOR? YES?
? YES
IS THERE A SCANNING READING ELECTRON BEAM?
? NO
MULTIPLIER GAIN?
? 5.E5
PC1        JEDEC-S20(ISS,SEC,II,ID)
SOURCE 2   SOLAR ABSOLUTE DATA
4100       143 ANGSTROM FILTER-5 PERCENT TRANSMISSION
      1.31469E-07          500000.00              1.00              1.50
      1.48796E-03         1100000.00       1.60000E-19              4.40
      1 PHOTOCHARGE 2        STORED CHARGE BEAM CUR DENS MULTIPLIER CUR
       0.              0.             0.             0.             0.
```

Figure C-8

```
EXPØSURE CURRENT=  3.2735120E+04 MICRØAMPERE
SIGNAL CURRENT  =  1.5932335E-02 MICRØAMPERE
NØISE CURRENT   =  1.3146951E-01 MICRØAMPERE
SIGNAL/NØISE    =  1.22E-01
PC1       JEDEC-S20(ISS,SEC,II,ID)
SØURCE 2  SØLAR ABSØLUTE DATA
5395.9    1/4 ANGSTRØM FILTER-5 PERCENT TRANSMISSIØN
      2.99463E-03        500000.00              1.00              1.50
      7.72047E-10       1100000.00     1.60000E-19              4.40
      1 PHØTØCHARGE 2       STØRED CHARGE BEAM CUR DENS MULTIPLIER CUR
       0.             0.             0.             0.             0.
EXPØSURE CURRENT=  1.6935034E+03 MICRØAMPERE
SIGNAL CURRENT  =  3.2926633E-04 MICRØAMPERE
NØISE CURRENT   =  2.9943285E-02 MICRØAMPERE-
SIGNAL/NØISE    =  2.77E-02

MAXIMUM HIGHLIGHT SIGNAL/NØISE FØR TV CAMERA.

BANDWIDTH IN KILØHERTZ?
? 11000.---.                                  Return Beam Vidicon
FRAME TIME IN SECØNDS
? 1.
ACTIVE FRACTIØN ØF HØRIZØNTAL AND VERTICAL SCANS?
? .95 .98
SCAN LINES/FRAME?
? 1500.
  1470 ACTIVE SCAN LINES.
  1393 SAMPLES PER HØRIZØNTAL LINE.
PHØTØCATHØDE AREA IN CM**2?
? 4.4
EXPØSURE TIME IN SECØNDS?
? 1.
SCENE SIGNAL CØNTRAST?
? 1.
PREAMPLIFIER NØISE CURRENT IN NANØAMP?
? .3
```

Figure C-8 (Continued)

```
IS THIS EITHER A VIDICON OR AN IMAGE DISSECTOR? YES?-
? NO
CURRENT GAIN OF THE IMAGE SECTION?
? .15
IS THERE A SCANNING READING ELECTRON BEAM?
? YES
IS THIS AN ISOCON?
? NO
IS THERE A PHOTOMULTIPLIER OUTPUT?
? YES
MULTIPLIER GAIN?
? 5.E+4.E2
PC4        RETURN BEAM VIDICON
SOURCE 2   SOLAR ABSOLUTE DATA
4100       1/3 ANGSTROM FILTER-5 PERCENT TRANSMISSION
      2.63656E-09          400.00      1.50000E-01          1.50
      5.17791E-08      1100000.00      1.60000E-19          4.40
      1 PHOTOCHARGE 2       STORED CHARGE BEAM CUR DENS MULTIPLIER CUR
       0.            0.            0.            0.            0.
EXPOSURE CURRENT=   1.3669632E+01 MICROAMPERE-
SIGNAL CURRENT   =  1.4632795E+01 MICROAMPERE
NOISE CURRENT    =  2.7032559E-03 MICROAMPERE
SIGNAL/NOISE     =  5.43E+03
PC4        RETURN BEAM VIDICON
SOURCE 2   SOLAR ABSOLUTE DATA
5895.9     1/4 ANGSTROM FILTER-5 PERCENT TRANSMISSION-
      9.53966E-10          400.00      1.50000E-01          1.50
      6.59733E-09      1100000.00      1.60000E-19          4.40
      1 PHOTOCHARGE 2       STORED CHARGE BEAM CUR DENS MULTIPLIER CUR
       0.            0.            0.            0.            0.
EXPOSURE CURRENT=   1.7416951E+00 MICROAMPERE
SIGNAL CURRENT   =  1.3707739E+00 MICROAMPERE
NOISE CURRENT    =  1.0047960E-03 MICROAMPERE
SIGNAL/NOISE     =  1.36E+03
```

Figure C-8 (Continued)

```
MAXIMUM HIGHLIGHT SIGNAL/NØISE FØR TV CAMERA.-

BANDWIDTH IN KILØHERTZ?
? 1100.                                                    ISS
FRAME TIME IN SECØNDS
? 1.
ACTIVE FRACTIØN ØF HØRIZØNTAL AND VERTICAL SCANS?
? .95 .98
SCAN LINES/FRAME?
? 1500.
  1470 ACTIVE SCAN LINES.
  1393 SAMPLES PER HØRIZØNTAL LINE.
PHØTØCATHØDE AREA IN CM**2?
? 4.4
EXPØSURE TIME IN SECØNDS?
? 1.
SCENE SIGNAL CØNTRAST?
? 1.
PREAMPLIFIER NØISE CURRENT IN NANØAMP?
? .3
IS THIS EITHER A VIDICØN ØR AN IMAGE DISSECTØR? YES?-
? NØ
CURRENT GAIN ØF THE IMAGE SECTIØN?
? 2.E3
IS THERE A SCANNING READING ELECTRØN BEAM?
? YES
IS THIS AN ISØCØN?
? NØ
IS THERE A PHØTØMULTIPLIER ØUTPUT?
? NØ
IS THERE AN AUXILIARY IMAGE INTENSIFIER?
? NØ
```

Figure C-8 (Continued)

```
PC1        JEDEC-S20(ISS,SEC,II,ID)
SOURCE 2   SOLAR ABSOLUTE DATA
4100       1/3 ANGSTROM FILTER-5 PERCENT TRANSMISSION
       6.47309E-12              1.00          2000.00              1.00
       1.48796E-03              1.00       1.60000E-19             4.40
       1 PHOTOCHARGE 2        STORED CHARGE BEAM CUR DENS MULTIPLIER CUR
        0.            0.            0.            0.            0.
EXPOSURE CURRENT=   1.3094043E+02 MICROAMPERE
SIGNAL CURRENT   =  1.4064493E+02 MICROAMPERE
NOISE CURRENT    =  3.0006983E-04 MICROAMPERE
SIGNAL/NOISE     =  4.69E+05
PC1        JEDEC-S20(ISS,SEC,II,ID)
SOURCE 2   SOLAR ABSOLUTE DATA
5895.9     1/4 ANGSTROM FILTER-5 PERCENT TRANSMISSION
       1.47443E-12              1.00          2000.00              1.00
       7.72047E-10              1.00       1.60000E-19             4.40
       1 PHOTOCHARGE 2        STORED CHARGE BEAM CUR DENS MULTIPLIER CUR
        0.            0.            0.            0.            0.
EXPOSURE CURRENT=   6.7940136E+00 MICROAMPERE
SIGNAL CURRENT   =  7.2975441E+00 MICROAMPERE
NOISE CURRENT    =  3.0000362E-04 MICROAMPERE
SIGNAL/NOISE     =  2.43E+04

MAXIMUM HIGHLIGHT SIGNAL/NOISE FOR TV CAMERA.

BANDWIDTH IN KILOHERTZ?
? 1100.                                          Image Isocon
FRAME TIME IN SECONDS
? 1.
ACTIVE FRACTION OF HORIZONTAL AND VERTICAL SCANS?
? .95 .98
SCAN LINES/FRAME?
? 1500.
  1470 ACTIVE SCAN LINES.
  1393 SAMPLES PER HORIZONTAL LINE.
PHOTOCATHODE AREA IN CM**2?
? 4.4
```

Figure C-8 (Continued)

```
EXPØSURE TIME IN SECØNDS?
? 1.
SCENE SIGNAL CØNTRAST?
? 1.
PREAMPLIFIER NØISE CURRENT IN NANØAMP?-
? .3
IS THIS EITHER A VIDICØN ØR AN IMAGE DISSECTØR? YES?
? NØ
CURRENT GAIN ØF THE IMAGE SECTIØN?
? 4.
IS THERE A SCANNING READING ELECTRØN BEAM?
? YES
IS THIS AN ISØCØN?
? YES
MULTIPLIER GAIN?
? 4.E2
PC1        JEDEC-S20(ISS,SEC,II,ID)
SØURCE 2   SØLAR ABSØLUTE DATA
4100       1/8 ANGSTRØM FILTER-5 PERCENT TRANSMISSIØN
       7.43702E-09            400.00              4.00              1.50
       1.48796E-08        1100000.00       1.60000E-19              4.40
       1 PHØTØCHARGE 2        STØRED CHARGE BEAM CUR DENS MULTIPLIER CUR
        0.             0.             0.             0.             0.
EXPØSURE CURRENT=   1.0475233E+02 MICRØAMPERE
SIGNAL CURRENT   =   1.1251599E+02 MICRØAMPERE
NØISE CURRENT    =   7.4430673E-03 MICRØAMPERE
SIGNAL/NØISE     =   1.51E+04
PC1        JEDEC-S20(ISS,SEC,II,ID)
SØURCE 2   SØLAR ABSØLUTE DATA
5395.9     1/4 ANGSTRØM FILTER-5 PERCENT TRANSMISSIØN
       1.69405E-09            400.00              4.00              1.50
       7.72047E-10        1100000.00       1.60000E-19              4.40
       1 PHØTØCHARGE 2        STØRED CHARGE BEAM CUR DENS MULTIPLIER CUR
        0.             0.             0.             0.             0.
```

Figure C-8 (Continued)

```
EXPØSURE CURRENT=   5.4352109E+00 MICRØAMPERE
SIGNAL CURRENT  =   5.8380353E+00 MICRØAMPERE
NØISE CURRENT   =   1.7204044E-03 MICRØAMPERE
SIGNAL/NØISE    =   3.39E+03

MAXIMUM HIGHLIGHT SIGNAL/NØISE FØR TV CAMERA.

BANDWIDTH IN KILØHERTZ?                                    Vidicon
? 1100.
FRAME TIME IN SECØNDS
? 1.
ACTIVE FRACTIØN ØF HØRIZØNTAL AND VERTICAL SCANS?
? .95 .93
SCAN LINES/FRAME?
? 1500.
  1470 ACTIVE SCAN LINES.
  1393 SAMPLES PER HØRIZØNTAL LINE.-
PHØTØCATHØDE AREA IN CM**2?
? 44-.4
EXPØSURE TIME IN SECØNDS?
? 1.
SCENE SIGNAL CØNTRAST?
? 1.
PREAMPLIFIER NØISE CURRENT IN NANØAMP?
? .3
IS THIS EITHER A VIDICØN ØR AN IMAGE DISSECTØR? YES?-
? NØ--YES
IS THERE A SCANNING READING ELECTRØN BEAM?
? YES
IS THIS AN ISØCØN?
? NØ
IS THERE A PHØTØMULTIPLIER ØUTPUT?
? NØ
IS THERE AN AUXILIARY IMAGE INTENSIFIER?
? NØ
```

Figure C-8 (Continued)

```
PC3        SLØW SCAN VIDICØN
SØURCE 2   SØLAR ABSØLUTE DATA
4100       1/3 ANGSTRØM FILTER-5 PERCENT TRANSMISSIØN-
      1.27442E-13              1.00              1.00              1.00
      1.15351E-03              1.00       1.60000E-19              4.40
      1 PHØTØCHARGE 2        STØRED CHARGE BEAM CUR DENS MULTIPLIER CUR
       0.             0.             0.             0.             0.
EXPØSURE CURRENT=   5.0754440E-02 MICRØAMPERE
SIGNAL CURRENT   =  5.4516047E-02 MICRØAMPERE
NØISE CURRENT    =  3.0000003E-04 MICRØAMPERE
SIGNAL/NØISE     =  1.82E+02
PC3        SLØW SCAN VIDICØN
SØURCE 2   SØLAR ABSØLUTE DATA
5895.9     1/4 ANGSTRØM FILTER-5 PERCENT TRANSMISSIØN
      5.20351E-14              1.00              1.00              1.00
      1.92305E-09              1.00       1.60000E-19              4.40
      1 PHØTØCHARGE 2        STØRED CHARGE BEAM CUR DENS MULTIPLIER CUR
       0.             0.             0.             0.             0.
EXPØSURE CURRENT=   8.4614200E-03 MICRØAMPERE
SIGNAL CURRENT   =  9.0885285E-03 MICRØAMPERE-
NØISE CURRENT    =  3.0000000E-04 MICRØAMPERE
SIGNAL/NØISE     =  3.03E+01
```

Figure C-8 (Continued)

```
BANDWIDTH   FRAMETIME   ACTIVE VERT   ACT HØRIZ
 1100.0        1.00         .95          .98
SCANLN/FRAME  EXP TIME   SCENE CØNTR   P.C.AREA
   1500.0       1.0          1.0          4.4
PREAMP NØISE CURRENT-NANØAMP    ISØCØN
               .3                 YES
  1470 ACTIVE SCAN LINES.
  1393 SAMPLES PER HØRIZØNTAL LINE.
VIDICØN ØR IMAGE DISSECTØR?
            NØ
CURRENT GAIN ØF THE IMAGE SECTIØN?
? 4.
SCANNING READING ELECTRØN BEAM?
              YES
MULTIPLIER GAIN?
      4.0E+02
QUANTUM EFFICIENCY?
? .07
SIGNAL CURRENT IN AMPS?
? 7.5E-9
EXPØSURE CURRENT    =   6.9825000E-03 MICRØAMPERE
SIGNAL CURRENT      =   7.5000000E-03 MICRØAMPERE
NØISE CURRENT-FLS   =   3.0608293E-04 MICRØAMPERE-
SIGNAL/NØISE-FLS    =   2.45E+01
NØISE CURRENT-JEN   =   2.8373086E-03 MICRØAMPERE
SIGNAL/NØISE-JEN    =   2.64E+00


SIGNAL CURRENT IN AMPS?
? 7.5E-8
EXPØSURE CURRENT    =   6.9825000E-02 MICRØAMPERE
SIGNAL CURRENT      =   7.5000000E-02 MICRØAMPERE
NØISE CURRENT-FLS   =   3.5618478E-04 MICRØAMPERE
SIGNAL/NØISE-FLS    =   2.11E+02
NØISE CURRENT-JEN   =   8.7899488E-03 MICRØAMPERE
SIGNAL/NØISE-JEN    =   8.53E+00


SIGNAL CURRENT IN AMPS?
? 7.5E-7
EXPØSURE CURRENT    =   6.9825000E-01 MICRØAMPERE
SIGNAL CURRENT      =   7.5000000E-01 MICRØAMPERE
NØISE CURRENT-FLS   =   6.7725623E-04 MICRØAMPERE
SIGNAL/NØISE-FLS    =   1.11E+03
NØISE CURRENT-JEN   =   2.7737916E-02 MICRØAMPERE
SIGNAL/NØISE-JEN    =   2.70E+01
```

Figure C-9

```
BANDWIDTH   FRAMETIME   ACTIVE VERT   ACT HØRIZ
 1100.0        1.00          .95          .98
SCANLN/FRAME   EXP TIME   SCENE CØNTR   P.C.AREA
   1500.0        1.0           1.0          4.4
PREAMP NØISE CURRENT-NANØAMP    ISØCØN
               .3                NØ
  1470 ACTIVE SCAN LINES.
  1393 SAMPLES PER HØRIZØNTAL LINE.
VIDICØN ØR IMAGE DISSECTØR?
          NØ
CURRENT GAIN ØF THE IMAGE SECTIØN?
? .15
SCANNING READING ELECTRØN BEAM?
             YES
PMT ØUTPUT?
    YES
MULTIPLIER GAIN?
      4.0E+02
QUANTUM EFFICIENCY?
? .63
SIGNAL CURRENT IN AMPS?
? 6.8E-7
EXPØSURE CURRENT    =   6.3308000E-01 MICRØAMPERE
SIGNAL CURRENT      =   6.8000000E-01 MICRØAMPERE
NØISE CURRENT-FLS   =   6.5135723E-04 MICRØAMPERE
SIGNAL/NØISE-FLS    =   1.04E+03
NØISE CURRENT-JEN   =   3.2835198E-02 MICRØAMPERE
SIGNAL/NØISE-JEN    =   2.07E+01


SIGNAL CURRENT IN AMPS?
? 6.8E-6
EXPØSURE CURRENT    =   6.3308000E+00 MICRØAMPERE
SIGNAL CURRENT      =   6.8000000E+00 MICRØAMPERE-
NØISE CURRENT-FLS   =   1.8527446E-03 MICRØAMPERE-
SIGNAL/NØISE-FLS    =   3.67E+03
NØISE CURRENT-JEN   =   1.0381841E-01 MICRØAMPERE
SIGNAL/NØISE-JEN    =   6.55E+01


SIGNAL CURRENT IN AMPS?
? 6.8E-6+5
EXPØSURE CURRENT    =   6.3308000E+01 MICRØAMPERE
SIGNAL CURRENT      =   6.8000000E+01 MICRØAMPERE-
NØISE CURRENT-FLS   =   5.7893544E-03 MICRØAMPERE
SIGNAL/NØISE-FLS    =   1.17E+04
NØISE CURRENT-JEN   =   3.2829770E-01 MICRØAMPERE
SIGNAL/NØISE-JEN    =   2.07E+02
```

Figure C-9 (Continued)

```
BANDWIDTH   FRAMETIME   ACTIVE VERT   ACT HØRIZ
 1100.0        1.00          .95          .98
SCANLN/FRAME   EXP TIME   SCENE CØNTR   P.C.AREA
   1500.0        1.0           1.0          4.4
PREAMP NØISE CURRENT-NANØAMP    ISØCØN
                .3                NØ
  1470 ACTIVE SCAN LINES.
  1393 SAMPLES PER HØRIZØNTAL LINE.
VIDICØN ØR IMAGE DISSECTØR?
          YES
SCANNING READING ELECTRØN BEAM?
            NØ
MULTIPLIER GAIN?
      5.0E+05
QUANTUM EFFICIENCY?
? .09
SIGNAL CURRENT IN AMPS?
? 6.4E-7
EXPØSURE CURRENT    =   1.3108480E+06 MICRØAMPERE
SIGNAL CURRENT      =   6.4000000E-01 MICRØAMPERE
NØISE CURRENT-FLS   =   8.3194221E-01 MICRØAMPERE
SIGNAL/NØISE-FLS    =   7.69E-01
NØISE CURRENT-JEN   =   4.8519912E-01 MICRØAMPERE
SIGNAL/NØISE-JEN    =   1.32E+00


SIGNAL CURRENT IN AMPS?
? 6.4E-6
EXPØSURE CURRENT    =   1.3108480E+07 MICRØAMPERE
SIGNAL CURRENT      =   6.4000000E+00 MICRØAMPERE-
NØISE CURRENT-FLS   =   2.6308321E+00 MICRØAMPERE
SIGNAL/NØISE-FLS    =   2.43E+00
NØISE CURRENT-JEN   =   1.5343333E+00 MICRØAMPERE
SIGNAL/NØISE-JEN    =   4.17E+00


SIGNAL CURRENT IN AMPS?
? 66.←←.4E-5
EXPØSURE CURRENT    =   1.3108480E+08 MICRØAMPERE
SIGNAL CURRENT      =   6.4000000E+01 MICRØAMPERE
NØISE CURRENT-FLS   =   8.3194215E+00 MICRØAMPERE
SIGNAL/NØISE-FLS    =   7.69E+00
NØISE CURRENT-JEN   =   4.8519875E+00 MICRØAMPERE
SIGNAL/NØISE-JEN    =   1.32E+01
```

Figure C-9 (Continued)

```
PC3         SLØW SCAN VIDICØN
SØURCE 3    P-20 SPECTRAL RESPØNSE (SØURCE 2 INPUT TØ INTENSIFIER)
4045.8      1/8 ANGSTRØM FILTER IN FRØNT END ØF TUBE
   8.90000E-01    1.00000E+00
   1.00546E-05    3.04630E+11    1.06712E-07
PC3         SLØW SCAN VIDICØN
SØURCE 3    P-20 SPECTRAL RESPØNSE (SØURCE 2 INPUT TØ INTENSIFIER)-
5500    1/4 ANGSTRØM FILTER IN FRØNT END ØF TUBE
   8.90000E-01    1.00000E+00
   7.91589E-04    2.39832E+13    8.40133E-06
PC3         SLØW SCAN VIDICØN
SØURCE 3    P-20 SPECTRAL RESPØNSE (SØURCE 2 INPUT TØ INTENSIFIER)
6562.8    1/2 ANGSTRØM FILTER IN FRØNT END ØF TUBE
   8.90000E-01    1.00000E+00
   1.78606E-04    5.41132E+12    1.89559E-06
PC3         SLØW SCAN VIDICØN
SØURCE 3    P-20 SPECTRAL RESPØNSE (SØURCE 2 INPUT TØ INTENSIFIER)
4100    1/8 ANGSTRØM FILTER IN FRØNT END ØF TUBE
   8.90000E-01    1.00000E+00
   4.79830E-04    1.45377E+13    5.09255E-06
PC3         SLØW SCAN VIDICØN
SØURCE 3    P-20 SPECTRAL RESPØNSE (SØURCE 2 INPUT TØ INTENSIFIER)
5895.9    1/4 ANGSTRØM FILTER IN FRØNT END ØF TUBE
   8.90000E-01    1.00000E+00
   2.48966E-05    7.54306E+11    2.64234E-07
PC4         RETURN BEAM VIDICØN
SØURCE 3    P-20 SPECTRAL RESPØNSE (SØURCE 2 INPUT TØ INTENSIFIER)-
4045.8    1/8 ANGSTRØM FILTER IN FRØNT END ØF TUBE
   8.90000E-01    1.00000E+00
   3.28070E-05    3.04630E+11    1.06712E-07
PC4         RETURN BEAM VIDICØN
SØURCE 3    P-20 SPECTRAL RESPØNSE (SØURCE 2 INPUT TØ INTENSIFIER)
5500    1/4 ANGSTRØM FILTER IN FRØNT END ØF TUBE
   8.90000E-01    1.00000E+00
   2.58286E-03    2.39832E+13    8.40133E-06
FC1         JEDEC-S20(ISS,SEC,II,ID)
SØURCE 2    SØLAR ABSØLUTE DATA
4045.8      1/8 ANGSTRØM FILTER-5 PERCENT TRANSMISSIØN
   9.10000E+01    1.00000E+00
   3.11795E-07    9.79489E+09    4.80856E-09
PC1         JEDEC-S20(ISS,SEC,II,ID)
SØURCE 2    SØLAR ABSØLUTE DATA
5500        1/4 ANGSTRØM FILTER-5 PERCENT TRANSMISSIØN
   8.10000E+01    1.00000E+00
   2.45473E-05    1.61846E+12    5.84463E-07
```

Figure C-10

```
PC1         JEDEC-S20(ISS,SEC,II,ID)
SØURCE 2    SØLAR ABSØLUTE DATA
6562.8      1/2 ANGSTRØM FILTER-10 PERCENT TRANSMISSIØN
   7.87000E+01    1.00000E+00
   5.53859E-06    8.17041E+11    2.47272E-07
PC1         JEDEC-S20(ISS,SEC,II,ID)
SØURCE 2    SØLAR ABSØLUTE DATA
4100        1/8 ANGSTRØM FILTER-5 PERCENT TRANSMISSIØN
   9.10000E+01    1.00000E+00
   1.48796E-05    4.75469E+11    2.30334E-07
PC1         JEDEC-S20(ISS,SEC,II,ID)
SØURCE 2    SØLAR ABSØLUTE DATA
5895.9      1/4 ANGSTRØM FILTER-5 PERCENT TRANSMISSIØN
   8.10000E+01    1.00000E+00
   7.72047E-07    6.39620E+10    2.15473E-08-
PC2A        SILICØN VIDICØN
SØURCE 2    SØLAR ABSØLUTE DATA
4045.8      1/8 ANGSTRØM FILTER-5 PERCENT TRANSMISSIØN
   9.10000E+01    1.00000E+00
   8.67509E-07    9.79489E+09    4.80856E-09
PC2A        SILICØN VIDICØN
SØURCE 2    SØLAR ABSØLUTE DATA
5500        1/4 ANGSTRØM FILTER-5 PERCENT TRANSMISSIØN
   8.10000E+01    1.00000E+00
   2.22096E-04    1.61846E+12    5.84463E-07
PC2A        SILICØN VIDICØN
SØURCE 2    SØLAR ABSØLUTE DATA
6562.8      1/2 ANGSTRØM FILTER-10 PERCENT TRANSMISSIØN
   7.87000E+01    1.00000E+00
   9.44097E-05    8.17041E+11    2.47272E-07
PC2A        SILICØN VIDICØN
SØURCE 2    SØLAR ABSØLUTE DATA
4100        1/8 ANGSTRØM FILTER-5 PERCENT TRANSMISSIØN
   9.10000E+01    1.00000E+00
   4.43163E-05    4.75469E+11    2.30334E-07
PC2A        SILICØN VIDICØN
SØURCE 2    SØLAR ABSØLUTE DATA
5895.8      1/4 ANGSTRØM FILTER-5 PERCENT TRANSMISSIØN
   8.10000E+01    1.00000E+00
   8.18796E-06    6.39620E+10    2.15473E-08-
PC3         SLØW SCAN VIDICØN
SØURCE 2    SØLAR ABSØLUTE DATA
4045.8      1/8 ANGSTRØM FILTER-5 PERCENT TRANSMISSIØN-
   9.10000E+01    1.00000E+00
   2.30085E-07    9.79489E+09    4.80856E-09
```

Figure C-10 (Continued)

```
PC3         SLØW SCAN VIDICØN
SØURCE 2    SØLAR ABSØLUTE DATA
5500        1/4 ANGSTRØM FILTER-5 PERCENT TRANSMISSIØN
   8.10000E+01    1.00000E+00
   6.42898E-05    1.61846E+12    5.84463E-07
PC3         SLØW SCAN VIDICØN
SØURCE 2    SØLAR ABSØLUTE DATA
6562.8      1/2 ANGSTRØM FILTER-10 PERCENT TRANSMISSIØN -
   7.87000E+01    1.00000E+00
   1.40541E-05    8.17041E+11    2.47272E-07
PC3         SLØW SCAN VIDICØN
SØURCE 2    SØLAR ABSØLUTE DATA
4100        1/8 ANGSTRØM FILTER-5 PERCENT TRANSMISSIØN
   9.10000E+01    1.00000E+00
   1.15351E-05    4.75469E+11    2.30334E-07
PC3         SLØW SCAN VIDICØN
SØURCE 2    SØLAR ABSØLUTE DATA
5895.9      1/4 ANGSTRØM FILTER-5 PERCENT TRANSMISSIØN
   8.10000E+01    1.00000E+00
   1.92305E-06    6.39620E+10    2.15473E-08
PC4         RETURN BEAM VIDICØN
SØURCE 2    SØLAR ABSØLUTE DATA
4045.8      1/8 ANGSTRØM FILTER-5 PERCENT TRANSMISSIØN
   9.10000E+01    1.00000E+00
   1.01777E-06    9.79489E+09    4.80856E-09
PC4         RETURN BEAM VIDICØN
SØURCE 2    SØLAR ABSØLUTE DATA
5500        1/4 ANGSTRØM FILTER-5 PERCENT TRANSMISSIØN
   8.10000E+01    1.00000E+00
   1.98717E-04    1.61846E+12    5.84463E-07
PC4         RETURN BEAM VIDICØN
SØURCE 2    SØLAR ABSØLUTE DATA
6562.8      1/2 ANGSTRØM FILTER-10 PERCENT TRANSMISSIØN
   7.87000E+01    1.00000E+00
   3.86494E-05    8.17041E+11    2.47272E-07
PC4         RETURN BEAM VIDICØN
SØURCE 2    SØLAR ABSØLUTE DATA
4100        1/8 ANGSTRØM FILTER-5 PERCENT TRANSMISSIØN
   9.10000E+01    1.00000E+00
   5.17791E-05    4.75469E+11    2.30334E-07
PC4         RETURN BEAM VIDICØN
SØURCE 2    SØLAR ABSØLUTE DATA
5895.9      1/4 ANGSTRØM FILTER-5 PERCENT TRANSMISSIØN
   8.10000E+01    1.00000E+00
   6.59733E-06    6.39620E+10    2.15473E-08
```

Figure C-10 (Continued)

```
PC4         RETURN BEAM VIDICØN
SØURCE 3  P-20 SPECTRAL RESPØNSE (SØURCE 2 INPUT TØ INTENSIFIER)-
6562.8    1/2 ANGSTRØM FILTER IN FRØNT END ØF TUBE
   8.90000E-01    1.00000E+00
   5.82768E-04    6.41132E+12    1.89559E-06
PC4         RETURN BEAM VIDICØN
SØURCE 3  P-20 SPECTRAL RESPØNSE (SØURCE 2 INPUT TØ INTENSIFIER)-
4100    1/8 ANGSTRØM FILTER IN FRØNT END ØF TUBE
   8.90000E-01    1.00000E+00
   1.56563E-03    1.45377E+13    5.09255E-06
PC4         RETURN BEAM VIDICØN
SØURCE 3  P-20 SPECTRAL RESPØNSE (SØURCE 2 INPUT TØ INTENSIFIER)
5895.9    1/4 ANGSTRØM FILTER IN FRØN END ØF TUBE
   8.90000E-01    1.00000E+00
   8.12345E-05    7.54306E+11    2.64234E-07
PC3         SLØW SCAN VIDICØN
SØURCE 3  P-20 SPECTRAL RESPØNSE (SØURCE 2 INPUT TØ INTENSIFIER)
2200    100 ANGSTRØM FILTER IN FRØNT END ØF TUBE
   8.90000E-01    1.00000E+00
   1.88692E-02    5.71690E+14    2.00263E-04
PC4         RETURN BEAM VIDICØN
SØURCE 3  P-20 SPECTRAL RESPØNSE (SØURCE 2 INPUT TØ INTENSIFIER)
2200    100 ANGSTRØM FILTER IN FRØNT END ØF TUBE
   8.90000E-01    1.00000E+00
   6.15678E-02    5.71690E+14    2.00263E-04
```

Figure C-10 (Continued)

```
100    PROGRAM FOTOCUR(INPUT,OUTPUT,TAPE1,TAPE2,TAPE3,TAPE4,TAPE5)
101C   PHOTOCATHODE CURRENT(MICROAMP) AND CURRENT DENSITY(MICROAMP/CM**2)
102C    GIVEN SPECTRAL DISTRIBUTIONS OF PHOTOCATHODE, ILLUMINATION,
103C    AND FILTERS; AND DATA ON OPTICS AND CAMERA.
109    DIMENSION NAME(3,6),KIND(6),KOD(3)
110    DIMENSION PCRESP(2,120),SOURCE(2,120),FILTRR(2,120)
111    COMMON TEMP,TX,F,AREA,IANS
112    COMMON/ANSWER/CURDEN,PHOTON,HSIG
120    DATA IPHOT/2HPH/,ILLUM/2HIL/,ISOURC/2HSO/,IFIL/2HFI/
121    DATA NO/2HNO/,IGO/2HGO/,NONE/4HNONE/,IBLACK/10H BLACKBODY/
122    DATA KIND/6HPHOTOC,6HATHODE,6HSOURCE,1H ,6HFILTER,1H /
124C:  INPUT DATA
125    NUM=0
126  11 NUM=NUM+1
127    I=NUM
128  10 KEY=0
129    J2=2*I
130    J1=J2-1
131    PRINT 102,KIND(J1),KIND(J2)
132 102 FORMAT(21HWHICH INDEX CODE FOR ,2A6,9H OR NONE?)
133    READ 103,KOD(I)
134 103 FORMAT(7A10)
135    IF(KOD(I).EQ.NONE)GO TO22
136  1 READ(I,103)KODE
137    IF(EOF,I)2,3
138  3 IF(KODE.EQ.KOD(I))4,1
139  2 REWIND I
140    IF(KEY.EQ.1)GO TO 5
141    KEY=1
142    GO TO 1
143  5 PRINT 104,KOD(I)
144 104 FORMAT(A10,22H NOT FOUND. TRY AGAIN.)
145    GO TO 10
146  4 READ(I,103)(NAME(I,J),J=1,6)
147    PRINT 103,KIND(4)
149    PRINT 103,KODE,(NAME(I,J),J=1,6)
150    PRINT 103,KIND(4)
```

Figure C-11

```
      KØDI=I
   23 IF(I.EQ.1)CALL PHØTØC(PCRESP,NPC)
      IF(I.EQ.2)CALL ILLUMI(SØURCE,NS,KØDI)
      IF(I.EQ.3)CALL FILTER(FILTRR,NFILTR,KØDI) -
      IF(NUM.LT.3)11,21
C     PRØCESS AND ØUTPUT
   20 CALL PRØCESS(PCRESP,NPC,FILTRR,NFILTR,SØURCE,NS)
      IF(KØD(2).NE.NØNE)GØ TØ 31
      WRITE(5,107)TEMP
  107 FØRMAT(F8.1,2H K)
      BACKSPACE 5
      READ(5,103)KØD(2)
      NAME(2)=IBLACK
   31 DØ 30 I=1,3
   30 WRITE(4,103)KØD(I),(NAME(I,J),J=1,6) -
      WRITE(4,106)F,TX
      WRITE(4,106)CURDEN,PHØTØN,HSIG
  106 FØRMAT(5E14.5)
C     REPEAT WITH NEW DATA
   21 PRINT 182
  182 FØRMAT(38HWHAT NEW DATA IS READY ØN TAPE? ØR GØ.)
      READ 185,IANS
      IF(IANS.EQ.IGØ) GØ TØ 20
  185 FØRMAT(A2)
      IF(IANS.EQ.NØ)GØ TØ 40
      IF(IANS.EQ.IPHØT)I=1
      IF(IANS.EQ.ILLUM)I=2
      IF(IANS.EQ.IFIL)I=3
      IF(IANS.EQ.ISØURC)I=2
      GØ TØ 10
   40 REWIND 4
      REWIND 5
      STØP
   22 KØDI=0
      DØ 39 J=1,6
   39 NAME(I,J)=KIND(4)
      GØ TØ 23
```

Figure C-11 (Continued)

```
199    END
200    SUBROUTINE PHOTOC(PCRESP,NPC)
201C READ TAPE1, WAVELENGTH IN MICRON, PHOTOCATHODE RESPONSE IN MA/W.
202    DIMENSION PCRESP(2,120)
203    COMMON TEMP,TX,FOCAL,AREA
206    PRINT 101
207  101 FORMAT(44HFOCAL RATIO, AND OPTICAL TRANSMISSION RATIO? )
208    READ,FOCAL,TX
211    NPC=120
215    CALL RDSORT(PCRESP,NPC,1)
218    RETURN
219    END
220    SUBROUTINE RDSORT(FUNC,N,NTAPE)
221C  READ X,Y-FILE AND SORT BY INCREASING X; X=1.E-32 STOPS READING.
222    DIMENSION FUNC(2,N),IFORM(2)
223    DATA IFORM/7H(E10.0,,9H1X,E14.4)/
224    READ(NTAPE,IFORM)(FUNC(J,1),J=1,2)
225    IF(EOF,NTAPE)7,5
226  5 IF(FUNC(1,1).EQ.1.E-32)GO TO 6
227    DO 1 I=2,N
228    READ(NTAPE,IFORM)(FUNC(J,I),J=1,2)
229    IF(EOF,NTAPE)2,3
230  3 IF(FUNC(1,I).EQ.1.E-32)GO TO 2
231C SORT
232    F1=FUNC(1,I)
233    F2=FUNC(2,I)
235    I2=I-1
237    IF(F1-FUNC(1,I2))14,16,1
238C IGNORE DUPLICATE VALUES
239  16 I=I-1
240    GO TO 1
241C FIND CORRECT POSITION
242  14 IF(I.EQ.2)GO TO 19
243    DO 15 J=2,I2
244    J2=I-J
246    IF(F1-FUNC(1,J2))15,16,17
248  15 CONTINUE
```

Figure C-11 (Continued)

```
250 19 J=I
252 17 DØ 18 J1=2,J
254    J2=I-J1+1
256    FUNC(1,J2+1)=FUNC(1,J2)
258 18 FUNC(2,J2+1)=FUNC(2,J2)
260    FUNC(1,J2)=F1
262    FUNC(2,J2)=F2
264 1 CØNTINUE
265    PRINT 267,N
266    RETURN
267 267 FØRMAT(4HØNLY,I3,23H PØINTS USED FRØM FILE.)
268 2 N=I-1
270    RETURN
271 7 REWIND NTAPE
272    READ(NTAPE,IFØRM)(FUNC(J,1),J=1,2)
273    IF(EØF,NTAPE)6,5
274 6 N=0
276    FUNC(1,1)=0.
277    FUNC(1,2)=1.E99
278    RETURN
279    END
300    SUBRØUTINE ILLUMI(SØURCE,NS,KØDI) -
301C   SØURCE SPECTRAL RADIANCE IN W/SR*MICRØN*CM**2 FRØM TAPE2
302C     ØR BLACKBØDY TEMPERATURE
305    DIMENSIØN SØURCE(2,120)
306    CØMMØN TEMP,TX,F,AREA -
307    DATA NØ/2HNØ/,PI/3.1415926536/
309 309 FØRMAT(A2)
312    IF(KØDI.EQ.2)1,2
316C EXPERIMENTAL FRØM TAPE2
317 1 TEMP=0.
319    NS=120
320    CALL RDSØRT(SØURCE,NS,2)
321    PRINT 115
322 115 FØRMAT(43HIS THIS THE GAIN SECTIØN ØF AN INTENSIFIER?)
323    READ,INT
```

Figure C-11 (Continued)

```
      IF(INT.NE.N0)G0 T0 116
      CURDN1=1.
      GINT=1.
      G0 T0 119
  116 PRINT 117
  117 F0RMAT(20HGAIN 0F INTENSIFIER?)
      READ,GINT
      PRINT 118
  118 F0RMAT(41HCURRENT DENSITY AT PH0T0CATH0DE-MA/CM**2?)
      READ,CURDN1
  119 PRINT 110
00342 110 F0RMAT(39HRADIANCE IN WATT/CM**2'MICR0N'STERADIAN)
00344   PRINT 111
00346 111 F0RMAT(36H 0R EMITTANCE IN WATT/CM**2*MICR0N?   )
00348   READ 309,IANS
00350   IF(IANS-N0)3,3,11
00352  11 D0 10 I=1,NS
  354  10 S0URCE(2,I)=PI*CURDN1*GINT*S0URCE(2,I)
  355     G0 T0 125
  356   3 D0 126 I=1,NS
  357 126 S0URCE(2,I)=CURDN1*GINT*S0URCE(2,I) -
  358 125 RETURN
  359C  BLACKB0DY
00360   2 NS=0
00362     S0URCE(1,2)=1.E99
00364     S0URCE(1,1)=0.
00366     PRINT 102
00368 102 F0RMAT(50HWHAT IS TEMPERATURE IN KELVIN 0F BLACKB0DY S0URCE?)
00370     READ,TEMP
00372   4 RETURN
00374     END
00376     SUBR0UTINE FILTER(FILTRR,NFILTR,K0DI)
00378C    TRANSMISSI0N SPECTRA 0F 0PTICAL FILTERS
00380     DIMENSI0N FILTRR(2,120)
00382     IF(K0DI.EQ.3)1,2
00384   1 NFILTR=120
```

Figure C-11 (Continued)

```
00386    CALL RDSØRT(FILTRR,NFILTR,3)
00388    RETURN
00390 2  NFILTR=0
00392    FILTRR(1,1)=0.
00394    FILTRR(1,2)=1.E99
00396    RETURN
00398    END
00400    SUBRØUTINE XVALUE(X,XMAX,A,NA,B,NB,C,NC,KEY)
00402C    FINDS XMIN AND XMAX, AND NEXT LARGER XVALUE ØF THREE ARRAYS
00404    DIMENSIØN A(2,NA),B(2,NB),C(2,NC)
00406    IF(KEY-1)1,59,20
00408C   MAXIMUM AND MINIMUM X-VALUES
00410 1  IF(NA.EQ.0)A(1,1)=0.
00412    IF(NB.EQ.0)B(1,1)=0.
00414    IF(NC.EQ.0)C(1,1)=0.
00416    XMIN=AMAX1(A(1,1),B(1,1),C(1,1))
00418    XMAX=1.E99
00420C    FIND START FØR EACH FILTER
00422    IF(NA.EQ.0)GØ TØ 14
00424    DØ 12 I=1,NA
00426    IF(A(1,I).GE.XMIN)GØ TØ 13
00428 12 CØNTINUE
00430 14 VA=1.E99
00432    GØ TØ 15
00434 13 JA=I
00436    IF(XMAX.GT.A(1,NA))XMAX=A(1,NA)
00438 15 IF(NB.EQ.0)GØ TØ 18
00440    DØ 16 I=1,NB
00442    IF(B(1,I).GE.XMIN)GØ TØ 17
00444 16 CØNTINUE
00446 18 VB=1.E99
00448    GØ TØ 26
00450 17 JB=I
00452    IF(XMAX.GT.B(1,NB))XMAX=B(1,NB)
00454 26 IF(NC.EQ.0)GØ TØ 24
00456    DØ 21 I=1,NC
00458    IF(C(1,I).GE.XMIN)GØ TØ 22
```

Figure C-11 (Continued)

```
00460 21 CONTINUE
00462 24 VC=1.E99
00464    GO TO 25
00466 22 JC=I
00468    IF(XMAX.GT.C(1,NC))XMAX=C(1,NC)
00470 25 KEY=1
00472C  FIND X AS MIN VALUE; INCREMENT INDICES INCLUDING DUPLICATES
00474 59 IB=0
00476    IC=0
00478    IF(NA.GT.0)VA=A(1,JA)
00480    IF(NB.GT.0)VB=B(1,JB)
00482    IF(NC.GT.0)VC=C(1,JC)
00484    IF(VA-VB)54,44,64
00486 64 IF(VB-VC)52,42,53
00488 44 IB=1
00490 54 IF(VA-VC)51,41,53
00492 53 JC=JC+1
00494    X=VC
00496    GO TO 60
00498 41 IC=1
00500 51 X=VA
00502    JA=JA+1
00504    JB=JB+IB
00506    JC=JC+IC
00508    GO TO 60
00510 42 IC=1
00512    52 JB=JB+1
00514    JC=JC+IC
00516    X=VB
00518 60 IF(X.EQ.XMAX)KEY=2
00520    RETURN
00522 20 X=XMAX
00524    RETURN
00526    END
00528    SUBROUTINE INTPOL(Y,X,FUNC,N,KEY)
00530C  QUADRATIC INTERPOLATION: OBTAINS VALUE Y=FUNC(X) FOR X WITHIN
```

Figure C-11 (Continued)

```
00532C   RANGE ØF GIVEN ARRAY WITH N VALUES NØT NECESSARILY EQUALLY SPACE
00534C   CØEFFICIENTS FØR INTERPØLATIØN ARE STØRED SØ THEY NEED ØNLY BE
00536C   CØMPUTED ØNCE.
00538C   AS MANY AS 3 DIFFERENT FUNCTIØNS MAY BE INTERPØLATED BEFØRE
00540C   A SET ØF CØEFFICIENTS MUST BE LØST.
00542    DIMENSIØN FUNC(2,N),CØEF(2,120,3)
00544C   CHECK RANGE ØF FUNCTIØN
00546    IF(X.LT.FUNC(1,1).ØR.X.GT.FUNC(1,N))GØ TØ 1 -
00548C   ZERØ ALL CØEFFICIENTS FIRST TIME USED
00550    IF(KEY.GT.0)GØ TØ 2
00552    KEY=-KEY
00554    DØ 10 J2=1,N
00556    CØEF(1,J2,KEY)=1.E-32
00558 10 CØEF(2,J2,KEY)=0.
00560C LØCATE VALUES REQUIRED
00562 2 DØ 11 J2=1,N
00564    IF(X-FUNC(1,J2))12,30,11
00566 11 CØNTINUE
00568    GØ TØ 1
00570 12 J1=J2-1
00572    IF(CØEF(1,J1,KEY).NE.1.E-32)GØ TØ 20
00574C CØMPUTE CØEFFICIENTS FIRST TIME NEEDED -
00576    J3=J2+1
00578    DX1=FUNC(1,J1)-FUNC(1,J2)
00580    DY1=FUNC(2,J1)-FUNC(2,J2)
00582    IF(J3.GT.N)GØ TØ 15
00584    DX2=FUNC(1,J3)-FUNC(1,J2)
00586    DY2=FUNC(2,J3)-FUNC(2,J2)
00588    DETX=DX1*DX2*(DX2-DX1)
00590    PRØD1=DX2*DY1
00592    PRØD2=DX1*DY2
00594    CØEF(1,J1,KEY)=(PRØD2-PRØD1)/DETX
00596    CØEF(2,J1,KEY)=(DX2*PRØD1-DX1*PRØD2)/DETX
00598    GØ TØ 20
00600 15 CØEF(1,J1,KEY)=0.
00602    CØEF(2,J1,KEY)=DY1/DX1
```

Figure C-11 (Continued)

```
00604C COMPUTE Y
00606 20 DX=X-FUNC(1,J2)
00608    DY=DX*(COEF(1,J1,KEY)*DX+COEF(2,J1,KEY))
00610    Y=FUNC(2,J2)+DY
00612    IF(Y.LT.0..AND.COEF(1,J1,KEY).NE.0.)GO TO 15
00614    RETURN
00616 1  Y=1.E-32
00618 101 FORMAT(I3,5E10.3)
00620    RETURN
00622 30 Y=FUNC(2,J2)
00624    RETURN
00626    END
00628    SUBROUTINE COMBIN(PROD,HLAMBD,XVALUE,A,NA,B,NB,C,NC,KEY)
00630C PRODUCT: PROD=A*B*C  FOR ONE X-VALUE OF ORDINATE.
00632    DIMENSION A(2,NA),B(2,NB),C(2,NC)
00634    COMMON TEMP,TX,FOCAL,AREA,IANS
00636    DATA NO/2HNO/
00638    PLANCK(W,T)=CONST/((-1.+EXP(C2/(W*T)))*W**5)
00640    IF(KEY.EQ.1)GO TO 30
00642    KEYA=-1
00644    KEY=1
00646    KEYB=-2
00648    KEYC=-3
00650    PI=3.1415926536
00652    PLNCK=6.6252E-34
00654    BOLTZ=1.38042E-23
00656    CLIGHT=2.99793E8
00658    C1=2.E20*PI*CLIGHT*PLNCK
00660    C2=1.E6*CLIGHT*PLNCK/BOLTZ
00662    CONST=CLIGHT*C1
00664    FAC=TX/(4*FOCAL**2)
00666 100 FORMAT(3I5,F7.0,4F10.4)
00668 101 FORMAT(F10.6,5E12.4)
00670C  EXPERIMENTAL CURVES
00672 30 PROD=FAC
00674C  FILTER
```

Figure C-11 (Continued)

```
00676 31 IF(NB.EQ.0)GØ TØ 32
00678    CALL INTPØL(Y,XVALUE,B,NB,KEYB)
00680    PRØD=PRØD*Y
00682C   SØURCE, EMITTANCE IN WATT/CM**2*MICRØN
00684 32 IF(NC.EQ.0)GØ TØ 33
00686    CALL INTPØL(Y,XVALUE,C,NC,KEYC)
00688    PRØD=PRØD*Y
00690C   BLACKBØDY SØURCE
00692 33 IF(TEMP.LT.1.)GØ TØ 50
00694    Y=PLANCK(XVALUE,TEMP)
00696    PRØD=PRØD*Y
00698 50 HLAMBD=PRØD
00700C   PHØTØCATHØDE RESPØNSE
00702    IF(NA.EQ.0)GØ TØ 53
00704    CALL INTPØL(Z,XVALUE,A,NA,KEYA)
00706    PRØD=PRØD*Z
00708    IF(IANS.GT.NØ)PRINT 101,XVALUE,Y,HLAMBD,Z,PRØD
00710 53 RETURN
00712    END
00714    SUBRØUTINE PRØCESS(P,NP,F,NNF,S,NS)
00716C   PRØCESS DATA AND ØUTPUT TØ TERMINAL AND TAPE.
00718    DIMENSIØN P(2,NP),F(2,NNF),S(2,NS)
00720    DIMENSIØN FUNC(2,3),HFUNC(2,3),PHUNC(2,3)
00722    CØMMØN TEMP,TX,FØCAL,AREA,IANS
00724    CØMMØN/ANSWER/CURDEN,PHØTØN,HSIG
00726    DATA NØ/2HNØ/
00728 106 FØRMAT(2X,7HMICRØN ,2(2X,10HW/CM**2*UM),3X,7HMA/WATT,
00730+          4X,11HMA/CM**2*UM/)
00732    PRINT 107
00734 107 FØRMAT(15HPRINT SPECTRUM?)
00736    READ 108,IANS
00738 108 FØRMAT(A10)
00740    KEY=0
00742    KEY1=0
00744    CURDEN=0.
00746    HSIG=0.
00748    PHØTØN=0.
```

Figure C-11 (Continued)

```
00750    HC=6.6252E-34*2.99793E8*1.E6
00752    CALL XVALUE(XMIN,XMAX,P,NP,F,NNF,S,NS,KEY)
00754    IF(IANS.LE.N0)G0 T0 2
00756    PRINT 103,XMIN,XMAX
00758    PRINT 105
00760    PRINT 106
00762  2 FUNC(1,1)=XMIN
00764    CALL C0MBIN(Y,HL,XMIN,P,NP,F,NNF,S,NS,KEY1)
00766    HFUNC(2,1)=HL
00768    HFUNC(1,1)=FUNC(1,1)
00770    PHUNC(1,1)=HFUNC(1,1)
00772    PHUNC(2,1)=HFUNC(2,1)*PHUNC(1,1)
00774    FUNC(2,1)=Y
00776  1 D0 10 J=2,3
00778    CALL XVALUE(X,XMAX,P,NP,F,NNF,S,NS,KEY)
00780    FUNC(1,J)=X
00782    HFUNC(1,J)=X
00784    PHUNC(1,J)=X
00786    CALL C0MBIN(Y,HL,X,P,NP,F,NNF,S,NS,KEY1)
00788    FUNC(2,J)=Y
00790    HFUNC(2,J)=HL
00792    PHUNC(2,J)=X*HL
00794    IF(X.GE.XMAX)G0 T0 11
00796 10 C0NTINUE
00798 12 CURDEN=CURDEN+QINTGL(FUNC)
00800    HSIG=HSIG+QINTGL(HFUNC)
00802    PH0T0N=PH0T0N+QINTGL(PHUNC)
00804    IF(X.GE.XMAX)G0 T0 20
00806    HFUNC(1,1)=HFUNC(1,3)
00808    FUNC(1,1)=FUNC(1,3)
00810    PHUNC(1,1)=PHUNC(1,3)
00812    HFUNC(2,1)=HFUNC(2,3)
00814    FUNC(2,1)=FUNC(2,3)
00816    PHUNC(2,1)=PHUNC(2,3)
00818    G0 T0 1
00820 11 IF(J.E0.3)G0 T0 12
```

Figure C-11 (Continued)

```
00822    CURDEN=CURDEN+(FUNC(2,2)+FUNC(2,1))*(FUNC(1,2)-FUNC(1,1))/2.
00824    HSIG=HSIG+(HFUNC(2,2)+HFUNC(2,1))*(HFUNC(1,2)-HFUNC(1,1))/2.
00826    PHØTØN=PHØTØN+(PHUNC(2,2)+PHUNC(2,1))*(PHUNC(1,2)-PHUNC(1,1))/2.
00828 20 CURDEN=CURDEN
00830    HSIG=HSIG
00832    PHØTØN=PHØTØN/HC
00834    CURENT=CURDEN*AREA
00836    PRINT 103,XMIN,XMAX
00838    PRINT 101,CURDEN
00840 101 FØRMAT(16HCURRENT DENSITY=,E12.5,18H MILLIAMPERE/CM**2)
00842 102 FØRMAT(23HPHØTØN CURRENT DENSITY=,E12.5,15H PHØTØN/S*CM**2)
00844 103 FØRMAT(14HSPECTRAL BAND:,F10.6,3H TØ,F10.6,11H MICRØMETER)
00846    PRINT 104,HSIG
00848 104 FØRMAT(21HIRRADIANCE ØN RETINA:,E12.5,11H WATT/CM**2)
00850    PRINT 102,PHØTØN
00852 105 FØRMAT(/10HWAVELENGTH,12H EMITTANCE  ,12H IRRADIANCE ,
00854+         12H PHØTØRESP  ,15HCURRENT DENSITY)
00856    RETURN
00858    END
00860    FUNCTIØN QINTGL(FUNC)
00862C QUADRATIC INTEGRAL ØF FUNCTIØN DEFINED BY 3 UNEQUALLY SPACED PØINTS
00864    DIMENSIØN FUNC(2,3)
00866    X1=FUNC(1,1)-FUNC(1,2)
00868    X3=FUNC(1,3)-FUNC(1,2)
00870    DY1=FUNC(2,1)-FUNC(2,2)
00872    DY2=FUNC(2,3)-FUNC(2,2)
00874    PRØDX=-X1*X3
00876    PRØD2=X1*DY2
00878    PRØD1=X3*DY1
00880    A=(PRØD1-PRØD2)/(PRØDX+PRØDX+PRØDX)
00882    B=(X1*PRØD2-X3*PRØD1)/(PRØDX+PRØDX)
00884    QINTGL=(X3-X1)*FUNC(2,2)+(X3+X1)*B
00886    QINTGL=QINTGL+((X3+X1)**2+PRØDX)*A
00888    RETURN
00890    END
```

Figure C-11 (Continued)

```
100    PROGRAM SIG2NOZ(INPUT,OUTPUT,TAPE1)
103    DIMENSION KIND(6),NAME(6)
106    DATA E/1.6E-19/,JA/3HYES/,NO/3HNO /
109    DATA KIND/6HPHOTOC,7HATHODE?,6HSOURCE,1H?,6HFILTER,1H?/
112    DATA IVID/3HVID/,INTEN/3HINT/
115    PRINT 100
118 100 FORMAT(/45HMAXIMUM HIGHLIGHT SIGNAL/NOISE FOR TV CAMERA./)
121C:  INPUT DATA
124C:   RASTER
127 1 PRINT 101
130 101 FORMAT(23HBANDWIDTH IN KILOHERTZ?)
133    READ,BANDO
136    BANDO=BANDO*1.E3
139    PRINT 102
142 102 FORMAT(21HFRAME TIME IN SECONDS?)
145    READ,FRAMEO
148    PRINT 103
151 103 FORMAT(49HACTIVE FRACTION OF HORIZONTAL AND VERTICAL SCANS?)
154    READ,HACT,VACT
157    SCANEF=HACT*VACT
160    SAMPLE=2.*FRAMEO*BANDO*SCANEF
163    PRINT 104
166 104 FORMAT(17HSCAN LINES/FRAME?)
169    READ,SCANLN
172    SCANLN=FLOAT(IFIX(SCANLN*VACT))
175    PRINT 105,SCANLN
178 105 FORMAT(F6.0,19H ACTIVE SCAN LINES.)
181    NUMH=IFIX(SAMPLE/SCANLN)
184    PRINT 106,NUMH
187 106 FORMAT(I6,29H SAMPLES PER HORIZONTAL LINE.)
190 2 PRINT 110
193 110 FORMAT(27HPHOTOCATHODE AREA IN CM**2?)
196    READ,AREA
199C:   EXPOSURE TIME AND CONTRAST
202 6 PRINT 111
205 111 FORMAT(25HEXPOSURE TIME IN SECONDS?)
208    READ,EXPTMO
```

Figure C-12

```
211    PRINT 112
214  112 FORMAT(22HSCENE SIGNAL CONTRAST?)
217    READ,CONTRS
220    CONFAC=(2.-CONTRS)/CONTRS
223    PRINT 113
226  113 FORMAT(38HPREAMPLIFIER NOISE CURRENT IN NANOAMP?)
229    READ,AMPNZ
232    AMPNZ=AMPNZ*1.E-9
235    AMPL=(2.*AMPNZ/(E*BANDO))**2
238C:   CAMERA TYPE
241    PRINT 120
244  120 FORMAT(52HIS THIS EITHER A VIDICON OR AN IMAGE DISSECTOR? YES?)
247    READ 121,IMAGE
250  121 FORMAT(A3)
253    GAINO=1.
262    IF(IMAGE.EQ.JA)GO TO 8
265    PRINT 122
268  122 FORMAT(34HCURRENT GAIN OF THE IMAGE SECTION?)
271    READ,GAINO
274  8 PRINT 123
277  123 FORMAT(42HIS THERE A SCANNING READING ELECTRON BEAM?)
280    ISOCON=NO
281    GMULTO=1.
282    ALPHA=1.
283    READ,IREAD
286    IF(IREAD.NE.JA)GO TO 26
289    PRINT 124
292  124 FORMAT(18HIS THIS AN ISOCON?)
295    READ,ISOCON
298    IF(ISOCON.EQ.JA)GO TO 23
301    PRINT 125
304  125 FORMAT(39HIS THERE AN ELECTRON MULTIPLIER OUTPUT?)
307    READ,MULTPO
310    IF(MULTPO.NE.JA)3,25
312  26 EXPTMO=0.5/BANDO
313  23 MULTPO=JA
316  25 PRINT 126
```

Figure C-12 (Continued)

```
319    IF(IREAD.EQ.JA)ALPHA=0.2
322  126 FORMAT(16HMULTIPLIER GAIN?)
325    READ,GMULTO
328C:  INTENSIFIER
331    3 PRINT 130
334  130 FORMAT(40HIS THERE AN AUXILIARY IMAGE INTENSIFIER?)
337    ETA1=2.
340    READ,INTO
343    GINTO=1.
346    IF(INTO.NE.JA)GO TO 4
349    PRINT 133
352  133 FORMAT(23HINTENSIFIER PHOTON GAIN?)
355    READ,GINTO
358    PRINT 134
361  134 FORMAT(46HCAMERA TUBE QUANTUM EFFICIENCY AT 0.55 MICRON?)
364    READ,ETA1
367    IF(ETA1.GT.1.)GO TO 5
370C:   EXPOSURE
373C:     INPUT FROM TAPE1
376  4 REWIND 1
379  11 DO 49 I=1,3
382  40 READ(1,41)KODE,NAME
385    IF(EOF,1)5,49
388  41 FORMAT(7A10)
391  49 PRINT 41,KODE,NAME
394    READ(1,44)FOCAL,TX
397    READ(1,44)CURDEN,PHOTON,HSIG
400    CURDEN=CURDEN*1.E-3
403  44 FORMAT(5E14.5)
406    GO TO 45
409C:    INPUT FROM TERMINAL
412  5 DO 48 I=1,3
415    J2=2*I
418    J1=J2-1
421    PRINT 46,KIND(J1),KIND(J2)
424  46 FORMAT(15HINDEX CODE FOR ,A6,A7)
```

Figure C-12 (Continued)

```
427    READ 41,KODE
430    IF(KODE.EQ.NO)GO TO 10
433    PRINT 47,KIND(J1),KIND(J2)
436 47 FORMAT(8HNAME OF ,A6,A7)
439 48 READ 41,NAME
442    PRINT 131
445 131 FORMAT(47HPHOTOCATHODE CURRENT DENSITY IN MILLIAMP/CM**2?)
448    READ,CURDEN
451    CURDEN=CURDEN*1.E-3
454    PRINT 132
457 132 FORMAT(49HPHOTOCATHODE PHOTON IRRADIANCE IN PHOTON/S*CM**2?)
460    READ,PHOTON
463C   COMPUTATION
466 45 CONTINUE
468C: LIMITED VARIABLES, INITIATION
469    EXPTIM=EXPTMO
472    INT=INTO
475    GINT=GINTO
478    GAIN=GAINO
481    BAND=BANDO
484    FRAME=FRAMEO
487    GMULT=GMULTO
490    MULTPL=MULTPO
492C: LIMITATIONS
493 61 FOTCHG=CURDEN*EXPTIM/CONTRS
496    IF(FOTCHG.LE.1.E-5)GO TO 62
499    EXPTIM=9.9E6*CONTRS/CURDEN
502    PRINT 161,EXPTIM
505 161 FORMAT(42HPHOTOCURRENT TOO HIGH; REDUCE EXPOSURE TO,E9.2,2H S)
508    GO TO 61
511 62 FOTCG2=FOTCHG*GINT
514    IF(FOTCG2.LE.1.E-5)GO TO 64
517    GINT=9.9E-6/FOTCHG
520    IF(GINT.GE.10.)GO TO 63
523    PRINT 162
526 162 FORMAT(46HINTENSIFIER OVERLOADS PHOTOCATHODE; REMOVE IT)
529    INT=NO
```

Figure C-12 (Continued)

```
532    GINT=1.
535    GO TO 64
538 63 PRINT 163,GINT
541 163 FORMAT(35HINTENSIFIER GAIN MUST BE REDUCED TO,E10.3)
544    GO TO 62
547 64 IF(IMAGE.EQ.JA)GO TO 65
550    SURFCG=FOTCG2*GAIN
553    IF(SURFCG.LE.3.E-8)GO TO 66
556    GAIN=2.9E-8/FOTCG2
559    PRINT 164,GAIN
562 164 FORMAT(24HALC LIMITS IMAGE GAIN TO,E10.3)
565    GO TO 64
568 65 SURFCG=FOTCG2
571 66 IF(IREAD.NE.JA)GO TO 67
574    BMCRDN=SURFCG*BAND/(2.*ALPHA)
577    IF(BMCRDN.LE.1.)GO TO 67
580    PRINT 165
583 165 FORMAT(43HBANDWIDTH EXCEEDS ELECTRON BEAM CAPABILITY.)
586    BAND=2.E-3*ALPHA/SURFCG
589    PRINT 166,BAND
592 166 FORMAT(19HREDUCE BANDWIDTH TO,E11.4,10H KILOHERTZ)
595    BAND=BAND*1.E3
598    FRAME=SAMPLE/(2.*BAND*SCANEF)
601    PRINT 167,FRAME
604 167 FORMAT(22HINCREASE FRAME TIME TO,E11.4,2H S)
607    GO TO 66
610 67 IF(MULTPL.NE.JA)GO TO 70
613 68 CURMUL=SURFCG*AREA*GMULT/(FRAME*SCANEF*ALPHA)
616    IF(CURMUL.LE.1.)GO TO 70
619    GMULT=FRAME*SCANEF*ALPHA/(SURFCG*AREA)
622    IF(GMULT.GE.10.)GO TO 69
625    PRINT 168
628 168 FORMAT(37HBEAM OVERLOADS MULTIPLIER. REMOVE IT)
631    MULTPL=NO
634    GMULT=1.
637    GO TO 70
640 69 PRINT 169,GMULT
```

Figure C-12 (Continued)

```
643 169 FORMAT(26HMULTIPLIER GAIN LIMITED TO,E10.3)
646   GO TO 68
648C: EQUATIONS
649 70 CONTINUE
652   ETA=CURDEN/(PHOTON*E)
655   IF(ETA.GT.1.)GO TO 42
658   GAINT=GINT/ETA
661   IF(INT.NE.JA)ETA1=ETA
664   EXPCUR=CURDEN*AREA*GAIN*GAINT*ETA1*GMULT
667   SIGE=EXPCUR*EXPTIM/(E*SAMPLE)
670   GNFAC=ETA+1.
673   IF(INT.EQ.JA)GNFAC=(GNFAC*GAINT+1.)*ETA1+1.
676   IF(IMAGE.NE.JA)GNFAC=GNFAC*GAIN+1.
679   IF(IREAD.EQ.JA)GNFAC=GNFAC+1.
682   IF(MULTPL.EQ.JA)GNFAC=(GNFAC+1.)*GMULT+1.
685   ECHGNZ=(SIGE*CONFAC*GNFAC+AMPL)
688   IF(ISOCON.NE.JA.AND.MULTPL.EQ.JA.AND.IREAD.EQ.JA)31,32
691 31 ECHGNZ=ECHGNZ+SIGE*(1.-ALPHA)*(2.*GMULT+1.)/ALPHA
694 32 ECHGNZ=SQRT(ECHGNZ)
697   CURNZ=2.*ECHGNZ*BAND*E
700   S2N=SIGE/ECHGNZ
703   SIGCUR=EXPCUR*EXPTIM/(FRAME*SCANEF)
706C: OUTPUT
707   PRINT 140
708   PRINT 44,FOTCHG,FOTCG2,SURFCG,BMCRDN,CURMUL
709   EXPCUR=EXPCUR*1.E6
710 140 FORMAT(6X,15H1 PHOTOCHARGE 2,7X,14HSTORED CHARGE ,
711+ 14HBEAM CUR DENS ,14HMULTIPLIER CUR )
712   PRINT 153,EXPCUR
715 153 FORMAT(17HEXPOSURE CURRENT=,E15.7,12H MICROAMPERE)
718   SIGCUR=SIGCUR*1.E6
721   PRINT 150,SIGCUR
724 150 FORMAT(17HSIGNAL CURRENT  =,E15.7,12H MICROAMPERE)
727   CURNZ=CURNZ*1.E6
730   PRINT 151,CURNZ
733 151 FORMAT(17HNOISE CURRENT   =,E15.7,12H MICROAMPERE)
```

Figure C-12 (Continued)

```
736    PRINT 152,S2N
739  152 FORMAT(17HSIGNAL/NOISE     =,E10.2)
742    GO TO 11
745   42 PRINT 200
748  200 FORMAT(49HQUANTUM EFFICIENCY GREATER THAN UNITY; TRY AGAIN.)
751C:   RESTART
754   10 PRINT 160
757  160 FORMAT(11H1 BEGINNING,10X,28H5 PHOTOCURRENT FROM TERMINAL)
760    PRINT 154
763  154 FORMAT(19H2 PHOTOCATHODE AREA,2X,15H6 EXPOSURE TIME)
766    PRINT 155
769  155 FORMAT(19H3 IMAGE INTENSIFIER,2X,6H7 STOP)
772    PRINT 156
775  156 FORMAT(25H4 PHOTOCURRENT FROM TAPE1,2X,14H8 READING BEAM)
778    PRINT 157
781  157 FORMAT(19HGO TO WHICH NUMBER?)
784    READ,NUMBER
787    GO TO(1,2,3,4,5,6,7,8),NUMBER
790   7 STOP
999    END
```

Figure C-12 (Continued)

```
10 PRØGRAM SIG2NZ1(INPUT,ØUTPUT)
15 DATA E/1.6E-19/,JA/3HYES/,NØ/3HNØ /
20   ISØCØN=JA
25 DATA AMPNZ/.3/
30 DATA BANDØ/1100./,FRAMEØ/1./,HACT/.95/,VACT/.98/
35 DATA SCANLN/1500./,EXPTMØ/1./,CØNTRS/1./,AREA/4.4/
40 PRINT 229
45 229 FØRMAT(44HBANDWIDTH  FRAMETIME  ACTIVE VERT  ACT HØRIZ)
50 PRINT 230,BANDØ,FRAMEØ,HACT,VACT
55 230 FØRMAT(1X,F6.1,7X,F4.2,7X,F4.2,7X,F4.2)
60 PRINT 231
65 231 FØRMAT(45HSCANLN/FRAME  EXP TIME  SCENE CØNTR  P.C.AREA)
70 PRINT 232,SCANLN,EXPTMØ,CØNTRS,AREA
75 232 FØRMAT(3X,F6.1,7X,F3.1,9X,F3.1,8X,F3.1)
80 PRINT 233
85 233 FØRMAT(37HPREAMP NØISE CURRENT-NANØAMP   ISØCØN)
90 PRINT 234,AMPNZ,ISØCØN
95 234 FØRMAT(14X,F2.1,17X,A3)
136   BANDØ=BANDØ*1.E3
157   SCANEF=HACT*VACT
160   SAMPLE=2.*FRAMEØ*BANDØ*SCANEF
172   SCANLN=FLØAT(IFIX(SCANLN*VACT+1E-8))
175   PRINT 105,SCANLN
178 105 FØRMAT(F6.0,19H ACTIVE SCAN LINES.)
181   NUMH=IFIX(SAMPLE/SCANLN+1E-8)
184   PRINT 106,NUMH
187 106 FØRMAT(I6,29H SAMPLES PER HØRIZØNTAL LINE.)
220   CØNFAC=(2.-CØNTRS)/CØNTRS
232   AMPNZ=AMPNZ*1.E-9
235   AMPL=(AMPNZ/(E*BANDØ))**2
238C:  CAMERA TYPE
239   IMAGE=NØ
241   PRINT 120
244 120 FØRMAT(27HVIDICØN ØR IMAGE DISSECTØR?)
247   PRINT 121,IMAGE
250 121 FØRMAT(12X,A3)
```

Figure C-13

```
253   GAIN0=1.
262   IF(IMAGE.EQ.JA)G0 T0 8
265   PRINT 122
268 122 F0RMAT(34HCURRENT GAIN 0F THE IMAGE SECTI0N?)
271   READ,GAIN0
274 8 PRINT 123
277 123 F0RMAT(31HSCANNING READING ELECTR0N BEAM?)
278   IREAD=JA
281   GMULT0=1.
282   ALPHA=1.
283   PRINT 248,IREAD
284 248 F0RMAT(14X,A3)
286   IF(IREAD.NE.JA)G0 T0 26
298   IF(IS0C0N.EQ.JA)G0 T0 23
300   PRINT 125
301 125 F0RMAT(11HPMT 0UTPUT?)
302   MULTP0=JA
303   PRINT 251,MULTP0
304 251 F0RMAT(4X,A3)
305   GMULT0=1.
306   C0NSTK=1.
308   INT0=N0
309   DELTAF=1/FRAME0
310   IF (MULTP0.NE.JA)241,25
312 26 EXPTM0=0.5/BAND0
313 23 MULTP0=JA
316 25 PRINT 126
317   GMULT0=4.E2
319   IF(IREAD.EQ.JA)ALPHA=0.2
320 126 F0RMAT(16HMULTIPLIER GAIN?)
321   PRINT 254,GMULT0
322 254 F0RMAT(6X,E7.1)
323   C0NSTK=1.5
324   DELTAF=BAND0
325 241 GINT0=1.
326   GAINCZ=GMULT0
```

Figure C-13 (Continued)

```
468C: LIMITED VARIABLES, INITIATION
469    EXPTIM=EXPTM0
472    INT=INT0
475    GINT=GINT0
478    GAIN=GAIN0
481    BAND=BAND0
484    FRAME=FRAME0
487    GMULT=GMULT0
490    MULTPL=MULTP0
648C: EQUATIONS
649  70 CONTINUE
652    PRINT 235
653  235 FORMAT(19HQUANTUM EFFICIENCY?)
654    READ,ETA
655  257 PRINT 239
656  239 FORMAT(23HSIGNAL CURRENT IN AMPS?)
657    READ,SIGCUR
658    GAINT=GINT/ETA
661    ETA1=ETA
664    EXPCUR=SIGCUR*FRAME*SCANEF/EXPTIM
665    CURDEN=EXPCUR/(AREA*GAIN*GAINT*ETA1*GMULT)
667    SIGE=SIGCUR*(FRAME*SCANEF)/(E*SAMPLE)
670    GNFAC=ETA+1.
673    IF(INT.EQ.JA)GNFAC=(GNFAC*GAINT+1.)*ETA1+1. -
676    IF(IMAGE.NE.JA)GNFAC=GNFAC*GAIN+1.
679    IF(IREAD.EQ.JA)GNFAC=GNFAC+1.
682    IF(MULTPL.EQ.JA)GNFAC=(GNFAC+1.)*GMULT+1.
685    ECHGNZ=(SIGE*CONFAC*GNFAC+AMPL)
688    IF(ISOCON.NE.JA.AND.MULTPL.EQ.JA.AND.IREAD.EQ.JA)31,32
691  31 ECHGNZ=ECHGNZ+SIGE*(1.-ALPHA)*(2.*GMULT+1.)/ALPHA
694  32 ECHGNZ=SQRT(ECHGNZ)
697    CURNZ=SQRT(2*E*GAINCZ*GAIN*CONSTK*CURDEN*AREA*DELTAF)
698    CURNZ1=2.*ECHGNZ*BAND*E
700    CURNZ=SQRT(CURNZ**2+AMPNZ**2)
704    S2N=SIGCUR/CURNZ
705    S2N1=SIGE/ECHGNZ
```

Figure C-13 (Continued)

```
*06C: ØUTPUT
709    EXPCUR=EXPCUR*1.E6
712    PRINT 153,EXPCUR
715 153 FØRMAT(20HEXPØSURE CURRENT    =,E15.7,12H MICRØAMPERE)
718    SIGCUR=SIGCUR*1.E6
721    PRINT 150,SIGCUR
724 150 FØRMAT(20HSIGNAL CURRENT      =,E15.7,12H MICRØAMPERE) -
727    CURNZ=CURNZ*1.E6
728    CURNZ1=CURNZ1*1.E6
730    PRINT 151,CURNZ
733 151 FØRMAT(20HNØISE CURRENT-FLS   =,E15.7,12H MICRØAMPERE)
736    PRINT 152,S2N
737    PRINT 179,CURNZ1
738 179 FØRMAT(20HNØISE CURRENT-JEN   =,E15.7,12H MICRØAMPERE)
739 152 FØRMAT(20HSIGNAL/NØISE-FLS    =,E10.2)
740    PRINT 176,S2N1
741 176 FØRMAT(20HSIGNAL/NØISE-JEN    =,E10.2)
744    EXPCUR=EXPCUR*1.E-6
747    SIGCUR=SIGCUR*1.E-6
750    CURNZ=CURNZ*1.E-6
753    CURNZ1=CURNZ1*1.E-6
756    PRINT 271
759 271 FØRMAT(3H    )
762    PRINT 274
765 274 FØRMAT(3H    )
800 GØ TØ 257
999    END
```

Figure C-13 (Continued)

APPENDIX D

REFERENCES

1. Electro-Optics Handbook, RCA, 1968.
2. C.W. Allen, Astrophysical Quantities, The Athlone Press, 1963.
3. "Project Plan for a 65 cm Solar Photoheliograph," Mission and Payload Planning Office Astronomy Group, NASA, July 1, 1970.
4. "Scientific Requirements for ATM Photoheliograph, "Cal Tech Memorandum, updated April 15, 1971.
5. "CIT Photoheliograph Definition Study, Final Report," Ball Bros. Research Corp, April 1971.
6. S. Wert, "Functional Requirements for Photoheliograph Image Recording," Cal Tech ATM Memorandum 002, August 1969.
7. A. Eisenman, P. Fowkal, "Intensifier Vidicon Television Subsystem, ATM-B Photoheliograph Detail Specification" California Institute of Technology and JPL.
8. "Solar Payload, ATM-A," Martin Marietta Corp, Document ED-2002-426.
9. "Skylab B Study, Phase I Technical Summary Report," Marshall Space Flight Center, August 3, 1970.
10. S.M. Seltzyer and W.B. Chubb, "Skylab Attitude and Pointing Control System," Marshall Space Flight Center, October 1970.
11. M. Nein, J. Oliver, Techniques for Conducting Scientific Research and Application Studies from an Orbiting Space Shuttle; 22nd International Astronautical Congress, September 1971.
12. T. Trott, The Effects of Motion on Resolution, Photogrammetric Engineering, December 1960.
13. G. Glasford, Fundamentals of Television Engineering, McGraw Hill, 1955.
14. A.S. Jensen, Proximity Focus Photocathodes, Westinghouse Aerospace Division, April 1969.

15. L.M. Biberman and S. Nudelman, Photoelectronic Imaging Devices, Plenum Press, 1971.

16. F.A. Rosell and G.V. Smith, "Television Camera Tube Performance and Data," Westinghouse AESD Technical Memo E0515, April 1970.

17. J.M. Watts, "Film Degradation Resulting from Magnetically Trapped Protons in ATM Orbits," NASA TM-X-53922, September 1969.

18. C.W. Hill, "Space Radiation Hazards to Project Skylab Photographic Film," NASA CR-61329, June 1970.